MINISTRY OF NATIONAL EDUCATION
AND SCIENTIFIC RESEARCH

THE ANNALS OF "DUNAREA DE JOS" UNIVERSITY OF GALATI

Fascicle IX
METALLURGY AND MATERIALS SCIENCE

YEAR XXXIV (XXXIX)
March 2016, no. 1

ISSN 1453-083X

2016
GALATI UNIVERSITY PRESS

EDITORIAL BOARD

EDITOR-IN-CHIEF

Prof. Marian BORDEI – "Dunarea de Jos" University of Galati, Romania

EXECUTIVE EDITOR

Assist. Prof. Marius BODOR – "Dunarea de Jos" University of Galati, Romania

PRESIDENT OF HONOUR

Prof. Nicolae CANANAU – "Dunarea de Jos" University of Galati, Romania

SCIENTIFIC ADVISORY COMMITTEE

Assoc. Prof. Stefan BALTA – "Dunarea de Jos" University of Galati, Romania
Prof. Lidia BENEA – "Dunarea de Jos" University of Galati, Romania
Prof. Acad. Ion BOSTAN – Technical University of Moldova, the Republic of Moldova
Prof. Bart Van der BRUGGEN – Katholieke Universiteit Leuven, Belgium
Prof. Francisco Manuel BRAZ FERNANDES – New University of Lisbon Caparica, Portugal
Prof. Acad. Valeriu CANTSER – Academy of the Republic of Moldova
Prof. Anisoara CIOCAN – "Dunarea de Jos" University of Galati, Romania
Assist. Prof. Alina CIUBOTARIU – "Dunarea de Jos" University of Galati, Romania
Prof. Alexandru CHIRIAC – "Dunarea de Jos" University of Galati, Romania
Assoc. Prof. Stela CONSTANTINESCU – "Dunarea de Jos" University of Galati, Romania
Assoc. Prof. Viorel DRAGAN – "Dunarea de Jos" University of Galati, Romania
Prof. Valeriu DULGHERU – Technical University of Moldova, the Republic of Moldova
Prof. Jean Bernard GUILLOT – École Centrale Paris, France
Assoc. Prof. Gheorghe GURAU – "Dunarea de Jos" University of Galati, Romania
Prof. Iulian IONITA – "Gheorghe Asachi" Technical University Iasi, Romania
Prof. Philippe MARCUS – École Nationale Supérieure de Chimie de Paris, France
Prof. Vasile MARINA – Technical University of Moldova, the Republic of Moldova
Prof. Rodrigo MARTINS – NOVA University of Lisbon, Portugal
Prof. Strul MOISA – Ben Gurion University of the Negev, Israel
Prof. Daniel MUNTEANU – "Transilvania" University of Brasov, Romania
Prof. Viorica MUSAT – "Dunarea de Jos" University of Galati, Romania
Prof. Maria NICOLAE – Politehnica University Bucuresti, Romania
Prof. Petre Stelian NITA – "Dunarea de Jos" University of Galati, Romania
Prof. Florentina POTECASU – "Dunarea de Jos" University of Galati, Romania
Assoc. Prof. Octavian POTECASU – "Dunarea de Jos" University of Galati, Romania
Prof. Cristian PREDESCU – Politehnica University of Bucuresti, Romania
Prof. Iulian RIPOSAN – Politehnica University of Bucuresti, Romania
Prof. Antonio de SAJA – University of Valladolid, Spain
Prof. Wolfgang SAND – Duisburg-Essen University Duisburg Germany
Prof. Ion SANDU – "Al. I. Cuza" University of Iasi, Romania
Prof. **Georgios SAVAIDIS –** Aristotle University of Thessaloniki, Greece
Prof. Elisabeta VASILESCU – "Dunarea de Jos" University of Galati, Romania
Prof. Ioan VIDA-SIMITI – Technical University of Cluj Napoca, Romania
Prof. Mircea Horia TIEREAN – "Transilvania" University of Brasov, Romania
Assoc. Prof. Petrica VIZUREANU – "Gheorghe Asachi" Technical University Iasi, Romania
Prof. Maria VLAD – "Dunarea de Jos" University of Galati, Romania
Prof. François WENGER – École Centrale Paris, France

EDITING SECRETARY

Prof. Marian BORDEI – "Dunarea de Jos" University of Galati, Romania
Assist. Prof. Marius BODOR – "Dunarea de Jos" University of Galati, Romania

Table of Contents

THE ANNALS OF "DUNAREA DE JOS" UNIVERSITY OF GALATI
FASCICLE IX. METALLURGY AND MATERIALS SCIENCE
N°. 1 - 2016, ISSN 1453 – 083X

NUMERICAL STUDY ON BALLISTIC PHENOMENA - PART TWO

Vasile BĂLAN[1], Marian BORDEI[2*]
[1]Tehnical Military Academy of Bucharest, Romania
[2]"Dunarea de Jos" University of Galati, Faculty of Engineering, Romania
[*]Corresponding author
email: mbordei@ugal.ro

ABSTRACT

The study of ballistic phenomena (interior ballistics, exterior ballistics and terminal ballistics) is an activity that involves the use of complex and at the same time very expensive equipment. Also, another aspect worth taking into account is the existence of risks when it comes to investigating the phenomena in this area.

The use of numerical methods for making the pre-digital tests can be seen as a logical and inexpensive approach. Furthermore, besides these advantages, the simulations of various ballistic phenomena allow for an otherwise impossible observation of different sizes and details regarding the polygon tests. In the case studied in this paper, the numerical modelling of the phenomenon of the charge of water propulsion allows for, as an example, the average speed evaluation of the whole amount of water, while in the case of polygon tests only the speed of peak flow value may be shown.

This paper is a numerical study on disrupting agent propulsion (internal ballistics), the speed water flow development and its distribution within the flow (the balancing kickback agent) being observed.

KEYWORDS: numerical modelling, ballistic phenomena

1. Case study

This paper was a numerical study on disrupting agent propulsion (internal ballistics), the speed water flow development and its distribution within the flow (the balancing kickback agent) being observed.

Thus, considering the geometrical and structural characteristics of the pipe and the mechanical characteristics of the disruption agent, the modeling and mesh parts were carried out.

Following the mesh of the structures involved in the water propulsion phenomenon, 169011 Euler type items, 2840 Lagrange type items and 24570 SPH items were obtained [14]. The schematization of the shaped assembly is shown in Fig. 1.

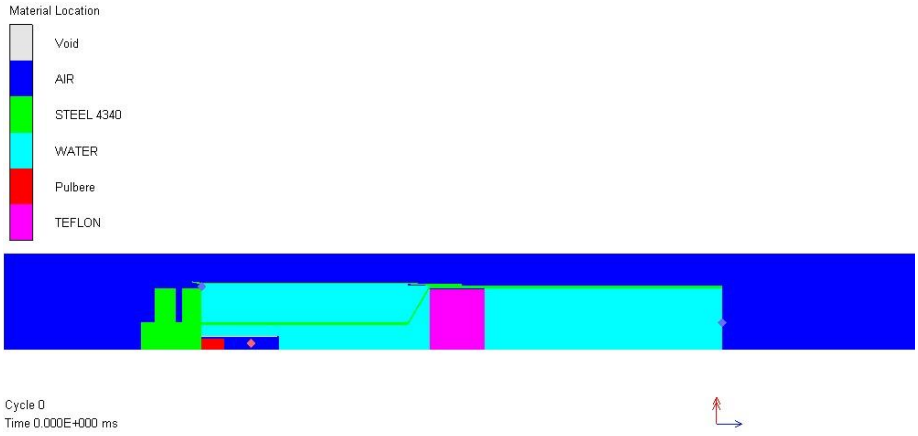

Fig. 1. *MEF Model*

The numerical simulation of propulsion was performed in AUTODYN v15.0, the type of analysis being the one stated.

The materials used were taken from the library and, for the powder, the model described in [17] was adopted. The material behavior is described by the following equations:

- AIR
- Density – 0.001225 g/cm^3;
- State equation of ideal gas type
  - Gamma: 1.4;
  - Adiabatic constant: 0;
  - Reference temperature: 288.2 K;
  - Specific heat: 717.599 J/kgK.
- WATER
- Density – 0.998 g/cm^3;
- State equation of shock type
  - Gruneisen coefficient: 0;
  - C1 Parameter: 1.647e3;
  - S1 Parameter: 1.921.
- TEFLON
- Density – 2.153 g/cm^3;
- State equation of shock type
  - Gruneisen coefficient: 0.59;
  - C1 Parameter: 1.841e3;
  - S1 Parameter: 1.707.
- POWDER
- Density – 1.86 g/cm^3;
- State equation of Powder Burn (Beta) type
  - EOS for solid phase - Linear type (Volume elasticity modulus: 1.35e7 kPa, Reference temperature: 293 K);
  - EOS for reactive phase - Exponential type (G=52.169998; c=0.5; C1=500; C2=0; D=1.0033; e=1.8185e6 kJ/m^3; p1=1e-5kPa; p2=2.5e6; p3=5e6; p4=7.5e6; p5=1e7; p6=1.25e7; p7=1.5e7; p8=1.75e7; p9=2e7; p10=1e9; H1=0,0071; H2=2,0432; H3=3,8692; H4=5.6236; H5=7.3329; H6=9.0095; H7=10.6606; H8=12,2906; H9=13,9029; H10=515,278015; ρ1=1e-6; ρ2=1; ρ3=2; ρ4=3; ρ5=4; ρ6=5; ρ7=6; ρ8=7; ρ9=8; ρ10=9; γ1..γ10=1);
- Von Mises resistance model
  - G=1.38e6kPa; σ_c= 2e3kPa.
- Steel 4340 type
- Density – 7.83 g/cm^3;
- State equation of Linear type
  - Volume elasticity modulus: 1.59e8 kPa,
  - Reference temperature: 300K;
  - Specific heat: 477 J/kgK;
- Johnson-Cook resistance model
  - G=8.18e7kPa;
  - A= 7.92e5 kPa; B=5.1e5 kPa; n=0.26; C=0.014; m=1.03; T_t=1.793e3; $d\varepsilon_o/dt=1s^{-1}$.

Another key element in defining the parameters of the simulation was the definition of contacts between the three parts of the model (pipe, piston and agent of disruption).

The water dispersing mode is shown in Fig. 2.

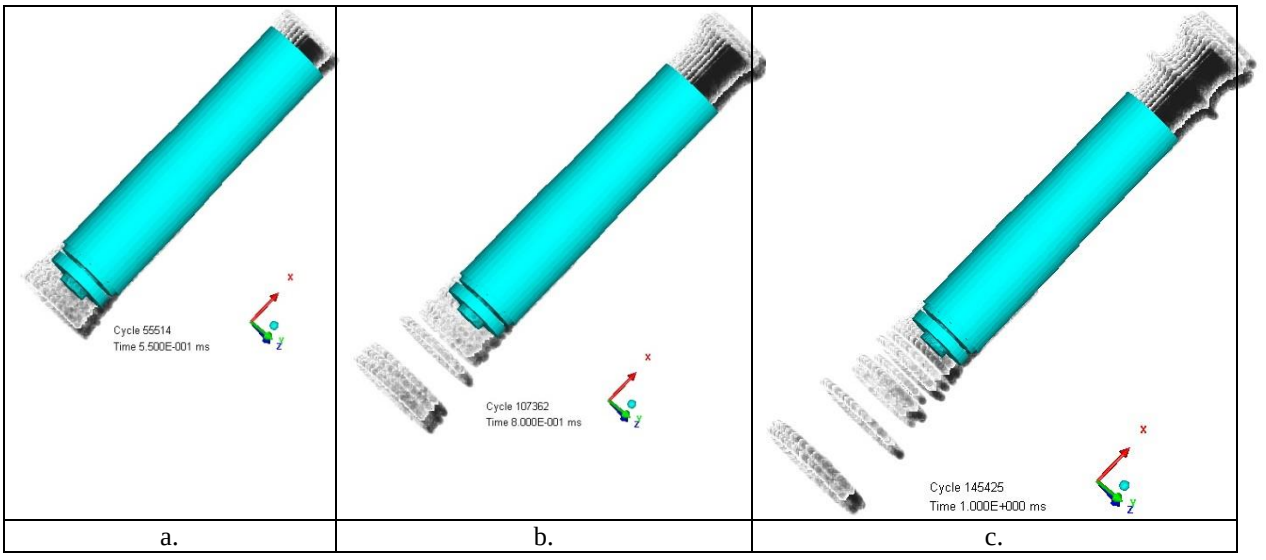

a. b. c.

Fig. 2. *Water dispersing mode in time*

The variation of the average speed of both water loads used by the disruptor is shown in Fig. 3 and Fig. 4.

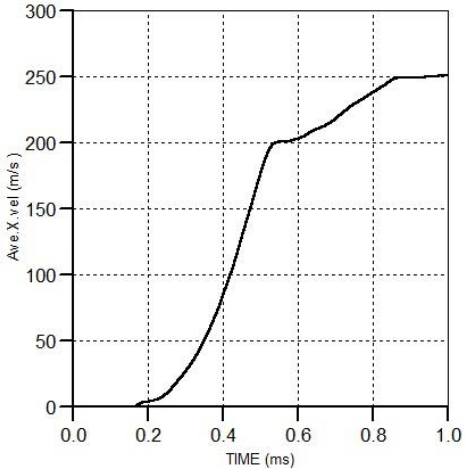

Fig. 3. *Average speed of the water (disrupting agent)*

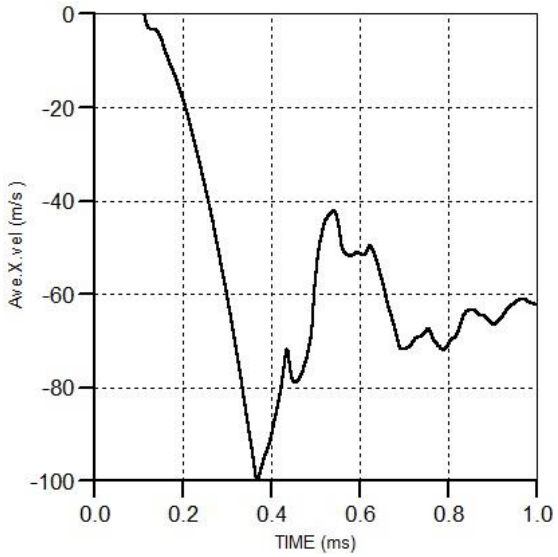

Fig. 4. *Average water speed (balancing agent kickback)*

Although the average speed chart of the disrupting agent and of the annulling agent of the kickback indicates a value of 250m/s, respectively, 62m/s, inside the flow there are also particles that record higher values of the speed (Fig. 5 and Fig. 6).

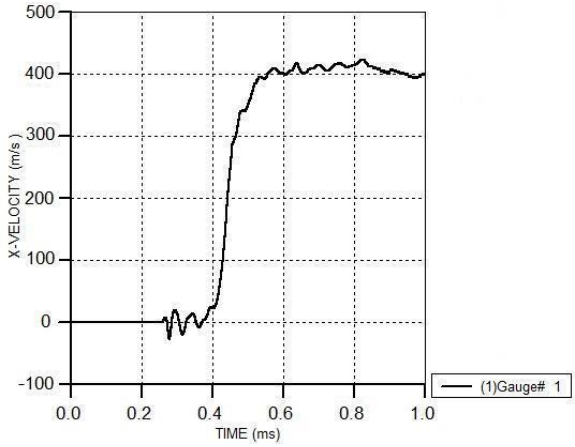

Fig. 5. *Evolution of the peak speed flow of the disruptor agent*

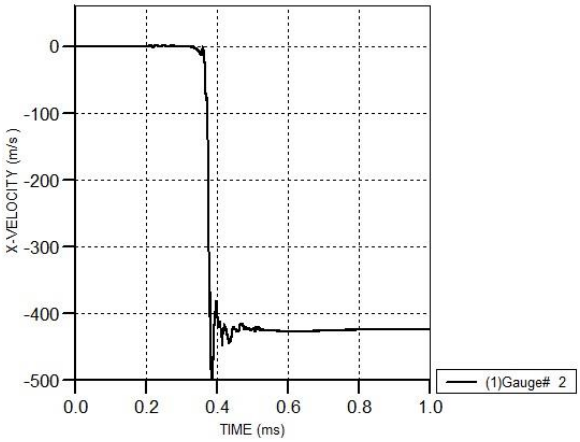

Fig. 6. *Evolution of the peak speed flow for water kickback compensation*

2. Conclusions

From those presented in the numerical modelling of the water propulsion phenomenon it results that the numerical approach is an easy way to achieve a detailed investigation and reduced costs.

The use of the SPH method allows for the numerical modelling of the phenomenon without the danger of blocking the problem because of the characteristic large deformations.

The analysis of the water speed field during covering 120mm highlights an average speed of the disrupting agent of 251m/s and a speed of the recoil agent of 62m/s. Also, the simulation shows a loss of flow coherence because of the water interaction with the adjacent environment (air). The flow peak speed presents a decrease after reaching a maximum value due to the interaction with air.

The comparative analysis of the numerical simulation results with the experimental results shows a good agreement in terms of the peak speed flow.

References

[1]. O. C. Zienkiewicz, *Origins, milestones and directions of the finite element method - A personal view***,** Archives of Computational Methods in Engineering, vol. 2, Issue 1, p. 1-48, 1995.

[2]. K. K. Gupta, J. L. Meek, *A brief history of the beginning of the finite element method*, International Journal for Numerical Methods in Engineering, vol. 39, p. 3761-3774, 1996.

[3]. R. W. Clough, *Early history of the finite element method from the view point of a pioneer*, Int. J. Numer. Meth. Engng, vol. 60, p. 283-287, 2004.

[4]. Vidar Thomee, *From finite diferences to finite elements. A short history of numerical analysis of partial diferential equations*, Journal of Computational and Applied Mathematics, vol. 128, p. 1-54, 2001.

[5]. Lucy L. B., *A numerical approach to the testing of the fission hypothesis*, Astron J., vol. 82 (12), p. 1013-1024, 1977.

[6]. Gingold R. A., Monaghan J. J., *Smoothed particle hydrodynamics—theory and application to non-spherical stars*, Mon Not R Astron Soc, vol. 181, p. 375-389, 1977.

[7]. Gingold R. A., Monaghan J. J., *Kernel estimates as a basis for general particle method in hydrodynamics*, J Comput Phys, vol. 46, p. 429-453, 1982.

[**8]. Monaghan J. J.,** *Particle methods for hydrodynamics*, Comput Phys Rep, vol. 3, p. 71-124, 1985.

[**9]. Dyka C., Ingel R.**, *An approach for tension instability in smoothed particle hydrodynamics (sph)*, Computers and Structures, vol. 57 (4), p. 573-580, 1995.

[10]. Swegle J., Hicks D., Attaway S., *Smooth particle hydrodynamics stability analysis*, J. Comp. Phys., vol. 116, p. 123-134, 1995.

[11]. Johnson J., Beissel S., *Normalized smoothing functions for sph impact computations*, Computer Methods in Apllied Mechanics and Engineering, vol. 139, p. 347-373, 1996.

[12]. Liu W., Jun S., Zhang Y., *Reproducing kernel particle methods*, International Journal for Numerical Methods in Engineering, vol. 20, p. 1081-1106, 1995.

[13]. Ştefan I. Maksay, Diana A. Bistrian, *Introducere în Metoda Elementelor Finite*, Ed. CERMI Iaşi, 2008.

[14]. Năstăsescu V., Bârsan G., *Metoda SPH*, Ed. Academiei Forţelor Terestre „Nicolae Bălcescu", Sibiu, 2012.

[15]. M. Vesenjak, Z. Ren, *Application Aspects of the Meshless SPH Method*, Journal of the Serbian Society for Computational Mechanics, vol. 1 (1), p. 74-86, 2007.

[**16]. M. B. Liu, G. R. Liu**, *Smoothed Particle Hydrodynamics (SPH): an Overview and Recent Developments*, Arch Comput Methods Eng, vol. 17, p. 25-76, 2010.

[**17]. E. Smestad, J. F. Moxnes, G. Odegardstuen**, *Modelling of deflagration, establishing material data into Ansys Autodyn's powder burn model*, 2012.

[18]. E. Trană, *Solicitarea materialelor metalice în regim dinamic. Legi constitutive*, Editura Univers Ştiinţific, Bucureşti, 2007.

THE ANNALS OF "DUNAREA DE JOS" UNIVERSITY OF GALATI
FASCICLE IX. METALLURGY AND MATERIALS SCIENCE
N°. 1 - 2016, ISSN 1453 – 083X

THERMO-MECHANICAL ANALYSIS OF SPRAYED LAYERS USING THE FINITE ELEMENT METHOD

Roxana-Alexandra GHEŢA, Bogdan DUMITRU, Gabriel Marius DUMITRU, Mădălina-Elena MILITARU
Politehnica University of Bucharest, Department for Industrial Engineering, Romania
email: roxana_gheta@yahoo.com; militaruemadalina@yahoo.com; bogdan_dmt@yahoo.com; gmdumitru@yahoo.com

ABSTRACT

The present paper presents an analysis performed in order to determine the thermo-mechanical behavior at the layer-substrate interface in case of thermal spraying, by using the ANSYS R15.0 software. The analysis was made on high alloyed steel samples thermal sprayed on one side. For the 1st sample, the material used for the deposited layer was ZrO_2 stabilized with Y_2O_3 (ZrO_2+20% Y_2O_3) using the HVOF process. The 2nd sample was sprayed with stellite using the plasma spraying process. This analysis follows the idea of temperature distribution along with the other characteristics that define the thermal state in an object: the heat quantities released or absorbed, thermal gradient and thermal flow. In order to determine the causes of thermal expansions or contractions, the analysis is followed by a stress analysis. The obtained results show that the interface stresses are lower in the case of stellite coating, both steel and stellite having closer thermo-physical characteristics than steel and YSZ also including the intermediate layer.

KEYWORDS: reconditioning, sprayed layer, bond coat, stellite, thermal shock

1. Introduction

Metal spraying reconditioning is a method of remaking the nominal dimensions of the part by deposing additional material melted particles on the work piece surface. The purpose is to obtain improved properties of the deposited layers thanks to special materials which can be sprayed [1].

The chosen material, used for reconditioning, needs to have better mechanical features and the reconditioned part will be up to two or three times more resistant to wear, fatigue or corrosion, depending on the application [1].

The reconditioned parts, obtained through material deposition, are made of two distinct components, the basic material and the sprayed layer.

In terms of chemical composition, thermo-physical properties and the behavior to mechanical and thermal stresses, these two components usually have totally different expansion and contraction coefficients. This way, the risk of developing internal stresses which can compromise the entire structure appears [1].

The **HVOF** (High Velocity Oxygen Fuel) is a thermal spray process which utilizes a combination of oxygen with various fuel gases including hydrogen, propane, propylene, hydrogen and even kerosene (Figure 1). Fuel and oxygen mix and atomize within the combustion area under conditions that monitor the correct combustion mode and pressure [1, 2].

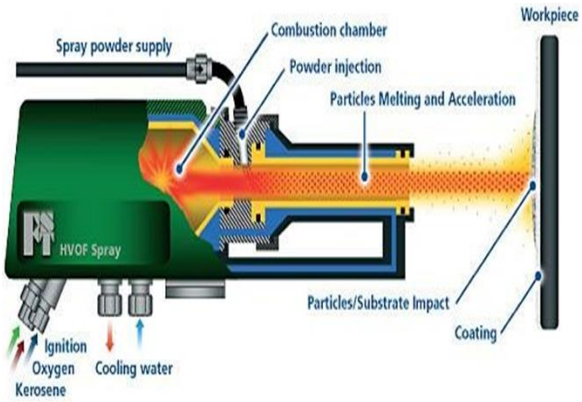

Fig. 1. *Schematic of HVOF Combustion Chamber* [2]

The process creates a very high velocity which is used to propel the particles at supersonic speeds before impact onto the substrate.

One of the key benefits of this system's high velocity is the extremely high coating density and low oxide content. The low oxides are due partly to the speed of the particles spending less time within the heat source and partly due to the lower flame temperature (around 3000 °C) of the heat source compared with alternative processes.

The **plasma spraying** process involves the latent heat of ionized inert gas being used to create the heat source, which melts the coating material and propels it to the work piece (Figure 2). The most common gas used to create the plasma is argon. Helium tends to expand the plasma and when used in combination with argon produces a "high velocity plasma" that exits the nozzle at about 488 m/sec. [1, 2].

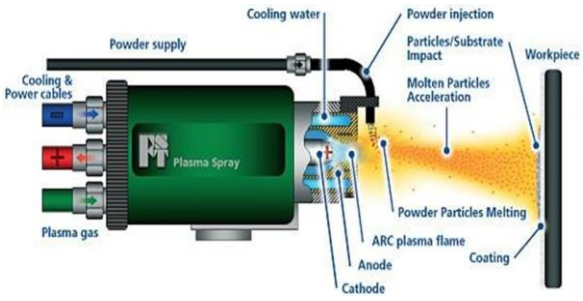

Fig. 2. *Plasma Spray Process* [2]

In commercial technology, plasmas are considered as hot streams of particles reaching temperatures higher than 10 000 °C. Today's plasma spray guns are sufficiently robust to produce temperatures from 5000 °C to 16 000 °C for long time periods [1].

2. Experimental part

2.1. Data entry

In the case study presented below, the thermo-mechanical behavior at the layer-substrate interface in case of thermal spraying is highlighted.

The experiment started with the increase of the wear resistance of the steam turbine blades subjected to harsh conditions of high temperature and cavitation/erosion caused by the steam condensate. In order to perform the analysis, high alloyed steel samples X22CrMoV12-1 for turbine blades, thermal sprayed on one side were chosen.

The two X22CrMoV12-1 plates have the dimensions (XxYxZ) 100x60x5 millimeters. For sample no.1, the deposition was made in three steps: first was added a bond-coat of Sultzer Metco Amdry 997 powder of 0.01 mm thickness, secondly was deposed an intermediate layer of Zirconia stabilized pseudo-alloy ceria-yttrium, 0.01 mm thickness and thirdly the material used for the top coat was ZrO_2 stabilized with Y_2O_3 (ZrO_2+20% Y_2O_3) metal-sprayed using HVOF process, this layer being 0.3 mm thick (Figure 3).

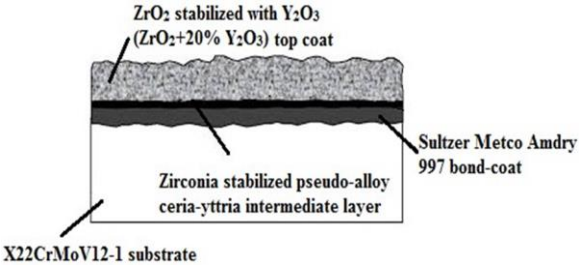

Fig. 3. *No. 1 specimen section*

Sample no. 2 (represented in Figure 4) was sprayed with Stellite 6 powder using the plasma spraying process. This layer is 0.3 mm thick.

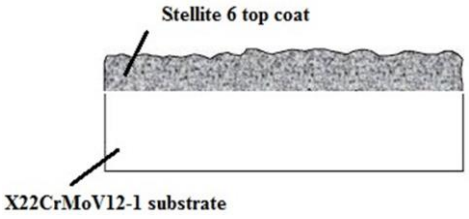

Fig. 4. *No. 3 specimen section*

2.2. ANSYS R15.0 data processing and results

Once the volumes of the entire studied structures defined, the characteristics and properties for each material were assigned and the next step - discretization of the structures – was defined like in Figure 5.

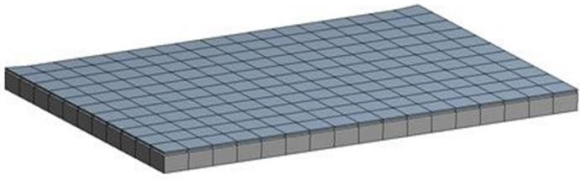

Fig. 5. *Structure discretization*

Figure 6 shows the block diagram of the simulation, containing the thermal and structural transient of the two analyzed specimens.

Fig. 6. *Block diagram of the simulation*

In choosing a material, to create a new one or to modify an existing material found in the library workbench, the module Engineering Data of ANSYS R15.0 was accessed (Figure 7) [5, 6].

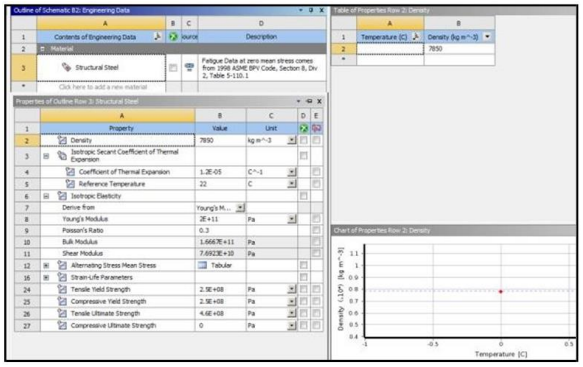

Fig. 7. *Engineering Data module*

The material characteristics of the high alloyed steel X22CrMoV12-1 taken into account for running the finite element analysis are presented in Table 1 [3, 4].

Table 1. *X22CrMoV12-1 characteristics*

	Properties	Values	Unit of measurement
X22CrMoV12-1	Density	7700	kg m^-3
	Thermal conductivity	47.9	W m^-1 K^-1
	Heat capacity	460	J kg^-1 K^-1
	Thermal expansion coefficient	12.1 e-006	K^-1
	Young's Modulus	200 e+09	Pa
	Poisson's ratio	0.3	-

In Table 2 are presented the material characteristics of ZrO_2 stabilized Y_2O_3 [3, 4].

Table 2. *ZrO_2 stabilized Y_2O_3 characteristics*

	Properties	Values	Unit of measurement
ZrO_2 stabilized Y_2O_3 (ZrO_2+20 % Y_2O_3)	Density	6600	kg m^-3
	Thermal conductivity	2.2	W m^-1 K^-1
	Heat capacity	540	J kg^-1 K^-1
	Thermal expansion coefficient	6 e-006	K^-1
	Young's Modulus	160 e+09	Pa
	Poisson's ratio	0.32	-

The material characteristics of Stellite 6 are presented in Table 3 [3, 4].

Table 3. *Characteristics of stellite 6*

	Properties	Values	Unit of measurement
Stellite 6	Density	7800	kg m^-3
	Thermal conductivity	55	W m^-1 K^-1
	Heat capacity	456	J kg^-1 K^-1
	Thermal expansion coefficient	6.6 e-006	K^-1
	Young's Modulus	195 e+09	Pa
	Poisson's ratio	0.32	-

The two structures are kept at an environmental temperature of 22 ºC.

In Figure 8 below is presented the thermal shock testing diagram depending on time. This was scheduled in 3 steps, as explained below.

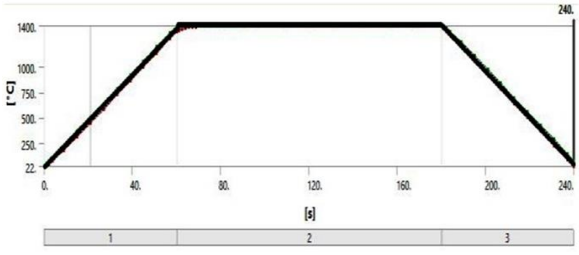

Fig. 8. *Temperature Graph depending on time*

In the first part of the experiment, each of them is submitted to a thermal shock, the heat source being oriented towards the sprayed layer (Figure 9). In 60 s the pieces are brought to 1400 ºC, then maintained for 120 s at this constant temperature of 1400 ºC.

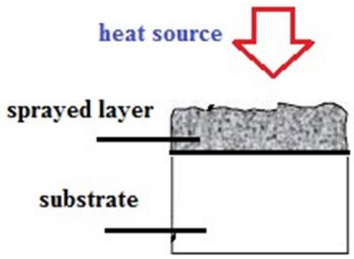

Fig. 9. *Heat source principle scheme*

In the last part of the experiment a sudden cooling in air jet was applied to the structures, thus the parts being brought back at ambient temperatures of 22 ºC within 60 seconds.

From the beginning of the cycle heat-cold in specially heating, we can observe the minimum and maximum tensions from the interface between the basic material and the deposited one.

The equivalent stresses for plate no. 1 sprayed with ceramic are in a range of 0.8-3200 MPa (Figure 10).

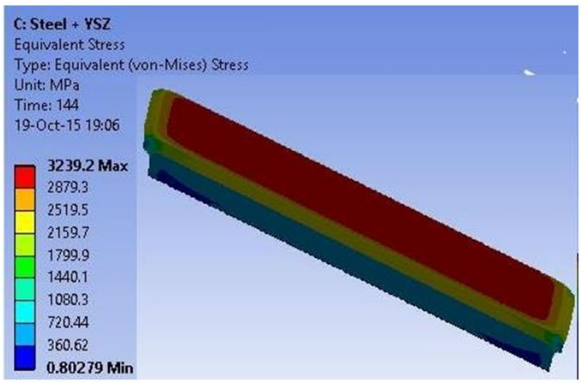

Fig. 10. *Equivalent stresses (von-Mises) steel + YSZ*

On the other hand, the range of equivalent stresses in the stellite coated plate is 0-22.8 MPa (Figure 11).

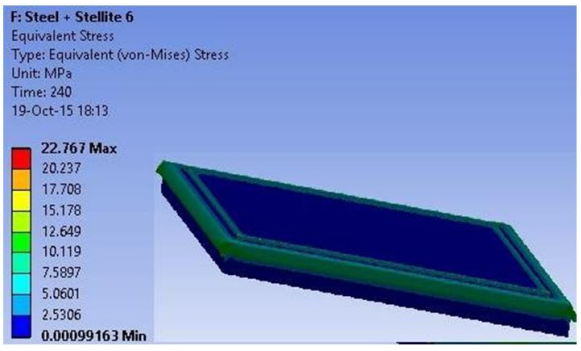

Fig. 11. *Equivalent stresses (von-Mises) steel + stellite*

Regarding the characteristics that define the thermal state in object, we could observe that the total heat flux reaches a maximum value of 0.433 W/mm^2 in the steel-stellite structure (Figure 12).

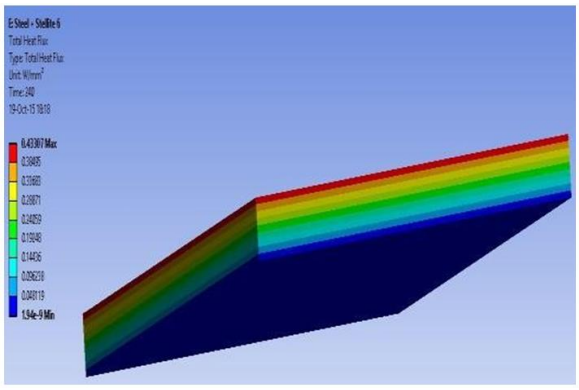

Fig. 12. *Total heat flux steel + stellite*

An almost insignificant difference can be observed in the case of steel-ceramic specimen, where the maximum heat flux value is 0.433 W/mm^2 (Figure 13).

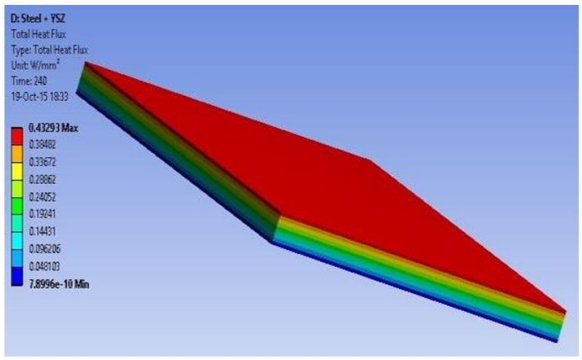

Fig. 13. *Total heat flux steel + ceramic*

A graph of total heat flux in the steel-stellite structure depending on time was generated, as can be seen in Figure 14 below.

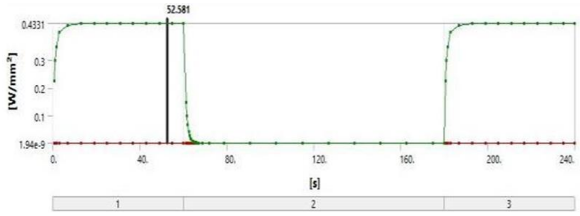

Fig. 14. *Steel-stellite total heat flux depending on time*

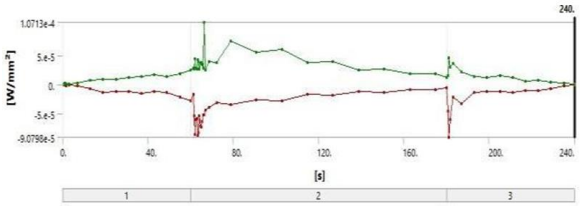

Fig. 15. *Steel-stellite directional heat flux in X*

At the end of the 3rd stage, after cooling the structures, the difference of temperature at the interface between the top coating and the basic material can be observed. If zirconia is used, 22 ºC were indicated at the surface, the intermediate layer went up to 79 ºC, then, at the level of the steel, the structure's temperature was 100 ºC (Figure 16).

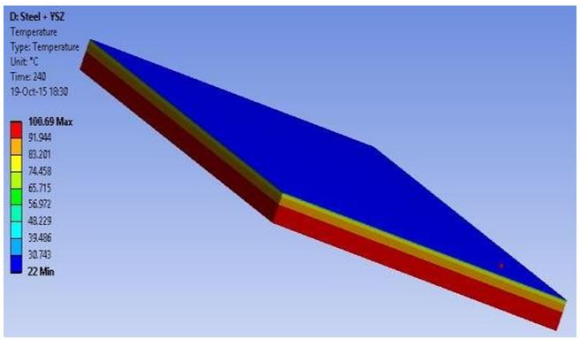

Fig. 16. *Steel-YSZ temperature after cooling*

At the steel-stellite interface, the structure reached a temperature value of 24 ºC. Then, at the base of the high alloyed steel plate, it gets up to 45 ºC (Figure 17).

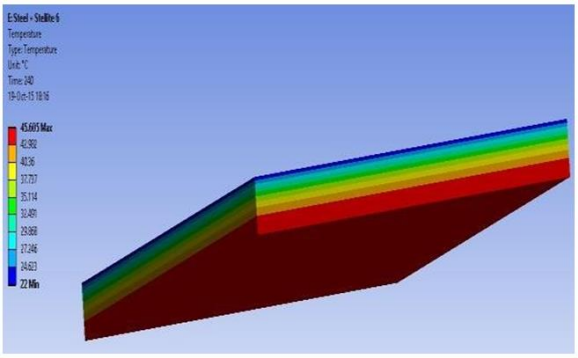

Fig. 17. *Steel-stellite temperature after cooling*

3. Conclusions

Conclusion (1). By the FEM analysis, applied through the ANSYS software, we could understand and interpret the thermo-mechanical phenomena that take place at the basic material – sprayed layer interface.

Conclusion (2). The obtained results show that the interface stresses are lower in case of stellite coating, both steel and stellite having closer thermo-physical characteristics than steel and YSZ also including the intermediate layer.

Conclusion (3). The low thermal conductivity of the ceramic layer does not allow for fast transmission of temperature. Ceramic has a smaller heat variation than steels. As time passes, the temperature curve flattens.

Conclusion (4). An optimization of the technological process of metal spraying, adapted to the requested working conditions in different situations of operating can be achieved through modifying the layer's thickness.

Acknowledgements

The work has been funded by the Sectoral Operational Programme Human Resources Development 2007-2013 of the Ministry of European Funds through the Financial Agreement POSDRU 187/1.5/S/155420.

The work has been funded by the Sectoral Operational Programme Human Resources Development 2007-2013 of the Ministry of European Funds through the Financial Agreement POSDRU/159/1.5/S/132395.

References

[1]. Gabriel Marius Dumitru, Constantin Radu, Bogdan Dumitru, *Reconditioning and repairing of products*, Ed. Printech, Bucharest, 2010.
[2]. ***, http://www.fst.nl.
[3]. ***, http://www.steelnumber.com.
[4]. ***, http://www.steelglossary.com.
[5]. Dan Florin Nitoi, Gheorghe Amza, *Modelling and simulation of technological processes*, Ed. A.G.I.R., Bucharest, 2009.
[6]. Cristina Pupaza, Radu Constantin Parpala, *Modelling and structural analysis with ANSYS Workbench*, Ed. Politehnica, Bucharest, 2013.

THE ANNALS OF "DUNAREA DE JOS" UNIVERSITY OF GALATI
FASCICLE IX. METALLURGY AND MATERIALS SCIENCE
Nº. 1 - 2016, ISSN 1453 – 083X

ENERGY DISEQUILIBRIUM EFFECTS IN HEAT TREATMENT EQUIPMENT

Mihai COJOCARU[1], Leontin DRUGĂ[2], Florică TUDOSE[1], Daniela DRAGOMIR[3], Gheorghe TOADER[3]
[1]Politehnica University of Bucharest,
[2]Romanian Academy for Technical Sciences,
[3]UTTIS, Vidra, Romania,
e-mail: mocojocaru2005@yahoo.co.uk, ld@uttis.ro, metalurgice@yahoo.com, daniela@uttis.ro

ABSTRACT

The differences found between heat fluxes in different areas of the heat treatment equipment workspace, due to energy disequilibrium or due to improper positioning of loading, can cause non-uniform temperatures and heat stress distributions which will impair the quality of heat processing.

In industrial practices, the unilateral heating is often requested for heat processing of certain products and, as a consequence, the heating rate represents a key factor which has to be known and controlled in order to avoid the possible disequilibrium occurring in the distribution of heat stresses.

The paper aims to assess by calculation of asymmetric heating effects of heat treated products occurring by improper operation of heat treatment equipment or by improper positioning of loading in the heat treatment equipment workspace.

KEYWORDS: asymmetric heating, virtual (fictive) product, temperatures distribution, heat stress distribution

1. Introduction

The operating regimes of heat treatment equipment can be various so that the selection of optimal heat treatment variant can be realized in correlation with the load geometry characteristics and with the load material physical characteristics: the aim is to ensure a high heating rate (maximum admissible) and consequently safe operation and quality products.

Independently of the selected heat treatment regime, the positioning of parts/loading in the heat treatment equipment workspace has to be realized so as to ensure a balanced distribution of the property carriers fluxes of convective type (macroscopic associations and aggregates, turbions, fluid currents) or radiant type (photons, energy quanta) [1] to every load sides surface element.

$$\mu = \frac{S}{X} = \frac{J_1}{J_1 + J_2} \qquad (1)$$

When special fans, screens or other means for gas directing are available in order to ensure forced circulation of the working atmosphere with a view of heating intensification [2-4], the possibility of non-uniform heat fluxes distribution is also enhanced.

The differences found between the heat fluxes on load side surfaces generate asymmetric heating of load [5-8] and cause improper distribution of heat stresses on the parts/load section.

To estimate these effects, an asymmetric coefficient of heating, μ, with the following expression will be taken into consideration [5, 6] if $J_1 \geq J_2$ (eq. 1) or if $J_1 \leq J_2$ (eq. 2):

$$\mu = \frac{X - S}{X} = \frac{J_1}{J_1 + J_2} \qquad (2)$$

where: S - is the calculation dimension (semi-dimension) of a fictive (virtual) product, where the temperatures and heat stress distributions are uniformly around its symmetry axis and its symmetry is identical with that of the real product (plane, cylindrical or spherical); X - is the real specific dimension of the product which will be heat processed; J_1, J_2 - are heat flux values on side surfaces of heat processed product which determine the

temperatures and the evolution of heat stresses in fictive (virtual) products, after well-known calculation methodology [4, 5, 9-11], which suppose uniform distribution on heat fluxes on their side surfaces. Then, the results obtained by calculation for the virtual product can be extrapolated in the real product in order to determine the real distribution of temperatures and heat stresses in it.

In industrial practices, unilateral heating is often requested for heat processing of certain products, such as spherical large tanks. For these products, the heating rate represents a key factor which has to be known and controlled in order to avoid possible disequilibrium occurring in heat stress distribution.

2. Research methodology

The research aimed to theoretically substantiate the proper determination of uniform temperature distribution in the workspace of heat treatment equipment as well as to demonstrate that energy disequilibrium can strongly impair the heat processing results even starting from the first stage of heat processing of material-heating.

The heating of a product with plane symmetry (with temperature close to that of the ambient) introduced in a medium which maintains constant temperature on the heating time Tc = ct = 920 °C has been analyzed. Products have been considered to be made of steel with mean chemical composition of 0.15%C, 6%Cr, 0.5%Mo (~ C15E, acc. to SR EN 10084-00) such as heating at this temperature corresponds to the requirements of the normalizing step.

The mean thermo-physical characteristics of this steel in the temperature range of 20÷890 °C (austenitizing temperature) are: λ=58 W/m·K, a = 0.045 m^2/h, $\beta = 13.1 \cdot 10^{-6}$ K^{-1}, $E = 20.58 \cdot 10^4$ MPa [12]; concerning the heat transfer characteristics from the medium to the product surface, the global coefficient of heating transmissivity by convection and radiation is α=193.3 W/m^2·grd. The following possible situations have been considered for analysis:

a) the furnace is perfectly energy balanced and heat flux distribution on side surfaces of product ($J_1 = J_2$, on the direction of Ox axis, $\mu = 0.5$) is uniform;

b) the furnace is energy unbalanced and differences between the heat fluxes measured on different directions are possible; two extreme situations (corresponding to the end values of the interval (0÷1) related to the bilateral heating) have been considered;

b_1) $J_1 < J_2$; $J_2 \sim 2.7J_1$, which corresponds to an asymmetry coefficient of $\mu \sim 0.27$, close to the limit value of bilateral heating ($\mu = 0$ represents the limit condition for initiation of unilateral heating $J_1 = 0$, acc. to eq. 2);

b_2) $J_1 > J_2$; $J_1 \sim 4J_2$, which corresponds to an asymmetry coefficient of $\mu \sim 0.8$, very close to the limit value of bilateral heating ($\mu = +10$ represents the limit condition for initiation of unilateral heating, $J_2 = 0$, acc. to eq. 1).

The calculation aimed to determine the distribution of temperatures and heat stresses in the metallic product with plane symmetry (X = 600 mm), in the part of non-stationary regular regime of heating in the medium with constant temperature ($t \geq 0.3(X/2)^2/a$), considering a perfect isotropic product and a heat transfer in one direction (the product has not received or not released heat on the other two directions). The calculation algorithm of the distribution of temperatures and heat stresses in the real metallic product, with plane symmetry, is the following:

- determination of the heating asymmetry coefficient, μ, starting from the conditions requested to the heat fluxes ratio, measured on the heat transfer direction;
- determination of the specific calculation dimension of the fictive (virtual) product: $S = \mu X$; this product has one, or both sides surface in common with those of the real product. The virtual product has been identified with the real product when the asymmetry coefficient is $\mu = 0.5$.
- determination of the temperatures and heat stress distributions in the virtual product with plane symmetry and with the specific dimension S. Temperature distribution has been determined by using the graphical expressions of criterial solutions of heat conductivity differential equation obtained by solving in the conditions limit of III order and/or the tabular values of Russel [5, 6, 9, 11]. Heat stress distribution has been determined by using the graphical expressions of the solutions obtained by criterial solving [5, 6, 11].

It has to be considered that the distribution of the temperatures within the virtual product is symmetrical in relation to its symmetry axis, but subsequently, by extrapolation in the real product, this distribution becomes asymmetrical in the case of an asymmetry coefficient of $\mu \neq 0.5$. In the case of bodies which are strongly anisotropic or where the heating effect is significant on the other directions, the calculation procedure can be repeated similarly, the temperatures and heat stress distributions in the product volume resulting from the distributions on each transfer direction.

3. Assessment of asymmetry effects of heat flux distribution. Results and analysis

For uniform distribution of heat fluxes within the workspace of the heat treatment equipment (energy balanced), the temperatures and heat stresses (extension stresses in the product center and compressive stresses to the surface zone) are uniformly distributed on the product section (Fig. 1) while the heat gradient on product section registers a decrease as well as the level of the heat stresses. The product is "massive" from the point of view of its thermal-technical behavior (Bi = 1.0) and the calculation of the temperature distribution (using the graphical expressions of the criterial solutions and the tabular values calculated by Russel) in non-stationary regular regime, $t \geq 0.3(X/2)^2/a \geq 0.6$ h, has led to the following values (Table 1, Fig. 1).

Table 1. *Calculated values of the temperatures in different micro-volumes of the product section with the calculation dimension S=300 mm, heated in the furnace with Tm = ct= 920 °C (Bi = 1.0, μ = 0.5)*

x/S	0	0.5	0.8	1.0	0	0.5	0.8	1.0	0	0.5	0.8	1.0
t, h, Fo	1.0 h, Fo = 0.5				3.0 h, Fo = 1.5				8.0 h, Fo = 4.0			
Θ	0.774	0.703	0.597	0.504	0.369	0.335	0.285	0.240	0.058	0.0527	0.0448	0.0378
T, °C	223.4	287.3	382.7	466.4	587.9	618.5	663.5	704	867.8	871.4	879.6	885.98
ΔTm, °C	243 °C				116.1 °C				18.18 °C			

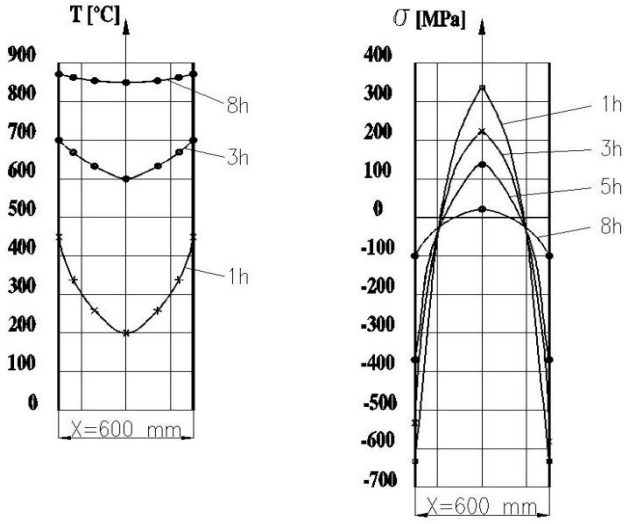

Fig. 1. *Distribution of temperatures and heat stresses in the heat processed product (plate with effective thickness X = 600 mm), heated in a medium with constant temperature, Tm = 920 °C, in the conditions of a symmetric distribution of heat fluxes (Bi = 1.0, μ = 0.5, $J_1 = J_2$)*

Table 2. *Calculated values of heat stresses in different micro-volumes of the product section with the real dimension X=600 mm, heated in the furnace with Tm = ct = 920 °C (Bi = 1.0, μ = 0.5)*

T, h, Fo	1 h, Fo = 0.5		3 h, Fo = 1.5		5 h, Fo = 2.5		8 h, Fo = 4	
x/[X/2]	0	1	0	1	0	1	0	1
f	-0.1	+0.18	-0.07	+0.17	-0.05	+0.11	-0.01	+0.03
σ, MPa	+346.5	-623.7	+242.5	-589	+173.2	-381.1	+34.64	-103.9

With regard to the heat stresses, their values can be calculated (Table 2, Fig. 1) starting from the criterial solution of the heat conductivity equation obtained by solving in condition limits of 3rd order and replacing the obtained result in the equation which gives the relation between the heat stresses and deformations implied (rel. 3). Thus, for the situation taken into consideration (asymmetric heating), different data was obtained.

The analysis of temperatures and heat stresses distributions on the section of the products which has been heated symmetrically (μ = 0.5) in the medium

with constant temperature has led to the following conclusions:

- the temperatures and heat stress distributions are absolutely symmetrical around the symmetry axis of the real product;

- the heat gradient maximum value on the product section (between its surface and center) is attained in the first moments of the initiation of the nonstationary common regime and does not exceed 250 °C;

- the heat stresses are compressive in surface and extension stresses in the product center; those of extension which are extremely dangerous are permanently under steel yield point, independently of temperature (Fig. 1, Fig. 2).

The disequilibrium of heat treatment equipment, indicated by the heat flux differences on the symmetrically opposite parts of the heat processed products/loads, determines a heating asymmetry the intensity of which increases with the increase of these differences.

When the asymmetry coefficient is about 0.27 (corresponding to the analyzed situation), thus when the heat flux from a sense of the direction of heat transfer becomes about two times higher than that occurs from the opposite sense, the asymmetry is high, the regime is not stabilized and regular (the dependence of the temperature on coordinate and time is relatively simple and poor influenced by the initial temperature distribution) and it is initiated in this new situation after a longer time ($t \geq 1.279$ h) by comparison with the previous case of the symmetrical heating ($t \geq 0.6$ h), because the semi-dimension of the virtual body is higher by comparison with that of the real body (S = 0.438 m, comparatively with X/2=0.3 m).

The calculation concerning the new distribution of temperatures (Table 3) and the heat stresses (Table 4), performed on this specific case of virtual product with S = 0.438 m, also massive by point of view of thermal-technical behavior (Bi = 1.46), have confirmed the significant effect of the disequilibrium of heat stresses and, more importantly, the fact that the distribution of heat stresses is extremely non-uniform in relation with the symmetry axis of the product which has been heat processed.

$$\frac{\sigma(1-\nu)}{E}\cdot\frac{1}{\beta(T_0-T_m)}=f\left(\frac{at}{\left(\frac{X}{2}\right)^2};\frac{\alpha\frac{X}{2}}{\lambda};\frac{x}{\frac{X}{2}}\right) \quad (3)$$

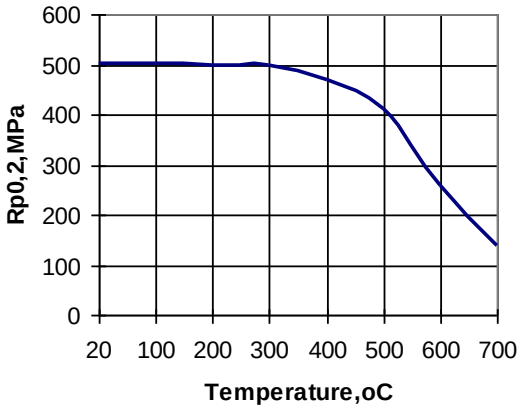

Fig. 2. *Dependency of yield strength $Rp_{0.2}$ on temperature, for steel with 0.15%C, 6%Cr and 0.5% Mo* [13]

Table 3. *Calculated values of the temperatures in different micro-volumes of the product section with the calculation dimension S = 438 mm, heated in furnace with Tm = ct = 920 °C (Bi = 1.46, μ = 0.27)*

x/S	0	0.7	1.0	0	0.7	1.0	0	0.7	1.0	0	0.7	1.0
t, h, Fo	2 h, Fo ~ 0.47			4 h, Fo = 0.936			8 h, Fo = 1.872			10 h, Fo = 2.34		
Θ	0.77	0.55	0.42	0.46	0.37	0.25	0.18	0.17	0.11	0.12	0.1	0.063
T, °C	227	425	542	506	587	695	758	767	821	812	830	863.3
ΔTm, °C	315			189			63			51.3		

Notice that, in this new case corresponding to the asymmetric heating, the explanation of heat stress values becomes possible by using calculation relation (rel. 4) and graphical expressions (graphical expression corresponding to the function Φ[μ;x/(X/2)], rel. 5) [5, 6] different by those used in the case of symmetric heating.

$$\frac{\sigma(1-\nu)}{E}\cdot\frac{1}{\beta\Delta T_m}=\Phi\left(\mu,\frac{x}{X/2}\right) \quad (4)$$

where:

$$\Phi\left(\mu,\frac{x}{X/2}\right)=\left[\frac{1}{3\mu^2}-\frac{1}{\mu}-\frac{\left(\frac{1}{2}\cdot\frac{x}{(X/2)}+\mu-\frac{1}{2}\right)^2}{\mu^2}+1\right] \quad (5)$$

and ΔTm represents the maximum temperature difference between the surface and center of virtual product which has been determined at a certain time.

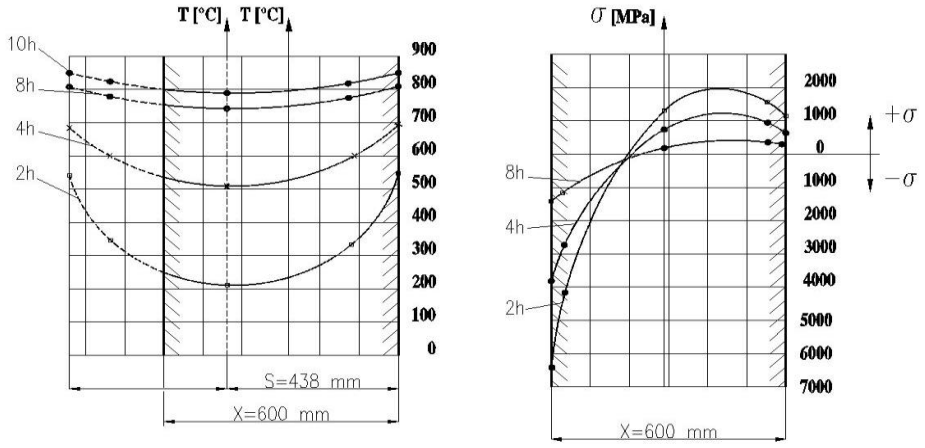

Fig. 3. *The distribution of heat stresses and temperatures in the heat processed product (plate with the effective thickness X = 600 mm and semi-dimension of fictive product S = 438 mm), heated in a medium with constant temperature, Tm = 920 °C in the case of asymmetric distribution of heat fluxes (Bi = 1.46, μ = 0.27, $J_1 < J_2$)*

Table 4. *The calculated values of heat stresses in different micro-volumes of the product section with real dimension, heated in furnace with Tm = ct = 920 °C (Bi = 1.46, μ = 0.27)*

x/(X/2)		0	+0.8	-0.8	+1	-1
t = 2.0 h	**Φ**	+1.144	+1.473	-3.571	+0.869	-5.441
	σ, MPa	+1386	+1786.4	-4330.7	+1053.8	-6598.5
t = 4.0 h	**Φ**	+1.144	+1.473	-3.571	+0.869	-5.441
	σ, MPa	+831.6	+1071.6	-2598.7	+631.2	-3957.6
t = 8.0 h	**Φ**	+1.144	+1.473	-3.571	+0.869	-5.441
	σ, MPa	+272.2	+357.2	-866.2	+210.4	-1319.2
t = 10.0 h	**Φ**	+1.144	+1.473	-3.571	+0.869	-5.441
	σ, MPa	225.7	+290.8	-705.4	+171.3	-1074.2

The distribution of heat stresses in the real product, which has been asymmetrically heated, with the symmetry coefficient of μ = 0.27, close to the limit conditions of the bilateral heating, is extremely inconvenient in relation to its integrity: the very high extension stresses on one of its sides of about 1786.4 MPa (much higher than the yield point of the product steel - Fig. 2) at 60 mm from surface (x/(X/2)= +0.8) and the extremely high compressive stresses on the other side of the product, starting with the first moments of the initiation of the non-stationary regular regime will certainly affect the integrity of the product from the heating stage (obviously in the above mentioned conditions). Another extreme situation taken into analysis is determined also by major differences between the values of heat fluxes, $J_1 \sim 4J_2$, differences which ensure a high heating asymmetry degree μ = 0.8.

The nonstationary regular regime is installed in this new situation for S = 0.48 m (semi-dimension of virtual product) after more than 1.536 h.

The calculation concerning the distribution of temperatures (Table 5) and heat stresses (Table 6) in this new hypothetical situation on a product which is also massive from the thermal-technical point of view (Bi = 1.6), have been performed in accordance with the algorithm mentioned previously.

In this new heating asymmetry case, the stress distribution is also non-uniform, with high extension stresses on one product side and extremely compressive high on the other product side.

It is true that the maximum extension stress calculated after 2 h from the beginning of the heating process has the maximum value ~ 400 MPa in the zone which is highly strained (at x/(X/2) ~ 0.8) and is below the yield point at the temperature related to this zone after this heating time (~440 °C, after 2 h). However, it is also very probable that during non-regular non-stationary regime (t << 1.536 h), therefore close to the moment of charge loading in the furnace, the expansion stresses level from the zones which are in the vicinity of the surface to be much higher than the yield point and thus the integrity of the product to be impaired earlier.

Table 5. *Calculated values of temperatures in various micro volumes in the product section with the calculation dimension S = 480 mm, heated in furnace with Tm = ct = 920 °C (Bi = 1.6, μ = 0.8)*

x/S	0	0.7	1.0	0	0.7	1.0	0	0.7	1.0	0	0.7	1.0
t, h, Fo	2 h, Fo ~ 0.4			4 h, Fo = 0.8			7.68 h, Fo = 1.5			10.24 h, Fo = 2		
Θ	0.78	0.644	0.4	0.52	0.42	0.26	0.27	0.23	0.118	0.16	0.13	0.09
T, °C	218	340.4	560	458	542	686	677	713	814	776	803	839
ΔTm, °C	342			228			137			63		

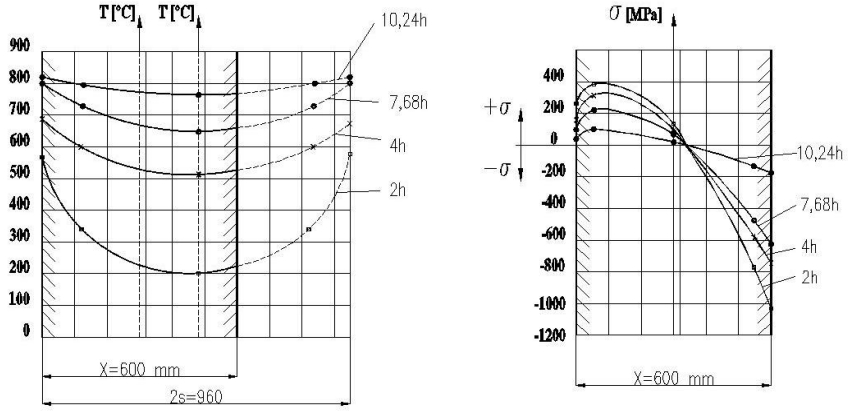

Fig. 4. *The temperatures and heat stresses distributions in the heat processed product (plate with effective thickness X = 600 mm and fictive product semi-dimension S = 480 mm), heated in medium with constant temperature, Tm = 920 °C for asymmetric distributions of heat fluxes (Bi = 1.6, μ = 0.8, $J_1 > J_2$; $J_1 \sim 4J_2$)*

Table 6. *Calculated values of heat stresses in different micro volumes of product section with real dimension X = 600 mm, heated in furnace with Tm = ct = 920 °C (Bi = 1.6, μ = 0.8)*

x/(X/2)		0	+0,8	-0.8	+1	-1
t = 2.0 h	**Φ**	+0.15	-0.56	+0.3	-0.81	+0.21
	σ, MPa	+197.5	-737.3	+395	-1066.5	+276.5
t = 4.0 h	**Φ**	+0.15	-0.56	+0.3	-0.81	+0.21
	σ, MPa	+135	-504.5	+270.3	-729.7	+189.2
t = 7.68 h	**Φ**	+0.15	-0.56	+0.3	-0.81	+0.21
	σ, MPa	+113.7	-424.7	+227.5	-614.3	+159.3
t = 10.24 h	**Φ**	+0.15	-0.56	+0.3	-0.81	+0.21
	σ, MPa	+36.4	-135.8	+72.65	-196.4	+51

4. Conclusions

The energy disequilibrium within the heat treatment equipment for the heat processing of metallic products can cause major heating asymmetry with very severe consequences on the distribution of heat stresses on the products section. It is compulsory to perform permanent and rigorous control of temperature within the heat treatment equipment so that the temperature differences occurring between different zones of the working space be known and kept at minimum level. The situations considered for analysis obviously represent extreme situations. At lower differences between the heat fluxes, the asymmetry coefficients have values close to μ = 0.5 (which corresponds to the energy balanced state), but there are also temperatures and non-uniform distributions of heat stresses that can cause deformation and even deterioration of the heat processes products/load.

In the case of unilateral heating, when requested, a rigorous control of the heating rate has to be performed so as the temperature evolution in the heated wall to avoid unusual distribution of temperature and heat stresses that can cause undesired effects.

Acknowledgement

The work has been funded by the Sectoral Operational Programme Human Resources Development 2007-2013 of the Ministry of European

Funds through the Financial Agreement POSDRU187/'1.5/S/155536.

References

[1]. W. H. McAdams, *Transmision de la Chaleur*, Ed. DUNOD, Paris, 1964.
[2]. J. H. Brunklaus, *Cuptoare industriale (Industrial Furnaces)*, Editura Tehnică, Bucureşti, 1977.
[3]. C. Samoilă, L. Drugă, *Cuptoare şi instalaţii de încălzire (Heating furnaces and installations)*, Ed. Didactică şi Pedagogică, Bucureşi, 1985.
[4]. C. Samoilă, L. Drugă, *Tehnologii şi instalaţii moderne de încălzire în metalurgie (Modern heating technologies and installations in metallurgy)*, Ed. Tehnică, Bucureşti, 1987.
[5]. N. Iu Taiţ, *Tehnologhia nagreva stali*, Metalurghizdat, Moskva, 1962.
[6]. M. Cojocaru, M. Târcolea, *Modelarea interacţiunilor fizico-chimice ale produselor metalice cu mediile*, (*Modelling of the phsico-chemical interaction of the metallic products*), MATRIX ROM, Bucureşti, 1998.
[7]. W. Aung, L. S. Fletcher, V. Semas, *Developing laminar free convection between vertical flat plates with asymmetric heating*, in International Journal of Heat and Mass Transfer, vol. 15, Issue 11, p. 2293-2304, 1972.
[8]. Y. Demirel, B. A. Abu-Al-Saud, H. H. Al-Ali, Y. Makkawi, *Packing size and Shape effects on forced convection in large rectangular packed ducts with asymmetric heating*, in International Journal of Heat and Mass Transfer, vol. 42, issue 17, p. 3267-3277, 1999.
[9]. A. I. Pehovici, V. M. Jidkih, *Rasciotî teplovogo tejima tveordîh tel*, Izd. Energhia, Leningrad, 1976.
[10]. L. S. Kaţevici, *Teoria teploperedaci i teplovîie rasciotî electriceskih pecei*, Izd. Energhia, Moskva, 1977.
[11]. ***, *Tratat de Ştiinţa şi Ingineria materialelor*, vol. VI - Proiectare-Calitatea produselor - Materiale speciale-Inginerie economică metalurgică, *(Book of Materials Science and Engineering, vol. VI, Design – Products Ouality – Special Materials – Economic metallurgical engineering)*, Editura AGIR, Bucureşti, 2014.
[12]. ***, *Tabliţî fiziceschih velicin*, Spravocinik, Atomizdat, Moskva, 1976.
[13]. ***, *Metallovedenie i termiceskaia obrabotka stali*, vol. I, Spravocinik, Moskva, 1961.

THE ANNALS OF "DUNAREA DE JOS" UNIVERSITY OF GALATI
FASCICLE IX. METALLURGY AND MATERIALS SCIENCE
N°. 1 - 2016, ISSN 1453 – 083X

ASPECTS REGARDING THE IMPACT OF ENERGY RECOVERY FROM DOMESTIC WASTE ON ATMOSPHERE

Adrian LEOPA, Anca SERBAN
"Dunarea de Jos" University of Galati, Faculty of Engineering and Agronomy, Braila
e-mail: adrian.leopa@ugal.ro, anca.serban@ugal.ro

ABSTRACT

The issue of domestic waste neutralization appeared with human civilization but got new dimensions in the context of the present consumer society. The diversity and increasing quantity of domestic waste imposed finding new methods for its neutralization, grouped into two categories, namely recycling and recovery. In the category of domestic waste recovery methods, incineration is mentioned among others. The main drawback of the incineration process is air pollution, which is present when the implementation of gaseous pollutant retention solutions at the source generation is avoided. In order to identify the areas that are potential sources of pollution, the present paper focuses on the dispersion modelling of gaseous pollutants from domestic waste incineration.

KEYWORDS: domestic waste, incineration, modelling, atmosphere

1. Introduction

The amount and complexity of waste make them a genuine challenge for any modern society concerning the identification of neutralizing solutions according to environmental protection standards.

The amount of waste worldwide generated is increasing due to the population growth of 7.3 billion in 2015 compared to 2 billion in 1927, but also due to policies encouraging excessive consumption [1]. Although some sociologists affirm that a high consumption level ensures larger production and thus increases the number of employees, this trend contradicts the primary resource conservation principle. Beyond this controversy on the population's moderate or excessive consumption, the problem of consumption waste neutralization remains topical.

The waste complexity derives from the plurality of substances and materials discovered in scientific research activity in various fields. For instance, according to ChemID*plus* database, in chemical industry alone about 408,898 compounds are known. This requires from the scientific community to identify some waste treatment and neutralization solutions (in particular, for industrial ones) specific to their composition.

Normally, when domestic waste removal is done selectively, the waste should have a low toxicity effect on the environment. In Romania, environmental education being still in an early stage, the infrastructure design for waste recycling is not 100% operational and the domestic waste contains toxic or potentially recyclable elements. Thus, in domestic waste composition one can find recyclable waste such as plastic materials, glass, paper and cardboard, aluminum and steel cans, etc. The dangerous waste includes batteries, residues of chemical substances used in households (nail polish, paint, diluents), spray tubes, etc.

The Eco-Rom Packaging firm, specialized in waste recycling in Romania, carried out a one year experimental study in order to establish precisely the waste composition in urban and rural areas Fig. 1 [3]. Figure 1 shows the important recycling potential of domestic waste: 52.32% in rural areas and 38.02% in urban areas. According to the Sustainable Development concept, the recovery of recyclable components from urban waste is an obligation for the current generation in order to avoid prejudicing the future generations.

In Romania, the main way of urban waste elimination is storage. Although this method is less expensive than others it also has some disadvantages such as occupying land that could be extended to other activities, the generation of greenhouse gaseous emissions, low density waste spreading to adjacent areas due to airflows, etc.

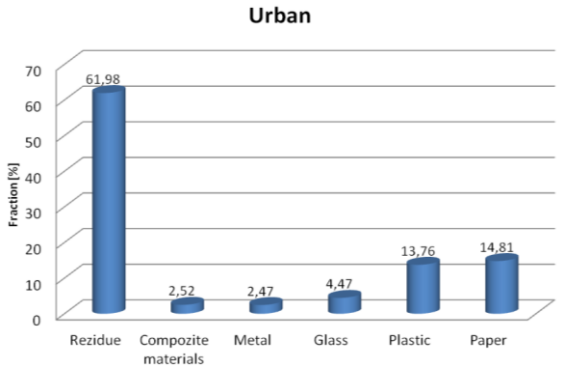

a. in urban areas

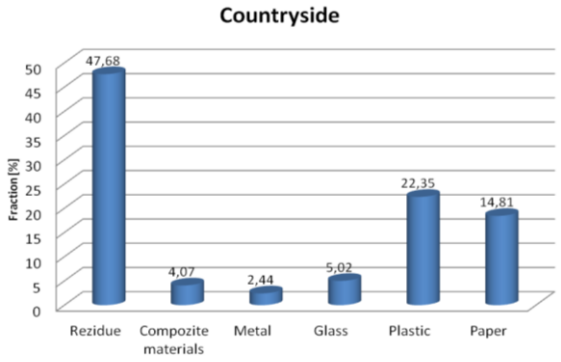

b. in the countryside

Fig. 1. *Waste composition*

A reduction of municipal waste deposited in landfills consists of the recovery of recyclable components, but a removal of 80-85% is achieved only by thermal treatment.

2. Public waste incineration

The thermal treatment of public waste can be achieved by several methods among which we recall: plasma pyrolysis (PGM - Plasma Gasification Melting), incineration and co-incineration [4]. In Romania, the thermal treatment of domestic waste is achieved by co-incineration in cement factories in the clinker production process.

In 2013 in the urban area, each Romanian citizen produced an average amount of 346 kg of domestic waste with a 38.02% recyclable rate; the countryside population produced only 95 kg of domestic waste of which 52.32% is recyclable. Considering that Romania would fulfill its environmental obligations and recycle 50% of the recyclable domestic waste up to 2020, the waste amount that needs to be discharged is a real challenge for the authorities.

Waste incineration is a viable solution for unrecyclable domestic waste removal provided that the best available techniques are implemented (the BATNEEC principle - Best Available Techniques Not Entailing Excessive Costs) for retaining pollutants at source. Placing an incinerator designed for medical waste treatment is a very important issue because its potential abnormal operation and especially in case of damage the equipment should not affect neighboring areas.

3. Evaluation of gaseous pollutant dispersion discharged through the chimney of municipal waste incineration plant

3.1. The INCREST incinerator

As follows from the above, based on the Gaussian model for a continuous source, this study evaluates the atmospheric dispersion of particulate matter generated by an INCREST incinerator designed for the thermal treatment of municipal waste in Braila municipality, Romania.

The thermic balance calculus of the INCREST type incinerator (Fig. 2) [6] was accomplished after the following assumptions:

- the incinerator's location was considered on the old plant platform Celhart Donaris located at 10 km from Braila city;
- the equipment services Braila county population. According to the latest census in 2011, the county population is 304,900 citizens and the municipality 168,300 citizens. Thus, the domestic waste volume generated within the county in one year is 71,208 tons of which 35,604 tons would remain to eliminate if 50% of them would be recycled;
- the incinerator capacity is 34,200 tons/year and the flow is variable depending on the season, in the range of 4-5 tons/hour;

Based on the calculus model of thermic balance presented in [6], the following parameters were found:

- the ash emission rate is Q = 0.44 g/s;
- the air flow evacuated on chimney is V = 2 m^3/s;
- the evacuated gas temperature is 135 ºC.

3.2. Gaussian model for continuous sources

As in [7, 9], the most general mathematical expression of Gaussian dispersion equation for a continuous emission source is:

$$X(x,y,z,H)=\frac{Q}{2\pi u\sigma_y\sigma_z}\exp\left[-\frac{y^2}{2\sigma_y^{\,2}}\right]\cdot \cdot\left\{\exp\left[-\frac{(z-H)^2}{2\sigma_z^{\,2}}\right]+\exp\left[-\frac{(z+H)^2}{2\sigma_z^{\,2}}\right]\right\} \quad (1)$$

As the interest lies on the degree of pollution on people, we considered the height z = 0 (ground level) that leads to a simplified equation as follows:

$$X(x,y,0,H)=\frac{Q}{2\pi u\sigma_y\sigma_z}\cdot \cdot\exp\left[-\frac{y^2}{2\sigma_y^{\,2}}\right]\exp\left[-\frac{H^2}{2\sigma_z^{\,2}}\right] \quad (2)$$

where: X (x, y, z, H) – is the concentration of the pollutant in the atmosphere, g/m^3; u – wind speed, u = 4-6 m/s, as in Fig. 2; σ_y, σ_z - the parameters of the dispersion or standard deviation; x - distance downwind to chimney, x = 2000 m; y - wind direction transverse distance from the center line of the pollutant plume, m; z - the height in the vertical direction from the ground, m; H - effective height of the pollutant plume, m.

$$H = h + \Delta h \quad (3)$$

h – gas exhaust chimney height, h = 50 m; Δh - pollutant plume ascension.

Determining the thickness of the pollutant plume Δh using the mathematical relation:

$$\Delta h=\frac{1.6F^{1/3}x^{2/3}}{u} \quad (4)$$

where: F - Buoyancy flow.

The Buoyancy flow is calculated with:

$$F=\frac{g}{\pi}V\left(\frac{T_s-T_a}{T_s}\right) \quad (5)$$

where: g – acceleration of gravity; V – gas volume to chimney, V = 2 Nm^3/s; T_s – exhaust gas temperature to chimney; T_s = 135 °C; T_a – ambient temperature, T_a = 25 °C.

In order to determine the dispersion parameters (Briggs model), the relations developed by Caraway [9] were used:

$$\sigma_y = cx^d \quad (6)$$

where: c, d - are coefficients that depend on atmospheric stability and distance of the valuation (chosen tabular [9]); x - distance for which the valuation is made, x = 2000 m.

$$\sigma_z = ax^b \quad (7)$$

where: a, b - are coefficients that depend on atmospheric stability and distance of the valuation (chosen tabular [9]); x - distance for which the valuation is made.

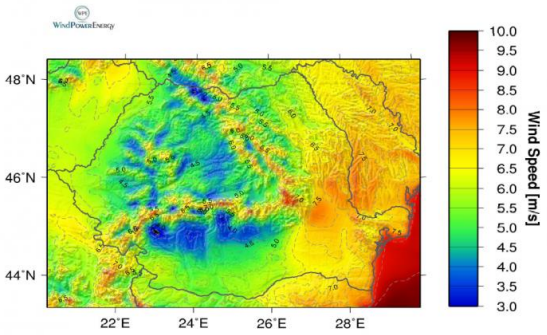

Fig. 2. *Wind map of Romania* [8]

The pollutant dispersion charts resulting from domestic waste incineration (in our case the pollutant being ash) were drawn up for different atmospheric conditions in order to identify the areas affected by pollution. Thus several iterations of the Gaussian model were achieved for a continuous source in the following numerical combinations of the atmospheric parameters:

- the wind speed 4 m/s;
- the atmospheric stability class E, nighttime with partly cloudy sky;
- the atmospheric stability class C, daytime with moderate insolation;
- the wind speed 5 m/s,
- the atmospheric stability class D, nighttime with partly cloudy sky;
- the atmospheric stability class C, daytime with moderate insolation;
- the wind speed 6 m/s,
- the atmospheric stability class D, nighttime with partly cloudy sky;
- the atmospheric stability class C, daytime with moderate insolation.

The classification of atmospheric stability is given in Table 1 [9].

The diffusion parameters evaluated using the calculation formulas presented in the paper [9] were integrated in the code source intended to solve the Gaussian equation for a continuous pollution source

that was developed in the programming field Matlab by Holzbecher E. in the paper [10].

Table 1. *The stability classification* [9]

The wind speed on surface (m/s)	Daytime			Nighttime	
	Strong	Mild	Light	Thin covered in clouds or > 4/8 Low nebulosity	< 3/8 nebulosity
< 2	A	A- B	B	-	-
2- 3	A- B	B	C	E	F
3- 5	B	B- C	C	D	E
5- 6	C	C- D	D	D	D
> 6	C	D	D	D	D

a. The ash concentration distribution for a continuous source with assumption of the following conditions: wind speed, v = 4 m/s; the atmospheric stability class E, nighttime, partly cloudy sky, Fig. 3.

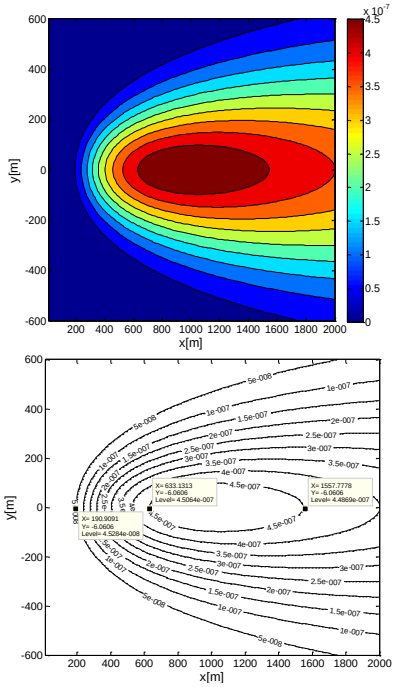

Fig. 3. *Gaussian distribution of pollutant concentration for a continuous source*

b. The ash concentration distribution for a continuous source with assumption of the following conditions: wind speed, v = 4 m/s; the atmospheric stability class C, daytime, moderate insolation, Fig. 4.

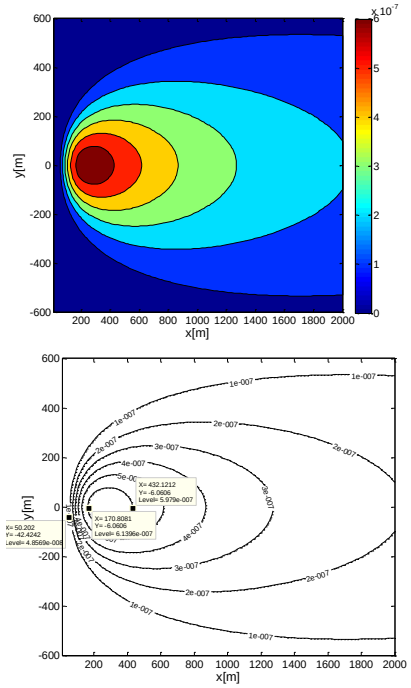

Fig. 4. *Gaussian distribution of pollutant concentration for a continuous source*

c. The ash concentration distribution for a continuous source with assumption of the following conditions: wind speed, v = 5 m/s; the atmospheric stability class C, daytime, moderate insolation.

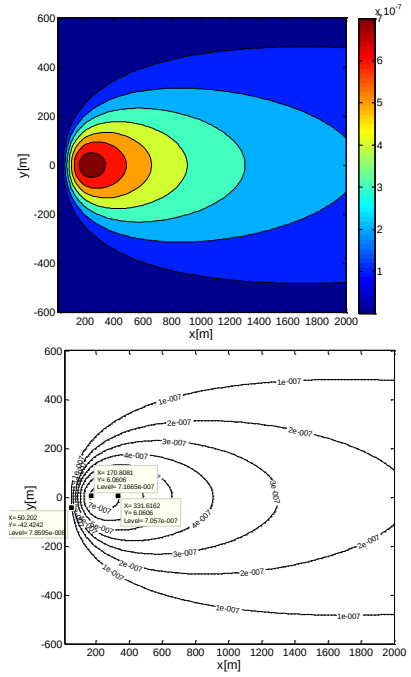

Fig. 5. *Gaussian distribution of pollutant concentration for a continuous source*

d. Pollutant concentration distribution for a continuous source for the next conditions: wind speed, v = 5 m/s; the atmospheric stability class D, nighttime, partly cloudy sky.

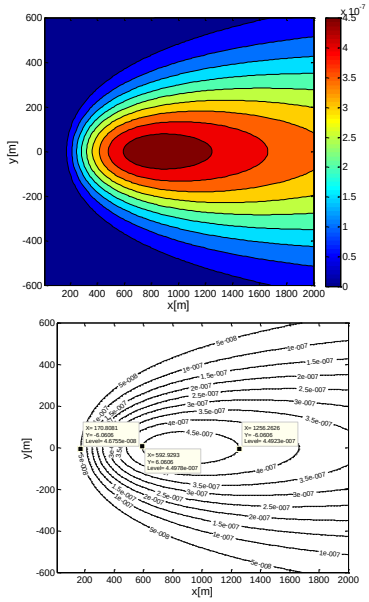

Fig. 6. *Gaussian distribution of pollutant concentration for a continuous source*

e. Pollutant concentration distribution for a continuous source for the next conditions: wind speed, v = 6 m/s; the atmospheric stability class D, nighttime, partly cloudy sky.

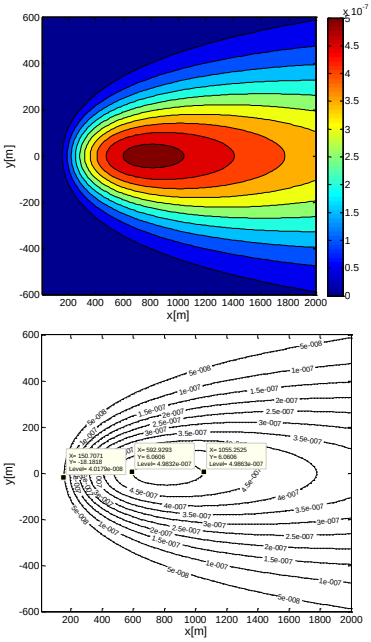

Fig. 7. *Gaussian distribution of pollutant concentration for a continuous source*

f. Pollutant concentration distribution for a continuous source for the next conditions: wind speed, v = 6 m/s; the atmospheric stability class C, daytime, moderate insolation.

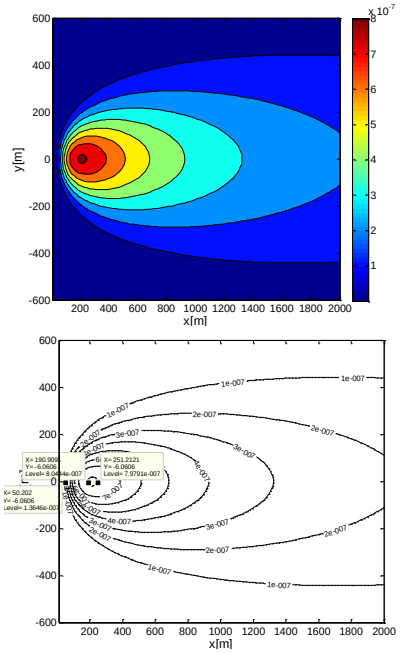

Fig. 8. *Gaussian distribution of pollutant concentration for a continuous source*

Chart analyses defined for the same wind speed and different atmospheric stability class outlined the following issues:

- the ground level pollution appears to the gases discharge point at a minimal distance of 50 m nighttime, respectively of 190 m daytime;
- the pollutant maximum concentration area begins at a distance of 633 m nighttime, respectively of 170 m daytime;
- the differences between the distances provided above for both moments of the day is explained by the different weather conditions. It is noted that during daytime the pollutant tendency is to remain concentrated near the chimney due to insolation.

The maximum concentration of ash released into the atmosphere is of 0.8 µg/m^3. The indicator PM10 (particulate matter with a diameter of up to ten micrometers), according to annex no. 3 of Law no. 104/2011 concerning the ambient air quality, in force since 28 July 2011 (repeals Order MAPM no. 592/2002) has a limit value during the mediation period of 24 hours for human health protection of 50 µg/m^3 (not to be exceeded more than 35 times in a calendar year).

Therefore, there is no exceeding of the limit values imposed by legislation for particulate matter with a diameter of up to ten micrometers.

3. Conclusions

The dispersion analyses of pollutants evacuated from fuel combustion is of great interest for the stage of placing the future industrial facilities because adjacent areas affected by pollution are evaluated for different values of atmospheric parameters. For the industrial units in operation designed for thermal treatment of urban waste, the Gaussian model for pollutant dispersion can also indicate the affected areas in case of incineration system breakdown by identifying the safe location areas of residential neighborhoods.

The study aimed mainly to theoretically evaluate particulate matter dispersion generated by operating a municipal waste incinerator, which can be adapted to dispersion evaluation of other pollutants, such as CO and NO_2.

References

[1]. ***, *Current World Population*, www.worldometers.info.
[2]. ***, *Toxnet - Toxology data network*, http://chem.sis.nlm.nih.
[3]. ***, *EcoRom*, http://ecoromambalaje.ro.
[4]. Marin I., *Procedeul de tratarea a deşeurilor: Incinerarea*, http://greenly.ro.
[5]. ***, *EcoRom*, http://ecoromambalaje.ro.
[6]. Antonescu N., Polizu R., Cândeanu-Muntean V., Popescu M., *Valorificarea energetică a deşeurilor menajere*, Editura Tehnică Bucureşti, p. 146-177, 1998.
[7]. Cuculeanu G., *Gaussian approach of the atmospheric pollutant diffusion*, A patra conferinţă internaţională Efectele crizei globale asupra economiilor în dezvoltare, Bucureşti, 2009.
[8]. Lascu M., *Energie eoliana – harta de vant a Romaniei, potential de 14.000 MW*, http://energielive.ro.
[9]. Allen and Durrenberger, *Gaussian Plume Modelling*, Chemical Engineering, 357, 2003.
[10]. Holzbecher E., *Environmental Modeling Using MATLAB*, Springer, 2007.
[11]. ***, *Lesson 6 Plume Dispersion and Air Quality Modeling*, http://yosemite.epa.gov.

THE ANNALS OF "DUNAREA DE JOS" UNIVERSITY OF GALATI
FASCICLE IX. METALLURGY AND MATERIALS SCIENCE
N°. 1 - 2016, ISSN 1453 – 083X

ECOTECHNOLOGIES – A MAJOR ROUTE FOR DURABLE-SUSTAINABLE DEVELOPMENT IN THE METAL MATERIALS INDUSTRY

Avram NICOLAE, Claudia Ionela DRAGAN*, Catalin Stefan GRADINARU, Valeriu RUCAI, Maria NICOLAE
Center for Research and Eco-Metallurgical Expertise, Politehnica University of Bucharest
313, Splaiul Independentei, 060042, Bucharest, Romania
e-mail: claudia.dragan@ecomet.pub.ro

ABSTRACT

The paper shows that the durable and sustainable development depends on the quality of the events occurring in the convergence area between the natural ecological system (N.E.S.) and the technological system (T.S.) represented by the metal materials industry. The analysis is carried out in the following situations:

- decrease in the level of negentropy (nS) of N.E.S., due to the consumption of natural resources by T.S., and

- increase in the level of entropy (S) of N.E.S., due to the discharge into the environment of the pollutants generated by T.S.

Ecotechnologies constitute a major tool for optimizing the correlations N.E.S.-T.S. Our study proposes a classification of ecotechnologies in four categories, according to their influence on nS and S. The role of ecotechnologies in reducing the environmental entropisation phenomenon is also highlighted.

KEYWORDS: sustainability, durability, ecotechnologies, environmental (neg)entropy

1. Introduction

At present, development is considered a complex process able to optimize the *interactions and interconditionings* found in the convergence areas of the four fundamental systems (*natural-ecological, social, economical and technological*) that make the *eco-socio-economic-technological mega-system (M.S.)*, the actual form in which the *sphere of human existence* manifests itself.

The designing of a new development model must propose qualitative and quantitative improvements regarding the *conception, dissemination and operationalisation of the new knowledge*. The following targets become compulsory:

- to use *multi and interdisciplinary integration tools* so that the new model provide the theoretical framework for understanding the adaptive and evolutionary transformations, i.e. the design and management of new methodological tools [1];

- to achieve the *integration of sectoral knowledge* offered by a wide range of disciplines, in order to understand the integrative events at the mega-system level; within the same framework, it becomes important to use the confirmed theoretical elements of all the partial theories for developing and explaining the organization, complexity, dynamics and evolution of nature [1, 2];

- to replace, especially in engineering, the *gogglewise knowledge* with the *fanwise knowledge* [3].

The new development model is operationalised on the basis of two modern principles of evolution: sustainability and durability.

The **sustainability** refers to the ability of the new development model to *create, sustain and maintain* processes of evolution and adaptation within the eco-socio-economic-technological complexes.

The main item used to make assessments on the system sustainability is the *carrying capacity*, which measures the ability, mainly of the natural-ecological system, to provide the resources and services needed to develop the other systems.

Durability, as a characteristic of the new development model, aims at:

- the co-development potential of the systems through *long-term* adaptive transformations, i.e. also at the *level of future generations*;

- the ability of the systems to be resistant; in this context, it is not about the notion of *resistance* within the mechanical engineering meaning, but about a special form represented by what is called *system resilience*, which measures the system's ability to withstand the action of disturbing items (shock actions). At present, it is considered that the main disturbing item acting in MS is *pollution*;

- the systems' opportunities to develop as *viable entities*.

Environment resilience is another parameter sometimes used to assess durability. It is the *maximum disturbance limit* permissible for an ecosystem, over which this one would cease to operate as environment stabilizer [1, 10].

As a global disturbing item, pollution includes many other disturbing items ($M_{per.}$) whose disturbance limits should not be exceeded. Some of them are mentioned below [11]:

- increase of CO_2 concentration in the atmosphere, which now exceeds 0.033%;
- disappearance of species of living creatures and plants;
- intensification of agriculture by exaggerate use of chemical fertilizers;
- deforestation;
- ozone layer depletion;
- aerosol release into the atmosphere;
- excessive consumption and wastage of freshwater;
- ocean acidification;
- growing volumes of anthropogenic waste disposed into the environment.

From the above context, we note that the society has already gone through the third period of history. Especially after 1950, the world passed from *Holocene* to *Anthropogenic era* (period in which man becomes the main modeller of the natural-ecological system).

The disturbing items, $M_{di.}$, mentioned above, present a *hockey stick* type development (Figure 1).

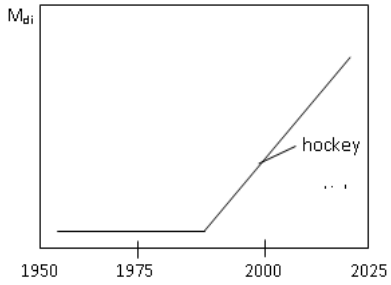

***Fig. 1.** Increase of disturbing items*

The differences between the two principles are also standing out when we take into account the assessment tools. Therefore:

- sustainability is based on carrying capacity, and
- durability is based on system resilience.

It is obvious that a differentiation as the above is not absolute, because there are many areas in which the two principles are intertwined.

Based on the above, we can briefly define the new development model as *that development that meets the needs of the present* (mainly by *sustainability*), *without compromising the ability of future generations* (mainly by *durability*) *to meet their own needs.*

As the new model is unitarily defined and operationalised based on the principles of durability and sustainability, this paper proposes the model to bear the name of ***durable-sustainable development* (D.S.D.)** [4].

2. Materials and products manufactured in metallurgical industry

2.1. Definition of the categories of materials

The **material** is the substance which, through a technological manufacturing process, generates *socially useful goods*. Steel is a material.

The **product** is the object (body) which, through a technological manufacturing process, *acquires social utility*. The steel sheet is a product.

Using the two notions interchangeably is not a serious mistake.

The materials listed below are manufactured in the metallurgical industry.

a) The **primary material (product), M.P.**, is the material subject to a technological manufacturing process. If it is a *complex process*, represented by a flow of more *sequences*, the following items can be found:

- *primary sequential material (product), P.S.M.;*
- *final sequential material (product), I.S.M.*

The steel made within the integrated flow consisting of *ore mine - blast furnace – steel plant - rolling mill* is a sequential primary product. Sometimes, this is referred to as *semi-finished product*. The steel sheet delivered to the beneficiary at the end of the above-mentioned flow is a final primary product.

b) The **pseudo-primary material (product), P.P.M.**, is the material used in the analysed process, but obtained in an adjacent manufacturing flow (cycle). The ferrosilicon used to make steel in the integrated flow is a pseudo-primary material, because

it is obtained in the ferroalloy plant adjacent to the integrated flow.

c) The **secondary material, S.M.**, is the material which, for technological reasons, accompanies the primary material. The following items are included in this category:

- The *by-product, B.P.*, is the secondary material that can be used within the technological flow that generated it. Ingot cut ends and mill scales are examples of by-products;

- The *waste, W.*, is the secondary material which leaves the technological flow that generated it, but has recovery potential, i.e. it can be used in other manufacturing cycles.

There are two categories of waste:

- The *manufacturing waste (technological waste)* is the waste that leaves the primary material manufacturing perimeter. Blast furnace slag is a manufacturing waste;

- The *usage waste (degradation waste)* is the waste generated by using the primary product, due to its degradation (transformation of the primary material into secondary material). Scrap is a degradation waste. The degradation product and the degradation waste must be assessed based on *degradation properties (characteristics).*

- The *residue, R (final waste)* is the secondary material disposed into the environment without usage possibilities. The *disposal* is the deposition of the secondary material into the environment (possibly after a neutralisation treatment) in all the three states of the material:

  - disposal in gaseous state (e.g. emission of CO_2 into the atmosphere);
  - disposal in liquid state (e.g. wastewater discharge);
  - disposal in solid state (e.g. slag dumping).

Pollutants are residues which, by disposal into the environment, have a negative impact on its quality.

The modality of placing the categories of materials into the manufacturing cycles is shown in Figures 1 and 2.

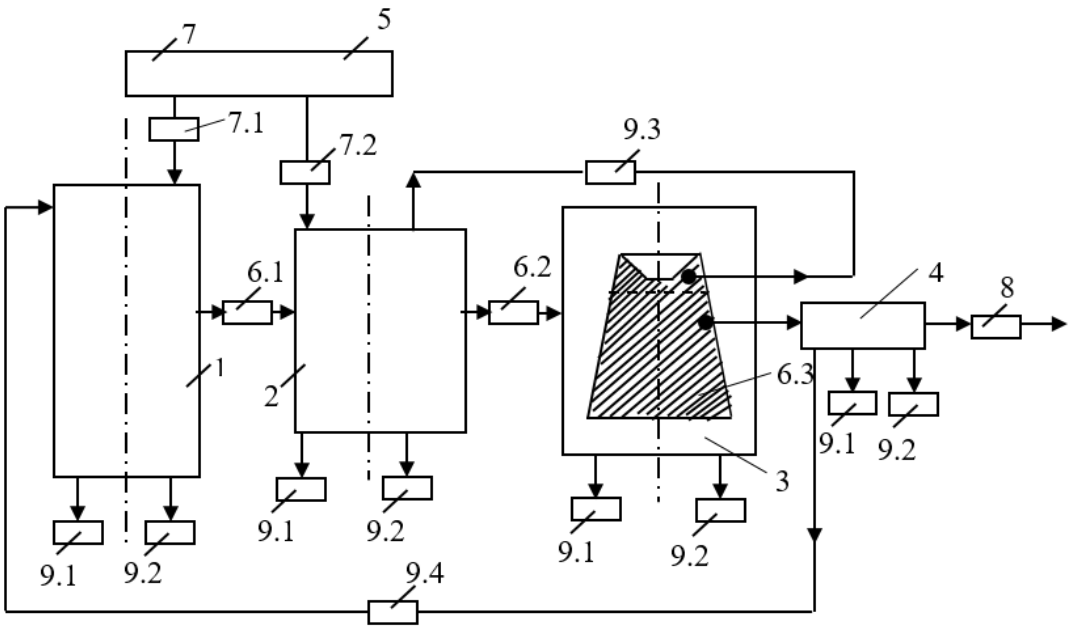

Fig. 1. *Modality of placing materials (product) in a steel-making flow based on ore and coke. 1 - blast furnace; 2 - steel-making furnace; 3 - casting mould; 4 - rolling mill; 5 - facilities for auxiliary (pseudo-primary) materials; 6 - sequential primary materials: 6.1 - pig-iron; 6.2 - steel, 6.3 - ingot (semi-finished product); 7 - pseudo-primary materials: 7.1 – coke; 7.2 – ferroalloys; 8 - final primary material; 9 - secondary materials: 9.1 – waste; 9.2 – residues; 9.3 - by-product (cut ends); 9.4 - by-product (scale briquettes).*
(Note: In this drawing, the perimeters are disproportionate)

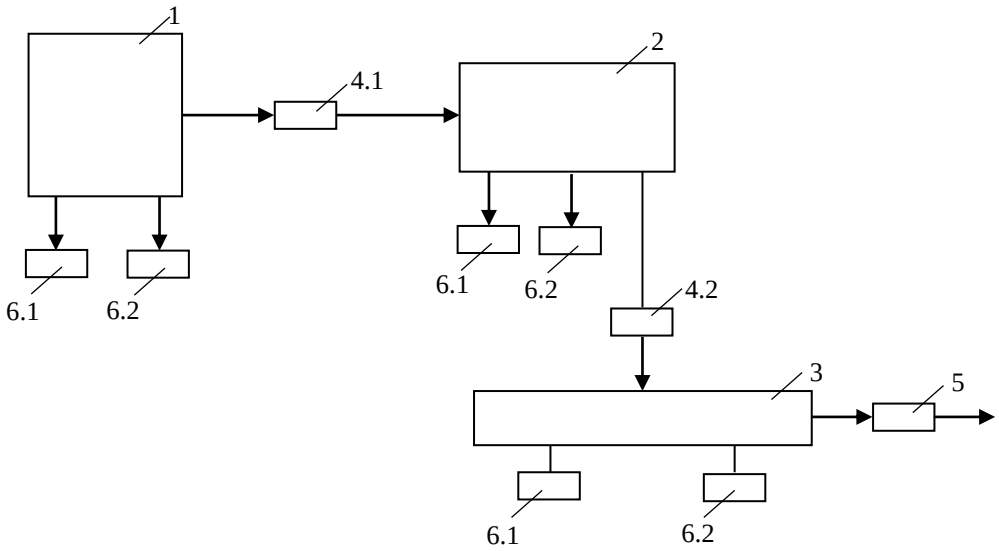

Fig. 2. *Modality of placing the materials (product) in a steel-making flow based on scrap. 1 - EAF; 2 - continuous casting machine; 3 - rolling mill; 4 - sequential primary materials: 4.1 – steel; 4.2 - semi-finished product (billet); 5 - final primary material (steel tubes and pipes); 6 - secondary materials: 6.1 – wastes; 6.2 - residues.*
(Note: In this drawing, the perimeters are disproportionate)

2.2. Characterisation of materials as thermodynamic system element

The technological system of metal materials manufacturing operates as a thermodynamic system (being a high temperature process, it is determined by heat exchange).

The modality of placing the materials into a thermodynamic system is shown in Figure 3.

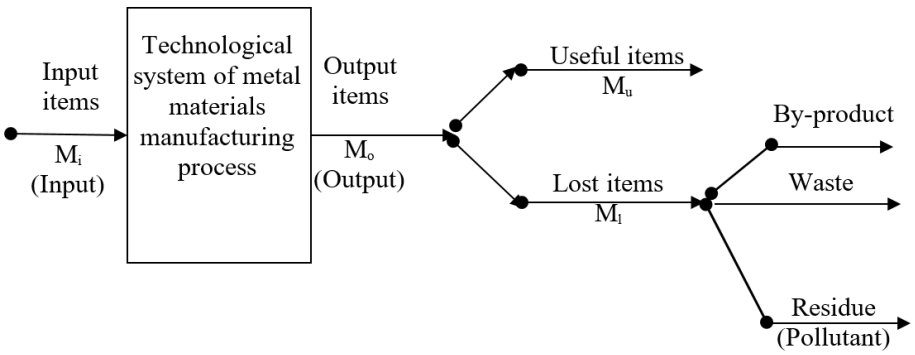

Fig. 3. *Thermodynamic structure of a technological process*

In terms of material balance or energy balance, we are working with:

- *input items*, M_i, represented by natural resources (*n.r.*), which can be:
  - material resources;
  - energy resources (real fuels and energies).
- *output items*, which are:
  - *useful items*, M_u, represented by raw materials;
  - *lost items*, M_l, represented by secondary materials; more specifically, they are:
    - by-products;
    - wastes;
    - residues.

It can be concluded that:

- From the thermodynamic point of view, as residues, *pollutants are lost items*.

- Because, according to the first law of thermodynamics, there are no zero loss systems, it follows that the metal materials manufacturing process is an objectively pollutant process.

- For the same reason as above, pollution projects such as *zero pollution* or *zero waste plant* are not thermodynamically justified, but they must be accepted as targets.

- From the ecological point of view, we are interested in the waste and residues leaving the technological system and being discharged into the environment.

3. (Neg)entropic characterization of materials

The changes in entropy or negentropy may be a possibility to characterise the transformations of materials when they undergo the life cycle (*l.c.*) [12].

Entropy (S) is the thermodynamic parameter that measures *the degree of matter disorder and degradation* in the environment. *The disorder degree and degradation increase* are measured by the entropy increase (*S)*.

The **negentropy (nS)**, or **anti-entropy (aS)**, is the thermodynamic parameter that measures the degree of matter ordering in the environment. The increase of the ordering degree is measured by the increase of negentropy *(nS)*.

Below, we are going to briefly characterise the variation of (neg)entropy when the material undergoes the life cycle.

a) Provision of resources

Resources (e.g. iron ore) represent the matter with a certain degree of ordering, i.e. a certain degree of negentropy $nS_{n.r.}$. It is admitted that underground resources are a low entropy reserve [6, 7]. The consumption of resources has therefore resulted in *lowering the environmental neg(entropy)*.

b) Manufacturing of material (product)

The technological process of material manufacturing results in enhancing the ordering of matter, hence the increase of the material negentropy. For example, we can write that:

$$nS_{steel\ sheet} > nS_{ore},$$

or that the *technological process is a negentropy producer* $nS_{t.p.}$ [5].

Materials engineers are a social category apt to create social neg(entropy).

c) Usage of material

In the use phase, *material degradation* occurs, which means the decreasing of the matter ordering degree.

d) Waste generation and disposal in the environment

Material degradation causes *waste generation*, which is considered a *disordered state of matter* (i.e. entropy carrier), equal to S_R.

Since some waste can be recovered, we are interested in the entropy $S_{R.}$ of the finally disposed wastes.

e) Waste reintegration is a process of matter reordering from the state of secondary material in *resource material*. Therefore, we are speaking about negentropy recovery through reintegrated material, $nS_{r.m.}$. It is also called *reintegration negentropy*.

Environment entropisation, as a process that must be prevented or minimised, is assessed by decreasing its negentropy basin, $(\Delta nS)_{env}$, calculable with the expression:

$$|(\Delta nS)_{env}| = [|nS_{n.r}| + |S_R|] - [|nS_{t.p}| + |nS_{r.m}|] \qquad (1)$$

At the limit, the condition $|(\Delta nS)_{env}| = 0$ should be satisfied. But, the laws of thermodynamics and the history of civilization proved that $|(\Delta nS)_{env}| > 0$, fact that characterizes an *irreversible phenomenon of environmental entropisation* [7, 8].

In reality, there is a situation characterized by the expression:

$$(|nS_{n.r} + |S_R|) > (|nS_{t.p.} + |nS_{r.m}|) \qquad (2)$$

4. About ecotechnologies

The *ways to operationalise the concept of durable-sustainable development* in industry constitute a fundamental component of the activities performed by metallurgical engineers. Practically, the D.S.D. model is a target for optimising the interactions and interconditionings between the natural-ecological (N.E.S.) and technological (T.S.) systems, aimed at maximizing life quality indicators in terms of economic efficiency increase.

Ecotechnologies represent the major vector based on which we can achieve the above objectives, whose content means the minimisation of $(\Delta nS)_{env}$, fact achievable through the minimisation of $|nS_{n.r}|$ & $|S_R|$ and maximisation of $|nS_{t.p}|$ & $|nS_{r.m}|$.

Based on the above assumptions, the possible correlations in the natural-ecological systems (N.E.S.) and technological system (T.S.) are plotted in Figure 4.

There are four situations:

A. The T.S. upstream area represents the N.E.S.-T.S. correlation, defined by the functions of these systems:

- SNE having the function of *basin (supplier) of natural resources;*
- ST having the function of *resource consumer*.

The negentropic content of the environment is decreasing with $nS_{r.n.}$. The correlation optimisation depends on the *environmental sustainability* assessed through the *carrying capacity* in ensuring the resources.

Applying **ecotechnologies** to **minimise the consumption of resources (ETmC)** is the main way of maintaining the carrying capacity of the environment. The *ecotechnologies for preservation and conservation of resources* are specific variants for ETmC.

Preservation is the provision of natural resources over a period as long as possible by minimum consumptions.

Conservation is putting under the ban of any anthropogenic interference within the natural resources perimeter, over a transitional period.

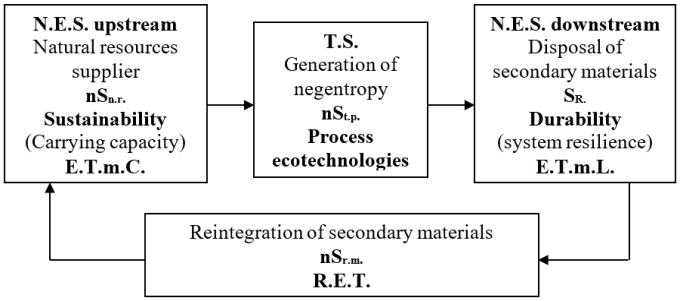

Fig. 4. *Ecotechnological interconditionings between N.E.S. and T.S.*

B. The SN downstream area represents the T.S.-N.E.S. correlation, defined by the functions of these systems:

- T.S. having the function of *pollutant generator*;
- SNE having the function of *takeover, processing and disposal of pollutants*.

Hypo-polluting ecotechnologies are the key industrial methods for optimising the N.E.S.-T.S. interconditionings on the foundation represented by the negative impact exerted by the pollutants.

Hypo-polluting ecotechnologies are the technologies applied to prevent or decrease the *negative impact of the pollutants on the quality of the environment*.

The **ecotechnologies** applied for **minimising the losses (ETmL)** are the industrial-scale operationalisation solution for hypo-polluting ecotechnologies. We adopt this name because, in the material and energy balances, pollutants are *lost quantities* from the T.S. perimeter to N.E.S.

Because ETmL finally concerns pollution, which is the main environment disruptive item, they constitute the major policy to improve the *system resilience* of N.E.S. for the future generations.

C. The intermediate zone

This situation is given by the upstream-downstream bilateral interconditioning, defined by the complex recovery function of reintegration in the industrial circuits of the secondary materials.

The **reintegration ecotechnologies (R.E.T.)** of the secondary materials (especially of the waste) are the major route to accomplish a double purpose:

- improving the N.E.S. carrying capacity (upstream area) by using reintegrated materials as substitutes for the natural resources;
- improving the N.E.S. system resilience (downstream area) by reducing the quantity of polluting waste discharged into the environment.

The positive effect of waste reintegration is assessed through *reintegration negentropy*, $nS_{r.m.}$.
Waste reintegration is carried out through the *3R technologies* (recirculation, recycling, regeneration).

Recirculation is the recovery achieved by reintroducing the materials or secondary energies in the same manufacturing flow. An example of recirculation diagram is shown in Figure 5. The object of recirculation is the *by-product.*

Recycling is the recovery of secondary materials by using them in other manufacturing cycles than those which generated them. An example of recycling diagram is shown in Figure 6.

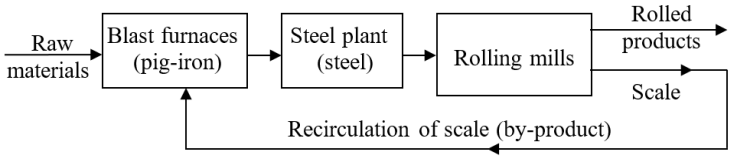

Fig. 5. *Recirculation diagram*

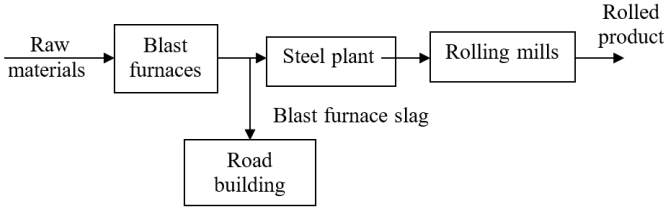

Fig. 6. *Recycling diagram*

The object of recycling is the *waste*.

Regeneration is the process of regaining the original properties of the secondary materials by physical, chemical, thermal or mechanical processing, for reuse in the manufacturing process. Regeneration is compulsorily followed by recirculation or recycling.

Regeneration is a term that should be used with caution, as shown below.

Regarding material resources, it appears that they are renewable. For example, the foundry sand which, after its degradation by use, is reintroduced in the manufacturing process thanks to the *sand regeneration technology*.

Regarding energy resources, the situation is more complicated. As we know from thermodynamics, the energy which follows a cycle of *generation - use - discharge into the environment* finally turns irreversibly into *degraded energy*, spread (dissipated) into the environment as *unusable entropy*. A simple example: In the history of civilization, there was no man, found outside a technological oven, able to take over the energy (heat) discharged into the environment, to regenerate it and to reintroduce it into the plant. We can say that the *dump of the energy (heat) discharged from the oven is the infinite environment*.

We can conclude that energy cannot be regenerated and, therefore, the term *renewable energy* is incorrect. For non-conventional energies, we recommend the term *renewable energies* [9]. This name highlights the fact that, for example, an amount of solar energy is permanently replaced (renewed) by another amount generated by the sun.

D. The technological process perimeter

As shown above, the process is generating negentropy $nS_{t.p.}$. Practically, this means the increase of the *added value*, V_a, through continuous technological processing. It can be writen as

$$nS_{ore} < nS_{steel} < nS_{black\ sheet} < nS_{tin\ sheet} \quad (3)$$

or as

$$V_{a\,ore} < V_{a\,steel} < V_{a\,black\ sheet} < V_{a\,tin\ sheet} \quad (4)$$

It follows that:

$$\Delta V_a = f\left(\Delta nS_{t.p.}\right) \quad (5)$$

Process ecotechnology is the technology which, by advanced technological processing, causes the increase of MS negentropy, reducing therefore the environmental entropisation process.

5. Conclusions

- The current development concept is based on two distinct pillars: sustainability (characterised by the carrying capacity of the environment) and durability (characterised by the environment system resilience), reason why we propose the name of *durable-sustainable development*.
- The events developed in the convergence area N.E.S.-T.S. must be assessed taking into account their influence on the *environmental entropisation* processes.
- Ecotechnologies are technologies used to minimise the environmental entropisation processes related to human activity.
- We define and characterize four categories:
  - ecotechnologies with minimisation of natural resources consumption;
  - ecotechnologies with minimisation of the polluting losses from the technological process perimeter to the environment;
  - ecotechnologies of secondary materials reintegration;
  - process ecotechnologies.

References

[1]. A. Vădineanu, *Development management: An ecosystemic approach*, Publisher: Ars Docendi, Bucharest, 2004.
[2]. S. Mincu, V. Stancovici, *Interdisciplinarity in the contemporary science*, Publisher: Politică, Bucharest, 1980.
[3]. A. Nicolae, *In metallurgy, the "gogglewise" knowledge is replaced by the "fanwise knowledge"*, Acta Tehnica Napucensis, series EESDE, no. 3, p. 17-23, 2014.
[4]. A. Nicolae, M. Nicolae, A. C. Berbecaru, A. M. Predescu, G. Coman, *Durable-sustainable development in metal materials*, Publisher: Printech, Bucharest, 2015.
[5]. C. Negrei, *Tools and methods in environmental management*, Publisher: Economică, Bucharest, 1999.
[6]. V. Rojanschi, *et al.*, *Elements of environmental economics and management*, Publisher: Economică, Bucharest, 2004.
[7]. N. Georgescu-Roegen, *The Entropy law and economic progress*, Publisher: Politică, Bucharest, 1979.
[8]. N. Georgescu-Roegen, *The energy, natural resources and economic theory*, Publisher: Expert, Bucharest, 2006.
[9]. I. Ionel, N. Robu, *Preface Proc. renewable energy resources*, Publisher: Politehnica, Timişoara, 2006.
[10]. A. Nicolae, B. F. Stroe, I. Borş, A. I. Mauthner, A. Semenescu, A. A. Minea, *Ecosociologie metalucrgică*, Ed. Matrix, Bucharest, 2012.
[11]. N. Sîrbu, *Complicata lume nouă, Caţavencii*, nr. 15, p. 18, 2015.
[12]. A. Nicolae, B. Stroe, *The use of some thermodynamic parameters in metallurgical ecosociology analisyses, Met. Int.*, 17, nr. 9, p. 155, 2012.

THE ANNALS OF "DUNAREA DE JOS" UNIVERSITY OF GALATI
FASCICLE IX. METALLURGY AND MATERIALS SCIENCE
N°. 1 - 2016, ISSN 1453 – 083X

A REVIEW ON THE THERMOPHYSICAL PROPERTIES OF WATER-BASED NANOFLUIDS AND THEIR HYBRIDS

Alina Adriana MINEA[1]
[1]"Gheorghe Asachi" Technical University of Iasi
Bd. D. Mangeron 63, Iasi, 700050, Romania
e-mail: aminea@tuiasi.ro

ABSTRACT

A nanofluid is a solid–liquid mixture which consists of nanoparticles and a base liquid. Nanoparticles are basically metal (Cu, Ni, Al, etc.), oxides (Al_2O_3, TiO_2, CuO, SiO_2, Fe_2O_3, Fe_3O_4, $BaTiO_3$, etc.) and some other compounds (SiC, $CaCO_3$, graphene, etc.) and base fluids usually include water, ethylene glycol, propylene glycol, engine oil, etc. Conventional fluids have poor heat transfer properties but their vast applications in power generation, chemical processes, heating and cooling processes, electronics and other micro-sized applications make the re-processing of those thermo fluids to have better heat transfer properties quite essential. Recently, it has been shown that the addition of solid nanoparticles to various fluids can increase the thermal conductivity and can influence the viscosity of the suspensions by tens of percent. The thermophysical properties of nanofluids were shown dependent on the particle material, shape, size, concentration, the type of the base fluid, and other additives. Therefore, a comprehensive analysis has been performed to evaluate the thermophysical properties of nanofluids due to variations of nanoparticle volume concentration. Actually, it is shown that no model is able to predict the thermophysical properties of nanofluids precisely in a broad range of nanoparticle volume fraction. Also, a review on hybrid nanofluids is inserted, even if the research is at the very beginning. As a conclusion, the results indicated that further work is needed due to a large uncertainty in termophysical properties method of estimation.

KEYWORDS: hybrid nanofluid, thermal conductivity, Nusselt number, oxide nanoparticles, viscosity

1. Introduction

The past decade has seen the rapid development of the science and technology of nanofluids in many respects but the present research is mostly focused on their thermal conductivity. Choi [1] in 1995 showed from a series of calculations that the thermal conductivity of a fluid can be enhanced by adding nanoparticles. However, nanofluid viscosity also deserves the same attention as thermal conductivity.

Due to the very small size and large specific surface areas of the nanoparticles, nanofluids have superior properties like high thermal conductivity, minimal clogging in flow passages, long-term stability, and homogeneity [2]. Conventional fluids such as ethylene glycol (EG), water and oil have poor heat transfer properties but their vast applications in power generation, chemical processes, heating and cooling processes, transportation, electronics, automotive and other micro-sized applications make the re-processing of those thermo fluids to have better heat transfer properties quite essential.

Viscosity describes the internal resistance of a fluid to flow and it is an important property for all thermal applications involving fluids [3]. The pumping power is related with the viscosity of a fluid. In laminar flow, the pressure drop is directly proportional to viscosity. Hence, viscosity is as important as thermal conductivity in engineering systems involving fluid flow [4].

Lee *et al.* [5] measured the thermal conductivity of Al_2O_3 (mean diameter 38 nm) and CuO (mean diameter 23.6 nm) nanofluids in water and ethylene glycol up to about 4% volumetric concentration, using the transient hot-wire method. Their experimental results showed that for a copper oxide-

ethylene glycol nanofluid the thermal conductivity can be enhanced by more than 20% for a particle volumetric concentration of 4%. Their measured thermal conductivity of CuO nanofluids with that obtained from the model of Hamilton and Crosser [6] did not agree. Therefore, the Hamilton-Crosser model, which was originally developed for microparticles, was found to be inadequate to predict the thermal conductivity of nanofluids correctly and new correlations were necessary.

Eastman *et al.* [7] measured the thermal conductivity of Cu nanoparticle of mean diameter <10 nm in ethylene glycol. They found that the effective thermal conductivity increased by up to 40% with approximately 0.3% volumetric concentration of Cu nanoparticles over the base fluid.

Das *et al.* [8] presented the temperature dependency of thermal conductivity of nanofluids with water-based CuO and Al_2O_3 nanoparticles of average particle diameter 28.6 nm and 30.4 nm respectively. Their measured thermal conductivity values of CuO-water nanofluid of 4% volumetric concentration exhibited an increase from 14 to 36% over the base fluid with temperature increasing from 21 °C to 51 °C. They also showed that at temperatures above the room temperature, the Hamilton and Crosser [6] model failed to predict the correct values of thermal conductivities for both nanofluids, consistently under-predicting the correct values.

Wang *et al.* [9] presented a model based on the fractal theory for the determination of the effective thermal conductivity of nanofluids. They compared the fractal model prediction to experimental data with 50 nm CuO particles in DI water of less than 0.5% volumetric concentration. They mentioned that beyond this dilute limit, the model needs to be refined by taking into account possible deposition effect. Koo and Kleinstreuer [10] derived a model for the effective thermal conductivity of nanofluids that combines the conventional static part represented by Hamilton-Crosser equation plus a dynamic part due to the Brownian motion. This model includes the effects of particle size, volume concentration, temperature, properties of the base fluid and the nanoparticles and the motion of the surrounding fluid moving with the particles. Using their model of effective thermal conductivity and viscosity, Koo and Kleinstreuer [11] showed through a numerical laminar flow analysis that there was an increase in the heat transfer performance of micro-heat sinks with the addition of CuO nanoparticles of particle diameter 20 nm and particle concentration of up to 4% in the base fluids of both water and ethylene glycol.

Viscosity and rheological properties are essential parameters to know for practical applications of nanofluids. In this study, it has been shown that a great amount of research has been done considering the viscosity of nanofluids. However, it does not seem to be sufficient to estimate any standard about the viscosity of nanofluids, as there are some inconsistencies among the published results [2, 12-21]. For example, some authors reported that nanofluids were Newtonian fluids [2, 12], while others observed a non-Newtonian behavior [12-16].

Some authors showed that relative viscosity is independent of temperature [12] and some authors showed that the viscosity of nanofluids decreases non-linearly or exponentially [19-21] with the increase of temperature.

From another perspective, some researchers showed viscosity increasing linearly with the increase of volume concentrations, while others showed a nonlinear trend [12, 13]. Also, the same nanofluids with the same concentration demonstrate different viscosity enhancement. Debates also exist about the particle size effect on the viscosity of nanofluids.

In this study, a comprehensive analysis was performed in order to compare and evaluate different models for thermal conductivity and viscosity for three different oxide nanofluids.

2. Thermophysical properties

Using classical formulas derived for a two-phase mixture, the density, specific heat capacity and thermal expansion coefficient of the nanofluid under consideration as a function of the particle volume concentration and individual properties can be computed using the following equations, respectively:

$$\rho_{eff} = \varphi\rho_p + (1-\varphi)\rho_f \quad (1)$$

$$(\rho c_p)_{eff} = \varphi(\rho c_p)_p + (1-\varphi)(\rho c_p)_f \quad (2)$$

$$(\rho\beta)_{eff} = \varphi(\rho\beta)_p + (1-\varphi)(\rho\beta)_f \quad (3)$$

However, the transport properties of nanofluid: dynamic viscosity and thermal conductivity are not only dependent on nanoparticle volume fraction, but are also highly dependent on other parameters, such as particle shape (spherical, disk shape or cylindrical), size, mixture combinations and slip mechanisms, surfactant, etc. Studies showed that viscosity, as well as thermal conductivity increases by use of nanofluid compared to base fluid. So far, various theoretical and experimental studies have been conducted and various correlations have been proposed for the dynamic viscosity and the thermal conductivity of nanofluids.

2.1. Thermal conductivity

Theoretical efforts and modeling of the thermal conductivity enhancement mechanisms in nanofluids have not come up with a universal theoretical model that carefully predicts the thermal conductivity for a variety of nanofluid compositions. The macroscopic effective medium theory (EMT) introduced by Maxwell [22] and further developed for non-spherical particle shapes by Hamilton and Crosser [6] predicts that thermal conductivity of two component heterogeneous mixtures is a function of the conductivity of pure materials, the composition of the mixture and the manner in which pure materials distributed throughout the mixture.

A review on existing models relevant to aluminum oxide (Al_2O_3), copper oxide (CuO) and titanium dioxide (TiO_2), dispersed in water is depicted in Table 1.

Table 1. *Correlations on thermal conductivity*

Model	Reference	Year	Correlation	Relevant information
Theoretical	Maxwell [22]	1881	$\frac{k_{eff}}{k_f}=\frac{k_p+2k_f+2\phi(k_p-k_f)}{k_p+2k_f-\phi(k_p-k_f)}$	spherical particles
	Bruggemann [23]	1935	$\frac{k_{eff}}{k_f}=\frac{1}{4}\left[(3\phi-1)\frac{k_p}{k_f}+(2-3\phi)\right]+\frac{k_f}{4}\sqrt{\Delta}$ $\Delta=\left[(3\phi-1)^2\left(\frac{k_p}{k_f}\right)^2+(2-3\phi)^2+2(2+9\phi-9\phi^2)\frac{k_p}{k_f}\right]$	spherical particles
	Hamilton and Crosser [6]	1962	$\frac{k_{eff}}{k_f}=\frac{k_p+(n-1)k_f+(n-1)\varphi(k_p-k_f)}{k_p+(n-1)k_f-\varphi(k_p-k_f)}$ $=4.97\varphi^2+2.72\varphi+1$	$k_p / k_f > 100$
	Wasp [24]	1977	$\frac{k_{eff}}{k_f}=\frac{k_p+2k_f+2\phi(k_p-k_f)}{k_p+2k_f-\phi(k_p-k_f)}$	
	Davis [25]	1986	$\frac{k_{eff}}{k_f}=1+\frac{3(k-1)}{(k-2)-\phi(k-1)}\left[\phi+f(k)\phi^2+O\phi^3\right]$	f(k) = 2.5 for k = 10 f(k) = 0.5 for k = ∞
	Lu and Lin [26]	1996	$\frac{k_{eff}}{k_f}=1+a\phi+b\phi^2$	For k = 10: a = 2.25, b = 2.27 For k = ∞ a = 3.00, b = 4.51
	Bhattacharya et al. [27]	2004	$\frac{k_{eff}}{k_f}=\frac{k_p}{k_f}\phi+(1-\phi)$ $k_p=\frac{1}{K_BT^2V}\sum_{j=0}^{n}(Q(O)Q(j\Delta T))\Delta T$	
	Xue [28]	2005	$\frac{k_{eff}}{k_f}=\frac{1-\phi+2\phi\frac{k_p}{k_p-k_f}ln\frac{k_p+k_f}{2k_f}}{1-\phi+2\phi\frac{k_f}{k_p-k_f}ln\frac{k_p+k_f}{+2k_f}}$	
Experimental	Li and Peterson [29]	2006	$\frac{k_{eff}-k_f}{k_f}=0.764\phi+0.0187(T-273.15)-0.462$	Al_2O_3/water

			$\frac{k_{eff}-k_f}{k_f}=3.761\phi+0.0179(T-273.15)-0.307$	CuO/water
	Buongiorno [30]	2006	$\frac{k_{eff}}{k_f}=1+2.92\phi-11.99\phi$	TiO_2/water
	Timofeeva *et al.* [31]	2007	$k_{eff}=(1+3\phi)k_f$	Al_2O_3/water
	Avsec and Oblak [32]	2007	$\frac{k_{eff}}{k_f}=\left[\frac{k_p+(n-1)k_f+(n-1)(1+\beta)^3\phi(k_p-k_f)}{k_p+(n-1)k_f-(1-\beta)^3\phi(k_p-k_f)}\right]$	n = (3/ψ) Al_2O_3/EG Cu/EG TiO_2/water Al_2O_3/water
	Chandrsekar et al. [33]	2009	$\frac{k_{eff}}{k_f}=\left[\frac{k_p+(n-1)k_f+(n-1)(1+\beta)^3\phi(k_p-k_f)}{k_p+(n-1)k_f-(1-\beta)^3\phi(k_p-k_f)}\right]+\frac{c\varphi(T-T_0)}{\mu k a^4}$	CuO/water TiO_2/water n = 3 for spherical particles
	Duangthongsu and Wongwises [34]	2009	$\frac{k_{eff}}{k_f}=a+b\phi$ a = 1.0225, b = 0.0272 for T = 15 °C a = 1.0204, b = 0.0249 for T = 25 °C a = 1.0139, b = 0.0250 for T = 35 °C	TiO_2/water
	Patel *et al.* [35]	2010	$\frac{k_{eff}}{k_f}=\left(1+0.135\left(\frac{k_p}{k_f}\right)^{0.273}\phi^{0.467}\left(\frac{T}{20}\right)^{0.547}\left(\frac{100}{d_p}\right)^{0.234}\right)$	Oxide and metallic nanofluids
	Chandrasekar *et al.* [2]	2010	$\frac{k_{eff}}{k_f}=\left(\frac{C_{p.eff}}{C_{pf}}\right)^a\left(\frac{P_{eff}}{P_f}\right)^b\left(\frac{M_f}{M_{eff}}\right)^c$ a = -0.023, b = 1.358, c = 0.125	Al_2O_3/water
	Vajjha *et al.* [36]	2010	$\frac{k_{eff}}{k_f}=\frac{k_p+2k_f+2\phi(k_p-k_f)}{k_p+2k_f-\phi(k_p-k_f)}+5*10^4\beta\rho_p C_p\sqrt{\frac{K_b T}{\rho_P d}}f(T,\phi)$ $f(T,\phi)=\left(-3.0669*10^{-2}\phi-3.91123*10^{-3}\right)+\left(2.8217*10^{-2}\phi+3.917*10^{-3}\right)\frac{T}{T_0}$	Al_2O_3 (60:40) EG/ water
	Corcione [37]	2011	$\frac{k_{eff}}{k_f}=1+4.4\,Re^{0.4}\,Pr^{0.66}\left(\frac{T}{T_{FR}}\right)^{10}\left(\frac{k_e}{k_f}\right)^{0.03}\phi^{0.66}$	Al_2O_3/water

2.2. Viscosity

Various models have been suggested to model the viscosity of a nanofluid mixture, that take into account the percentage of nanoparticles suspended in the base fluid.

Table 2 includes some data relevant to aluminum oxide (Al_2O_3), copper oxide (CuO) and titanium dioxide (TiO_2), dispersed in water picked from the literature.

Table 2. *Correlations on viscosity*

Model	Reference	Year	Correlation	Relevant information
Theoretical	Einstein [38]	1906	$\frac{\mu_{eff}}{\mu_f} = 1 + 2.5\phi$	spherical particles
	Saito [39]	1950	$\frac{\mu_{eff}}{\mu_f} = \left(1 + \frac{2.5}{(1-\varphi)}\varphi\right)$	spherical particles
	Brinkman [40]	1952	$\frac{\mu_{eff}}{\mu_f} = \frac{1}{(1-\phi)^{2.5}}$	spherical particles
	Lundgren [41]	1972	$\frac{\mu_{eff}}{\mu_f} = \frac{1}{1-2.5\phi}$	moderate concentration
	Batchelor [42]	1977	$\frac{\mu_{eff}}{\mu_f} = 1 + 2.5\phi + 6.2\phi^2$	spherical particles
Experimental	Wang *et al.* [43]	1999	$\frac{\mu_{eff}}{\mu_f} = 1 + 7.3\varphi + 123\varphi^2$	Al_2O_3/ water
	Tseng and Lin [44]	2003	$\frac{\mu_{eff}}{\mu_f} = 13.47\,exp(35.98\phi)$	Al_2O_3/EG TiO_2/water
	Maiga *et al.* [45]	2005	$\frac{\mu_{eff}}{\mu_f} = 1 + 7.3\varphi + 123\varphi^2$	Al_2O_3/water
	Koo and Kleinstreuer [46]	2005	$\mu_{Brownian} = 5*10^4\,\beta\rho_f\phi\sqrt{\frac{K_bT}{2\rho_P r_p}}\left[(-134.63+1722.3\phi)+(0.4705-6.04\phi)\frac{T}{T_0}\right]$ $\beta = \begin{cases} 0.0137(100\phi)^{-0.8229} & \phi \le 0.01 \\ 0.0011(100\phi)^{-0.7272} & \phi \ge 0.01 \end{cases}$	CuO/water
	Kulkarni *et al.* [47]	2006	$ln\,\mu_{eff} = -\left(2.8751 + 53548\phi - 107.12\phi^2\right) + \left(1078.3 + 15857\phi + 20587\phi^2\right)\left(\frac{1}{T}\right)$	CuO/water
	Buongiorno [30]	2006	$\frac{\mu_{eff}}{\mu_f} = 1 + 5.45\phi + 108.2\phi^2$ $\frac{\mu_{eff}}{\mu_f} = 1 + 39.11\phi + 533.9\phi^2$	TiO_2/water Al_2O_3/water
	Chen *et al.* [12]	2007	$\frac{\mu_{eff}}{\mu_f} = 1 + 10.6\phi + 112.36\phi^2$	TiO_2/EG
	Nguyen *et al.* [3]	2007	$\frac{\mu_{eff}}{\mu_f} = 0.904\,exp(0.1483\phi)$ for d_p = 47 nm $\frac{\mu_{eff}}{\mu_f} = 1 + 0.025\phi + 0.015\phi^2$ for d_p = 36 nm	Al_2O_3/water CuO/water

			$\frac{\mu_{eff}}{\mu_f} = 1.475 - 0.319\iota + 0.051\phi^2 + 0.009\phi^3$ for d_p = 29 nm	
	Namburu *et al.* [48]	2007	$Log(\mu_{eff}) = Ae^{-BT}$ $A = 1.8375\phi^2 - 29.643\phi + 165.56$ $B = 4 * 10^{-6}\phi^2 - 0.001\phi + 0.0186$	CuO/water
	Duangthongsu and Wongwises [34]	2009	$\frac{\mu_{eff}}{\mu_f} = a + b\phi + c\phi^2$ a = 1.0226, b = 0.0477, c = - 0.0112 for T = 15 °C a = 1.0130, b = 0.0920, c = - 0.0150 for T = 25 °C a = 1.0180, b = 0.1120, c = - 0.0177 for T = 35 °C	TiO_2/water
	Chandrasekar *et al.* [2]	2010	$\frac{\mu_{eff}}{\mu_f} = 1 + b\left(\frac{\varphi}{1-\varphi}\right)^n$; b = 1631, n = 2.8	Al_2O_3/water
	Vajjha [36]	2010	$\frac{\mu_{eff}}{\mu_f} = Ae^{C\varphi}$; A = 0.9197, C = 22.8539	CuO/water

3. Discussion

In this paper, an attempt has been made to cover most of the investigations performed on the thermal conductivity and viscosity of nanofluids available in the literature. It has been found that temperature, particle size and shape and volume fractions have significant effects over the viscosity and the thermal conductivity of nanofluids. Results indicate that viscosity increases as the particle volume fractions increase, and nanofluids behave in a Newtonian way for low particle volume concentrations. No existing model or correlation is capable of precise prediction of the viscosity enhancement with respect to volume fractions. Although there have been a few contradictory results in the field of temperature effect on viscosity, generally, researchers conclude that viscosity decreases with an increase of temperature. There are some correlations available for the temperature influence over viscosity; most of which are not versatile enough and a debate still exists about the particle size impact on viscosity.

To illustrate these uncertainties, three types of nanoparticles, Al_2O_3, CuO and TiO_2, were chosen because they have been widely studied in recent years as promising additives.

Accurate formulas for the thermophysical properties (density, viscosity, specific heat and thermal conductivity) are necessary for these nanofluids to perform a thermal and fluid dynamic analysis, so few correlations were selected.

Table 3. *Thermophysical properties of base fluid and nanoparticles at 293 K*

Property	**Base fluid (water)**	**Nanoparticle (Al_2O_3)**	**Nanoparticle (CuO)**	**Nanoparticle (TiO_2)**
specific heat (J/kg K)	4179	773	551	692
density (kg/m^3)	997.1	3960	6000	4230
thermal conductivity (W/m·K)	0.613	40	33	8.4
viscosity (kg/ms)	8.91 x 10^{-4}	-	-	-

Further on, Figure 1 presents several selected models on thermal conductivity.

One can notice that almost all correlations give an increase in thermal conductivity, excepting the Li and Peterson [29] correlation for alumina nanofluid that goes to a decrease of thermal conductivity when adding nanoparticles. Even so, the thermal conductivity is increasing to almost 25% by adding nanoparticles to water.

In regard to viscosity, Figure 2 contains the plotting of some correlations in connection with the particle volume fraction. Figure 2 a. plots some

theoretical correlations available in the open literature and one can see the increase in viscosity with volume fraction, going to an overall increase of about 15% for a 5% volume fraction.

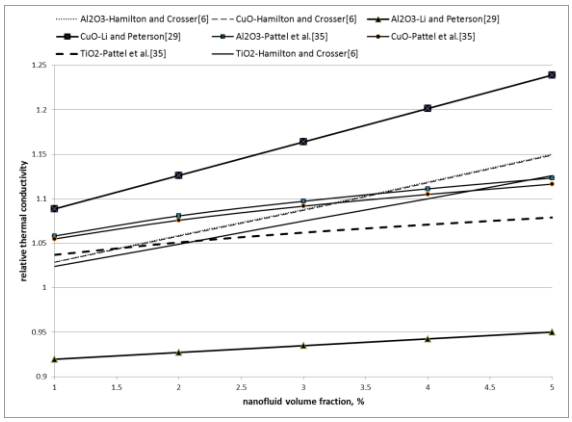

Fig. 1. *Relative thermal conductivity for selected nanofluids*

Figure 2 b shows the variation of viscosity for considered nanofluids in regard to some experimental correlations available in the open literature. It can be noticed that the highest increase was obtained for alumina-water nanofluid that goes to 400 % increase using Buongiorno [30] experimental formulae.

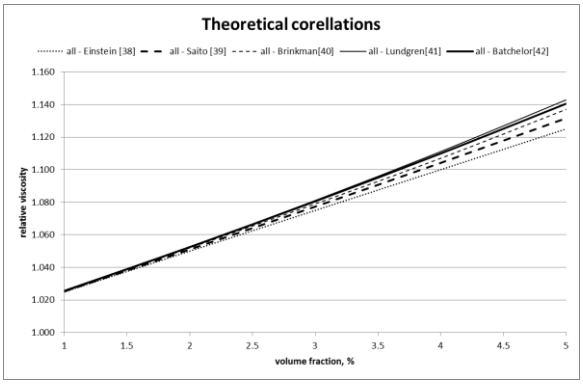

a.

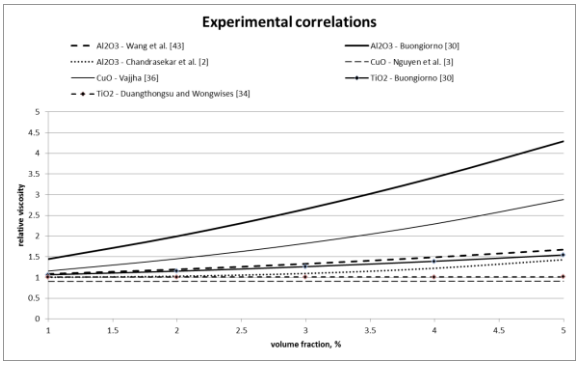

b.

Fig. 2. *Relative viscosity for selected nanofluids:*
a. theoretical correlations;
b. experimental correlations

Looking at Tables 1 and 2, one can notice that a lot of correlations are depending exclusively on particle volume fraction and eventually on temperature variations and this leads to the same thermal conductivity and viscosity enhancement regardless of nanoparticle material. Table 3 presents these correlations. Moreover, all theoretical models for viscosity prediction do consider only the particle volume fraction variation.

Table 4 is a review on viscosity and thermal conductivity enhancement for the considered nanofluids. One can notice that the results are highly dependent on each author research and their nanofluid method of approach. These results highly recommend a better approach to the theory of nanofluids and further work in this area.

Table 3. *Correlations depending only on particle volume fraction*

Model	Reference	Year	Correlation	Relevant information
THERMAL CONDUCTIVITY				
Theoretical	Hamilton and Crosser [6]	1962	$\frac{k_{eff}}{k_f} = 4.97\varphi^2 + 2.72\varphi + 1$	$k_p / k_f > 100$
	Lu and Lin [26]	1996	$\frac{k_{eff}}{k_f} = 1 + a\phi + b\phi^2$	For k = 10: a = 2.25, b = 2.27 For k = ∞ a = 3.00, b = 4.51

Experimental	Li and Peterson [29]	2006	$\frac{k_{eff}-k_f}{k_f}=0.764\phi+0.0187(T-273.15)-0.462$	Al_2O_3/water
			$\frac{k_{eff}-k_f}{k_f}=3.761\phi+0.0179(T-273.15)-0.307$	CuO/water
	Buongiorno [30]	2006	$\frac{k_{eff}}{k_f}=1+2.92\phi-11.99\phi$	TiO_2/water
	Timofeeva *et al.* [31]	2007	$k_{eff}=(1+3\phi)k_f$	Al_2O_3/water
	Duangthongsu and Wongwises [34]	2009	$\frac{k_{eff}}{k_f}=a+b\phi$ a = 1.0225, b = 0.0272 for T = 15 °C a = 1.0204, b = 0.0249 for T = 25 °C a = 1.0139, b = 0.0250 for T = 35 °C	TiO_2/water
VISCOSITY				
Theoretical	Einstein [38]	1906	$\frac{\mu_{eff}}{\mu_f}=1+2.5\phi$	spherical particles
	Saito [39]	1950	$\frac{\mu_{eff}}{\mu_f}=\left(1+\frac{2.5}{(1-\varphi)}\varphi\right)$	spherical particles
	Brinkman [40]	1952	$\frac{\mu_{eff}}{\mu_f}=\frac{1}{(1-\phi)^{2.5}}$	spherical particles
	Lundgren [41]	1972	$\frac{\mu_{eff}}{\mu_f}=\frac{1}{1-2.5\phi}$	moderate concentration
	Batchelor [42]	1977	$\frac{\mu_{eff}}{\mu_f}=1+2.5\phi+6.2\phi^2$	spherical particles
Experimental	Wang *et al.* [43]	1999	$\frac{\mu_{eff}}{\mu_f}=1+7.3\varphi+123\varphi^2$	Al_2O_3/water
	Tseng and Lin [44]	2003	$\frac{\mu_{eff}}{\mu_f}=13.47\exp(35.98\phi)$	Al_2O_3/EG TiO_2/water
	Maiga *et al.* [45]	2005	$\frac{\mu_{eff}}{\mu_f}=1+7.3\varphi+123\varphi^2$	Al_2O_3/water
	Kulkarni *et al.* [47]	2006	$\ln\mu_{eff}=-\left(2.8751+53548\phi-107.12\phi^2\right)+\left(1078.3+15857\phi+20587\phi^2\right)\left(\frac{1}{T}\right)$	CuO/water
	Buongiorno [30]	2006	$\frac{\mu_{eff}}{\mu_f}=1+5.45\phi+108.2\phi^2$ $\frac{\mu_{eff}}{\mu_f}=1+39.11\phi+533.9\phi^2$	TiO_2/water Al_2O_3/water
	Chen *et al.* [12]	2007	$\frac{\mu_{eff}}{\mu_f}=1+10.6\phi+112.36\phi^2$	TiO_2/EG
	Nguyen *et al.* [3]	2007	$\frac{\mu_{eff}}{\mu_f}=0.904\exp(0.1483\phi)$ for d_p = 47 nm	Al_2O_3/water CuO/water

			$\frac{\mu_{eff}}{\mu_f} = 1 + 0.025\phi + 0.015\phi^2$ for d_p = 36 nm $\frac{\mu_{eff}}{\mu_f} = 1.475 - 0.319\iota + 0.051\phi^2 + 0.009\phi^3$ for d_p = 29 nm	
	Namburu *et al.* [48]	2007	$Log(\mu_{eff}) = Ae^{-BT}$ $A = 1.8375\phi^2 - 29.643\phi + 165.56$ $B = 4 * 10^{-6}\phi^2 - 0.001\phi + 0.0186$	CuO/water
	Duangthongsu and Wongwises [34]	2009	$\frac{\mu_{eff}}{\mu_f} = a + b\phi + c\phi^2$ a = 1.0226, b = 0.0477, c = - 0.0112 for T = 15 °C a = 1.0130, b = 0.0920, c = - 0.0150 for T = 25 °C a = 1.0180, b = 0.1120, c = - 0.0177 for T = 35 °C	TiO_2/water
	Chandrasekar *et al.* [2]	2010	$\frac{\mu_{eff}}{\mu_f} = 1 + b\left(\frac{\varphi}{1-\varphi}\right)^n$; b = 1631, n = 2.8	Al_2O_3/water
	Vajjha [36]	2010	$\frac{\mu_{eff}}{\mu_f} = Ae^{C\varphi}$; A = 0.9197, C = 22.8539	CuO/water

Table 4. *Viscosity and thermal conductivity enhancement*

Nanofluid/correlation	***Nanofluid volume concentration, %***				
	1	**2**	**3**	**4**	**5**
VISCOSITY					
Al_2O_3 - Wang *et al.* [43]	8.53	19.52	32.97	48.88	67.25
Al_2O_3 - Buongiorno [30]	44.45	99.58	165.38	241.86	329.03
Al_2O_3 - Chandrasekar *et al.* [2]	0.42	3.02	9.67	22.28	42.85
CuO - Nguyen *et al.* [3]	-9.47	-9.33	-9.20	-9.06	-8.93
CuO - Vajjha [36]	15.58	45.26	82.56	129.43	188.34
TiO_2 - Tseng and Lin [44]	1828.57	2661.24	3853.42	5560.32	8004.18
TiO_2 - Buongiorno [30]	6.53	15.23	26.09	39.11	54.30
TiO_2 - Duangthongsu and Wongwises [34]	1.09	1.18	1.27	1.36	1.45
all - Einstein [38]	2.50	5.00	7.50	10.00	12.50
all - Saito [39]	2.53	5.10	7.73	10.42	13.16
all - Brinkman [40]	2.50	5.20	7.90	10.70	13.70
all - Lundgren [41]	2.56	5.26	8.11	11.11	14.29
all - Batchelor [42]	2.56	5.25	8.06	10.99	14.05
THERMAL CONDUCTIVITY					
Al_2O_3 - Hamilton and Crosser [6]	2.89	5.90	8.80	11.90	15.00
CuO-Hamilton and Crosser [6]	2.87	5.80	8.70	11.80	14.90
TiO_2-Hamilton and Crosser [6]	2.40	4.90	7.50	10.00	12.60

Al_2O_3-Li and Peterson [29]	-8.04	-7.27	-6.51	-5.74	-4.98
CuO-Li and Peterson [29]	8.86	12.62	16.38	20.14	23.91
Al_2O_3-Pattel *et al.* [35]	5.82	8.08	9.72	11.12	12.34
CuO-Pattel *et al.* [35]	5.49	7.59	9.17	10.49	11.65
TiO_2-Pattel *et al.* [35]	3.70	5.10	6.20	7.10	7.90

4. New challenge: hybrid nanofluids?

In spite of some inconsistency in the reported results and insufficient understanding of the mechanism of the heat transfer in nanofluids, it has emerged as a promising heat transfer fluid.

In the continuation of nanofluids research, the researchers have also tried to use hybrid nanofluids recently, which is engineered by suspending dissimilar nanoparticles either in mixture or composite form.

The idea of using hybrid nanofluids is to further improvement of heat transfer and pressure drop characteristics by trade-off between advantages and disadvantages of individual suspension, attributed to good aspect ratio, better thermal network and synergistic effect of nanomaterials.

The introduction of a new concept of combined/hybrid nanofluids will be clearly explained in this article. Furthermore, this very short review summarizes recent research on thermophysical properties, heat transfer and possible applications and challenges of hybrid nanofluids. Review showed that proper hybridization may make the hybrid nanofluids very promising for heat transfer enhancement; however, many research works are still needed in the fields of preparation and stability, characterization and applications to overcome the challenges.

Some research started in 2007, but their number slowly increases over the years, as one can see from Figure 3.

Moreover, Tables 5 and 6 are a summary of recent experimental results obtained in the area of hybrid nanofluids, in connection with thermophysical properties.

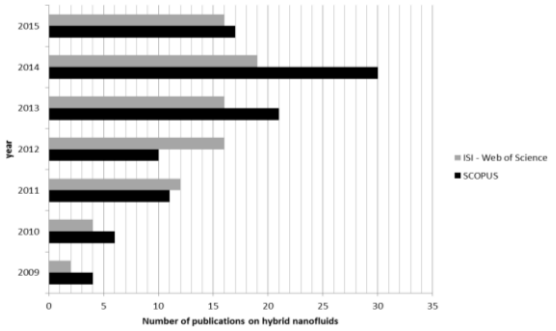

Figure 3. *Number of publications on hybrid nanofluids*

Table 5. *Investigations on density, heat capacity and viscosity of hybrid nanofluids*

Investigators	Nanofluids	Properties and important findings
Ho *et al.* [49]	Al_2O_3 - MEPCM/ water	Density and heat capacity: temperature independent measurement, classical correlations are applicable.
Ho *et al.* [49]	Al_2O_3 - MEPCM/ water	Viscosity: drastically increase of the effective dynamic viscosity of the hybrid suspension.
Suresh *et al.* [50]	Al_2O_3 - Cu/water	Viscosity: viscosity increases substantially higher than the increase in thermal conductivity.
Botha *et al.* [51]	Ag - Silica/oil	Viscosity: the nanofluid showed Newtonian behavior at lower silica concentrations and followed the Bingham flow model at high concentrations.
Baghbanzadeh *et al.* [52]	Silica/MWCNT water	Density and viscosity: at high concentration, better influence compared to mono nanofluids.

Table 6. *Investigations on thermal conductivity of hybrid nanofluids*

Investigators	Nanofluids	Important findings
Ho *et al.* [49]	Al_2O_3 - MEPCM/water	Significant enhancement of thermal conductivity of PCM suspension with Al_2O_3 nanoparticle dispersion relative to pure water.
Suresh *et al.* [50]	Al_2O_3 - Cu/water	A very significant enhancement in the effective thermal conductivity due to hybridization of alumina nanoparticles using metallic copper particles.

Botha *et al.* [51]	Ag - silica/oil	The theoretical increase in thermal conductivity is much lower than that observed.
Paul *et al.* [53]	Al-Zn/ethylene glycol	A maximum 16% thermal conductivity enhancement at 0.1 vol% particle concentration was achieved.
Baghbanzadeh *et al.* [54]	Silica/MWCNT	Thermal conductivity in case of hybrid nanofluids is between enhancement of MWCNT sand silica nanofluids.
Abbasi *et al.* [55]	γ-Al_2O_3/MWCNT	Enhancement of the thermal conductivity of hybrid nanofluids can reach up to 14.75 % at a volume fraction of 0.01.
Nine *et al.* [56]	Al_2O_3 - MWCNT/water	Thermal conductivity better with non-ground MWCNT s compared to ground MWCNTs.
Munkhbayar *et al.* [57]	Ag-MWCNT/water	Improved dispersion of CNT sinthematrix, as well as the decoration of the MWCNT s with silver may be the reason for enhancement in thermal conductivity.
Aravind *et al.* [58, 59]	Graphene-MWNT/water	High thermal transport characteristics of grapheme–MWNT composite nanofluids is attributed to the high aspect ratio of MWNT and graphene.
Chen *et al.* [60]	Fe_2O_3 - MWNT/ water	Significant enhancement of thermal conductivity due to synergistic effect.
Batmunkh *et al.* [61]	Ag - TiO_2/water	Thermal conductivity TiO_2/water nanofluid was enhanced by addition of Ag particle.

As one can see from Table 5 and Table 6, all the studies are encouraging in recommending hybrid nanofluids as new heat transfer fluids. Anyway, more experimental work is needed in order to attain a good stability for these new fluids.

5. Conclusions

Recently, important theoretical and experimental research works on convective heat transfer appeared in the open literature on the enhancement of heat transfer using suspensions of nanometer-sized solid particle materials, metallic or metallic oxides in base heat transfer fluids. Thus, this paper presents an overview of the recent investigations in the study the thermophysical characteristics of nanofluids.

General correlations for the effective thermal conductivity and viscosity of nanofluids are presented. Compared to the reported studies on thermal conductivity, investigations on viscosity of nanofluids are limited. Most of the experimental and numerical studies showed that nanofluids exhibit enhanced thermophysical properties compared to their base fluids, which increase significantly with increasing concentration of nanoparticles as well as Reynolds number.

Also, hybrid nanofluids containing composite nanoparticles yield significant enhancement of thermal conductivity. However, the long-term stability, production process, selection of suitable nanomaterials combination to get synergistic effect and the cost of nanofluids may be major challenges behind the practical applications.

Further theoretical and experimental research investigations on the effective thermal conductivity and viscosity are needed to demonstrate the potential of nanofluids and to understand their heat transfer characteristics, as well as to identify new and unique applications for these fields.

Nomenclature

c_p - specific heat, J/kg °C;
h - heat transfer coefficient, W/m^2 °C;
k - thermal conductivity, W/m °C;
n - shape factor;
Pr - Prandtl number;
Re - Reynolds number;
T - temperature, °C;
φ - volume concentration, %;
μ - viscosity, kg/ms;
ρ - density, kg/m^3;
Subscripts
eff - effective, refers to nanofluid effective property;
f - fluid;
p - particle.

References

[1]. S. Choi, *Enhancing thermal conductivity of fluids with nanoparticles*, in: D. A. Siginer, H. P. Wang (Eds.), Developments Applications of Non-Newtonian Flows, FED, vol. 231/MD, vol. 66, ASME, New York, 1995, p. 99-105.
[2]. M. Chandrasekar, S. Suresh, A. Chandra Bose, *Experimental investigations and theoretical determination of thermal conductivity and viscosity of Al_2O_3/water nanofluid*, Exp. Therm. Fluid Sci., 34 (2), p. 210-216, 2010.
[3]. C. Nguyen, F. Desgranges, G. Roy, N. Galanis, T. Mare, S. Boucher, H. Anguemintsa, *Temperature and particle-size dependent viscosity data for water-based nanofluids – hysteresis phenomenon*, Int. J. Heat Fluid Flow, 28 (6), p. 1492-1506, 2007.

[4]. M. Kole, T. K. Dey, *Viscosity of alumina nanoparticles dispersed in car engine coolant*, Exp. Therm. Fluid Sci., 34 (6), p. 677-683, 2010.
[5]. S. Lee, S. U. S. Choi, S. Li, J. A. Eastman, *Measuring thermal conductivity of fluids containing oxide nanoparticles*, J. Heat Transfer, 121, p. 280-289, 1999.
[6]. R. L. Hamilton, O. K. Crosser, *Thermal conductivity of heterogeneous two component system*, I EC Fund., 1, p. 187-191, 1962.
[7]. J. A. Eastman, S. U. S. Choi, S. Li, W. Yu, L. J. Thompson, *Anomalously increased effective thermal conductivities of ethylene glycol-based nanofluids containing copper nanoparticles*, Appl. Phys. Lett., 78 (6), p. 718-720, 2001.
[8]. S. K. Das, N. Putra, P. Thiesen, W. Roetzel, *Temperature dependence of thermal conductivity enhancement of nanofluids*, J. Heat Transfer, 125, p. 567-574, 2003.
[9]. B. X. Wang, L. P. Zhou, X. F. Peng, *A fractal model for predicting the effective thermal conductivity of liquid with suspension of nanoparticles*, Int. J. Heat Mass Transfer, 46, p. 2665-2672, 2003.
[10]. J. Koo, C. Kleinstreuer, *A new thermal conductivity model for nanofluids*, J. Nanoparticle Res., 6, p. 577-588, 2004.
[11]. J. Koo, C. Kleinstreuer, *Laminar nanofluid flow in microheat-sinks*, Int. J. Heat Mass Transfer, 48, p. 2652-2661, 2005.
[12]. H. Chen, Y. Ding, Y. He, C. Tan, *Rheological behaviour of ethylene glycol based titania nanofluids*, Chem. Phys. Lett., 444 (4-6), p. 333-337, 2007.
[13]. H. Chen, Y. Ding, C. Tan, *Rheological behaviour of nanofluids*, New J. Phys., 9 (10), p. 267, 2007.
[14]. Chen W. Yang, Y. He, Y. Ding, L. Zhang, C. Tan, A. A. Lapkin, D. V. Bavykin, *Heat transfer and flow behaviour of aqueous suspensions of titanate nanotubes (nanofluids)*, Powder Technol., 183 (1), p. 63-72, 2008.
[15]. H. Chen, Y. Ding, A. Lapkin, X. Fan, *Rheological behaviour of ethylene glycoltitanate nanotube nanofluids*, J. Nanopart. Res., 11 (6), p. 1513-1520, 2009.
[16]. H. Chen, S. Witharana, Y. Jin, C. Kim, Y. Ding, *Predicting thermal conductivity of liquid suspensions of nanoparticles (nanofluids) based on rheology*, Particuology, 7 (2), p. 151-157, 2009.
[17]. T. X. Phuoc, M. Massoudi, R. H. Chen, *Viscosity and thermal conductivity of nanofluids containing multi-walled carbon nanotubes stabilized by chitosan*, Int. J. Therm. Sci., 50 (1), p. 12-18, 2011.
[18]. P. Garg, J. L. Alvarado, C. Marsh, T. A. Carlson, D. A. Kessler, K. Annamalai, *An experimental study on the effect of ultrasonication on viscosity and heat transfer performance of multi-wall carbon nanotube-based aqueous nanofluids*, Int. J. Heat Mass Transfer, 52 (21-22), p. 5090-5101, 2009.
[19]. D. P. Kulkarni, D. K. Das, R. S. Vajjha, *Application of nanofluids in heating buildings and reducing pollution*, Appl. Energy, 86 (12), p. 2566-2573, 2009.
[20]. A. Turgut, I. Tavman, M. Chirtoc, H. P. Schuchmann, C. Sauter, S. Tavman, *Thermal conductivity and viscosity measurements of water-based TiO_2 nanofluids*, Int. J. Thermophys., 30 (4), p. 1213-1226, 2009.
[21]. M. T. Naik, G. R. Janardhana, K. V. K. Reddy, B. S. Reddy, *Experimental investigation into rheological property of copper oxide nanoparticles suspended in propylene glycol- water based fluids*, ARPN J. Eng. Appl. Sci., 5 (6), p. 29-34, 2010.
[22]. Maxwell C. A. *Treatise on electricity and magnetism. Oxford*, UK: Clarendon Press, 1881.
[23]. Bruggeman D. A. G., *Berechnung verschied enerphysikalischerkonstantenvon heterogenen substanzen, I-Dielektrizitatskonstanten undleitfahigkeiten der mischkorperausisotropen substanzen*. Annalender Physik, Leipzig, 24, p. 636-679, 1935.
[24]. Wasp F. J., *Solid–liquid slurry pipeline transportation. Transactionson Techniques*, Berlin, 1977.
[25]. Davis R. H., *The effective thermal conductivity of a composite material with spherical inclusions*, International Journal of Thermophysics, 7, p. 609-620, 1986.
[26]. Lu S., Lin H., *Effective conductivity of composites containing aligned spherical inclusions of finite conductivity*, Journal of Applied Physics, 79, p. 6761-6769, 1996.
[27]. Bhattacharya P., Saha S. K., Yadav A., Phelan P. E., Prasher R. S., *Brownian dynamics simulation to determine the effective thermal conductivity of nanofluids*, Journal Applied Physics, 95 (11), p. 6492-6494, 2004.
[28]. Xue Q. Z., *Model for thermal conductivity of carbon nanotube-based composites*, Physica B: Condensed Matter, 368 (1-4), p. 302-307, 2005.
[29]. Li C. H., Peterson G. P., *Experimental investigation of temperature and volume fraction variations on the effective thermal conductivity of nanoparticle suspensions (nanofluids)*. Journal of Applied Physics, 99 (8), 084314, 2006.
[30]. Buongiorno J., *Convective transport in nanofluids*, Journal of Heat Transfer, 128, p. 240-250, 2006.
[31]. Timofeeva E. V., Gavrilov A. N., McCloskey J. M., Tolmachev Y. V., *Thermal conductivity and particle agglomeration in alumina nanofluids: experiment and theory*, Physical Review, 76, 061203, 2007.
[32]. Avsec J., Oblak M., *The calculation of thermal conductivity, viscosity and thermodynamic properties for nanofluids on the basis of statistical nanomechanics*, International Journal of Heat and Mass Transfer, 50 (19), p. 4331-4341, 2007.
[33]. Chandrsekar M., Suresh S., Srinivasan R., Chandra Bose A., *New analyatical models to investigate thermal conductivity of nanofluids*, Journal of Nanoscience and Nanotechnology, p. 533-538. 2009.
[34]. Duangthongsuk W., Wongwises S., *Measurement of temperature-dependent thermal conductivity and viscosity of TiO_2-water nanofluids*, Experimental Thermal and Fluid Science, 33(4), p. 706-714, 2009.
[35]. Patel H. E., Sundararajan T., Das S. K., *An experimental investigation into the thermal conductivity enhancement in oxide and metallic nanofluids*, Journal of Nanoparticle Research, 12, p. 1015-1031, 2010.
[36]. Vajjha R. S., Das D. K., Namburu P. K., *Numerical study offluid dynamic and heat transfer performance of Al_2O_3 and CuO nanofluids in the flat tubes of a radiator*, International Journal of Heat and Fluid Flow, 31, p. 613-621, 2010.
[37]. Corcione M., *Rayleigh–Bernard convection heat transfer in nanoparticle suspensions*, International Journal of Heat and Fluid Flow, 32, p. 65-77, 2011.
[38]. Einstein A., *Eine neue best immung der molekul dimensionen*, Annalen der Physik, Leipzig, 19, p. 289-306, 1906.
[39]. Saito N., *Concentration dependence of the viscosity of high polymer solutions*, Journal of the Physical Society of Japan, 5, p. 4-8, 1950.
[40]. Brinkman H. C., *The viscosity of concentrated suspensions and solution*, Journal of Chemical Physics, 20, p. 571-581, 1952.
[41]. Lundgren T., *Slow flow through stationary random bed sand suspensions of spheres*, Journal of Fluid Mechanics, 51, p. 273-99, 1972.
[42]. Batchelor G. K., *The effect of Brownian motion on the bulk stress in a suspension of spherical particles*, Journal of Fluid Mechanics, 83 (1), p. 97-117, 1977.
[43]. Wang X., Xu X., Choi S. U. S., *Thermal conductivity of nanoparticles - fluid mixture*, Journal of Thermophysics and Heat Transfer, 13 (4), p. 474-480, 1999.
[44]. Tseng W., Lin K. C., *Rheology and colloidal structure of aqueous TiO_2 nanoparticle suspensions*, Material Science Engineering, A, 355, p. 186-192, 2003.
[45]. Maiga S., Palm S. J., Nguyen C. T., Roy G., Galanis N., *Heat transfer enhancement by using nanofluids in forced convection flows*, International Journal of Heat and Fluid Flow, 26, p. 530-546, 2005.
[46]. Koo J., Kleinstreuer C., *Impact analysis of nanoparticle motion mechanisms on the thermal conductivity of nanofluids*,

International Communicationsin Heat and Mass Transfer, 3, 2 (9), p. 1111-1118, 2005.

[47]. Kulkarni D. P., Das D. K., Chukwu G., *Temperature dependent rheological property of copper oxide nanoparticles suspension (Nanofluid)*, Journal of Nanoscience and Nanotechnology, 6, p. 1150-1154, 2006.

[48]. Namburu P. K., Kulkarni D. P., Misra D., Das D. K., *Viscosity of copperoxide nanoparticles dispersed in ethyleneglycol and water mixture*, Experimental Thermal and Fluid Science, 32, p. 67-71, 2007.

[49]. Ho C. J., Huang J. B., Tsai P. S., Yang Y. M., *Preparation and properties of hybrid water- based suspension of Al_2O_3 nanoparticles and MEPCM particles as functional forced convection fluid*, Int Commun Heat Mass Transf, 37, p. 490-494, 2010.

[50]. Suresh S., Venkitaraj K. P., Selvakumar P., Chandrasekar M., *Synthesis of Al_2O_3-Cu/water hybrid nanofluids using two step method and its thermophysical properties*, Colloids Surf A: Physicochem Eng. Asp., 388, p. 41-48, 2011.

[51]. Botha S. S., Ndungu P., Bladergroen B. J., *Physicochemical properties of oil-based nanofluids containing hybrid structures of silver nanoparticles supported on silica*, Ind. Eng. Chem. Res., 50, p. 3071-3077, 2011.

[52]. Baghbanzadeh M., Rashidi A., Soleimanisalim A. H., Rashtchian D., *Investigating the rheological properties of nanofluids of water/hybrid nanostructure of spherical silica/MWCNT*, Thermochim Acta, 578, p. 53-58, 2014.

[53]. Paul G., Philip J., Raj B., Das P. K., Manna I., *Synthesis, characterization, and thermal property measurement of nano-$Al_{95}ZnO_5$ dispersed nanofluid prepared by a two-step process*, Int J Heat Mass Transf, 54, p. 3783-3788, 2011.

[54]. Baghbanzadeha M., Rashidib A., Rashtchiana D., Lotfib R., Amrollahib A., *Synthesis of spherical silica/multiwall carbon nanotubes hybrid nanostructures and investigation of thermal conductivity of related nanofluids*, Thermochim Acta, 549, p. 87-94, 2012.

[55]. Abbasi S. M., Nemati A., Rashidi A., Arzani K., *The effect of functionalisation method on the stability and the thermal conductivity of nanofluid hybrids of carbon nanotubes/gamma alumina*, Ceram. Int., 39 (4), p. 3885-3891, 2013.

[56]. Nine M. J., Batmunkh M., Kim J. H., Chung H. S., Jeong H. M., *Investigation of Al_2O_3-MWCNTs hybrid dispersion in water and their thermal characterization*, J Nanosci Nanotechnol, 12, p. 4553-4559, 2012.

[57]. Munkhbayar B., Tanshen M. R., Jeoun J., Chung H., Jeong H., *Surfactant-free dispersion of silver nanoparticles into MWCNT-aqueous nanofluids prepared by one-step technique and their thermal characteristics*, Ceram. Int., 39 (6), p. 6415-6425, 2013.

[58]. Aravind S. S. J., Ramaprabhu S., *Graphene wrapped multiwalled carbon nano-tubes dispersed nanofluids for heat transfer applications*, J. Appl. Phys., 112, 124304, 2012.

[59]. Aravind S. S. J., Ramaprabhu S., *Graphene-multiwalled carbon nanotube-based nanofluids for improved heat dissipation*, RSCA dv, 3, 4199-4206, 2013.

[60]. Chen L. F., Cheng M., Yang D. J., Yang L., *Enhanced thermal conductivity of nanofluid by synergistic effect of multi-walled carbon nanotubes and Fe_2O_3 nanoparticles*, Appl. Mech. Mater., 548-549, p. 118-123, 2014.

[61]. Batmunkh M., Tanshen M. R., Nine M. J., Myekhlai M., Choi H., Chung H., *Thermal conductivity of TiO_2 nanoparticles based aqueous nanofluids with an addition of a modified silver particle*, Ind. Eng. Chem. Res., 53 (20), p. 8445-8451, 2014.

THE ANNALS OF "DUNAREA DE JOS" UNIVERSITY OF GALATI
FASCICLE IX. METALLURGY AND MATERIALS SCIENCE
N°. 1 - 2016, ISSN 1453 – 083X

EFFECT OF HEAVY METALS ON THE GERMINATION OF WHEAT SEEDS: ENZYMATIC ASSAY

Olga PINTILIE[1], Marius ZAHARIA[2,*], Adelina COSMA[2], Alina BUTNARU[3], Manuela MURARIU[4], Gabi DROCHIOIU[2], Ion SANDU[1,5*]

[1] Department of Geography and Geology, Al. I. Cuza University of Iași, 20A Carol I, Iasi-700505, Romania
[2] Department of Chemistry, Al. I. Cuza University of Iași, 11 Carol I, Iasi-700506, Romania
[3] Department of Biology, Al. I. Cuza University of Iași, 20A Carol I, Iasi-700505, Romania
[4]Petru Poni Institute of Macromolecular Chemistry, 41A Gr. Ghica Voda Alley, 700487 Iasi, Romania
[5]ARHEOINVEST Interdisciplinary Platform, Laboratory of Scientific Investigation and Conservation of Cultural Heritage, Al. I. Cuza University of Iasi, 22 Carol I, 700506, Iasi, Romania
e-mail: zaharia.marius2011@yahoo.com; ion.sandu@uaic.ro

ABSTRACT

Stress caused by heavy metals is a major problem which affects agricultural productivity and, implicitly, human health. Natural flora presents differences of tolerance to heavy metals. Some plants grow well in a soil enriched with heavy metals, while others cannot develop in such conditions. This study investigates the effect of heavy metals on plant viability at molecular level and draws attention to the danger of the widespread use of toxic compounds.

KEYWORDS: heavy metals; genetic conservation; toxicity; enzymatic determination; germination tests

1. Introduction

Plant viability can be partly and irreversibly degraded under the action of certain physical agents or chemical substances [1,2]. The phenomenon can occur under the action of metabolic inhibitors, heat, electricity, UV radiation, or it can occur spontaneously or in different physiological, pathological and experimental conditions [3]. Therefore, the state of living matter should be looked at as being dependent on the state of biostructural matter [4, 5]. Namely, living organisms being affected can signify physiological and even morphological modifications.

The toxicity of heavy metals that enter vegetal tissues can inhibit multiple physiological processes, such as: growth factors, photosynthesis, water absorption and nitrates assimilation [6, 10]. The gravity of these effects largely depends on the concentration of ions in heavy metals and the sensitivity or tolerance of plants affected by their presence [11, 12]. Some metals in small concentrations (Co, Cr, Cu, Fe, Mn, Mo, Ni, V and Zn) are considered essential to plant growth [13]. Zn and Co, as well as Mn and Fe, are essential elements [14] to the superior part of plants and are involved in more metabolic processes, while Pb and Cd do not have any physiological function in plants. A deficit of Zn and Co determines modifications in the fundamental processes of plant metabolism, which leads to a reduced growth. Root growth is more sensitive to heavy metal contamination [15, 16]. An immediate effect of plant contamination with a high concentration of Co is the side roots growth inhibition; these stay shorter, very ramified and without a solid structure. The experiment proved the fact that treating wheat seeds with heavy metals leads to a biomass reduction [15]. Consequently, the leaf function can be directly affected by local accumulation of heavy metals, or indirectly, by affecting the roots [17].

Nosko *et al.*, 1988 signals the fact that using Al in various concentrations does not inhibit the *Picea glauca* seed germination rate, modifying their viability on the other hand [18]. Peralta *et al.*, 2001 shows that different concentrations of Cr, Cu, Cd, Ni and Zn reduce the germination rate of *Medicago sativa L.* seeds and the elongation of rootlets and stemlets of future plants [19].

Munzuroglu and Geckil, 2002, after studying the influence of heavy metals Hg, Cd, Co, Cu, Pb and Zn upon the germination of *Triticum aestivum* și *Cucumis sativum* seeds, highlight a different inhibition of this process based on the used

concentration, as well as a reduction of the rootlet, hypocotyl and coleoptile length [20].

In our research, we emphasized the toxic effect on the viability of wheat seeds, using plants exposed to germination in the presence of heavy metal salts. Also, molecular modifications were highlighted through enzymatic measurements.

2. Materials and methods

In this study, we used analytical grade reagents, while all solutions were prepared with milliQ grade water with R = 18.2 Ω. Heavy metals were purchased from Sigma Aldrich (USA), Merck and Fluka.

Biological material. Wheat seeds (*Triticum Aastivum*), Gasprom variety, acquired from the Agricultural Research Station Suceava.

Instruments. Absorbance spectra were recorded with a Libbra S35 PC UV/VIS spectrophotometer endowed with quartz cuvettes with optical path length of 1 cm. Microprocessor Cole Parmer Ultrasonic (USA, Illinois) used for enzymatic extraction. Mikro22R centrifuge (Hettich) used for the separation of soluble protein mixture containing insoluble components (cell membrane). HANNA pH meter PH 211 used for determining and adjusting the pH buffers.

Germination determining. Lots of 50 seeds each were treated with different solutions of heavy metals inhibitors (solution 10^{-3} M salt of Cu^{2+}, Cd^{2+}, Hg^{2+}, Ni^{2+}, Pb^{2+}, Ba^{2+}, Ag^{+}, etc.), then left to germinate on filter paper in Petri dishes. Treatment duration is 1 hour, after which seeds are disposed in Petri dishes as uniformly as possible, on double filter paper, together with a treatment solution. Thus, 7-day wheat plantlets were harvested from their seeds, measured (height **H**, expressed as cm) and weighed (**M**, expressed as grams).

Enzymatic assay. The biochemical study of wheat seeds and plantlets consisted of determining the activity of some enzymes of oxidative stress [21]. Thus, to determine the peroxidase activity, we used the Gudkova and Degtiari, 1968 method (Artenie *et al.*, 2008), which is based on measuring the wave length of 540 nm of the color intensity of the oxidation product of o-Dianisidine with the help of peroxide. For the catalase activity, we used Sinha, 1972 method cited by Artenie *et al.*, 2008, by colorimetrically determining (λ = 570 nm) the chromic acetate obtained through the reaction of reduction of the potassium dichromate in acid environment by the peroxide which remained undecomposed after the enzyme inactivation. The superoxide dismutase activity was evaluated with the Winterbourn *et al.* (1975) method adapted by Artenie *et al.*, 2008, the method consisting of the enzyme capacity to inhibit the reduction of Nitro Blue Tetrazolium by the superoxide radicals generated in the reaction environment through riboflavin photoreduction (λ = 560 nm) [22].

The concentration of total soluble proteins was obtained based on the Bradford (1976) method, by forming a complex at an absorption maximum of 595 nm [23] between the proteins and the Coomassie Brilliant Blue G-250 dye.

3. Results and discussions

Germination test.

Fig. 1 shows that the effect of heavy metals at low concentrations (10^{-3} M) barely differs, manifesting a slightly inhibitory effect upon the germination of wheat seeds. As a result of this experiment, we can affirm that the toxic effect of heavy metals increases together with the concentration [24].

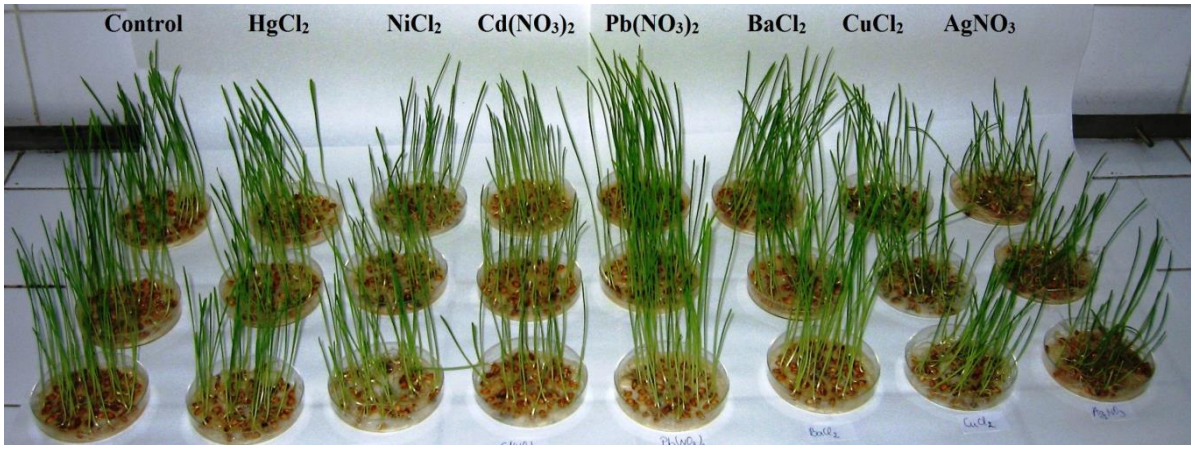

Fig. 1. *Effect of heavy metals (10^{-3}M) on wheat seeds after 7 days of germination*

After processing the obtained results (see Table 1), we noticed that plantlet length is similar in case of $HgCl_2$, $NiCl_2$, $Cd(NO_3)_2$, $CuCl_2$ and $AgNO_3$, but significantly differs from the blank sample, which leads to us affirming that these heavy metals inhibit the height growth of wheat plantlets. $Pb(NO_3)_2$ and $BaCl_2$ salts enhance the height growth of plantlets: from 409.50 cm in case of the blank sample, to 442.60 cm for $Pb(NO_3)_2$ and 434.83 cm for $BaCl_2$.

Tabel 1. *Effect of heavy metals ($10^{-3}M$) on wheat seeds*

Treatment *)	**No. plantlets**	**No. germinated seeds**	**No. dead seeds**	**Heights of plantlets in 50-seed lots (cm)**	**Plantlet weight of 50-seed lots (g)**
Control	34.60±0.20	1.30±0.10	14±0.12	2.54±0.33	409.50±2.54
$HgCl_2$	33.60±0.24	1.30±0.05	15±0.14	2.09±0.20	313.80±0.76
$NiCl_2$	35±0.43	0.30±0.10	14.60±0.98	2.02±0.36	302.20±0.50
$Cd(NO_3)_2$	37.30±0.15	0.60±0.01	15.30±0.25	1.94±0.05	302.80±5.78
$Pb(NO_3)_2$	35.30±0.23	0.30±0.02	17.60±0.45	2.40±0.10	442.60±3.64
$BaCl_2x2H_2O$	33.64±1.25	0.30±0.01	16±0.50	2.55±0.20	434.83±6.57
$CuCl_2$	35.30±0.50	1.30±0.25	13.30±0.75	2.17±0.37	314.30±5.73
$AgNO_3$	35±1	1.30±0.02	13.60±1.23	1.92±0.53	299.10±7.89
*) mean of three independent values					

The variation of enzymatic activities based on the treatment with heavy metals $10^{-3}M$.

Practical study of the superoxide dismutase (SOD) activity from vegetal extracts.

The data in Table 2 shows that the activity of this enzyme stabilizes the cellular abilities of removing oxygen radicals and attenuating cellular damage. Therefore, compared to the plantlets in the control batch, where the average activity of the SOD was 5.43 USOD/mg protein, the level of SOD activity increased significantly up to 14.36 USOD/mg protein in case of seeds treated with $NiCl_2$. The increase of oxidoreductase activity in the experimental group can be consequently attributed to the intensification of processes that release superoxide radicals under the initial influence of heavy metals.

Table 2. *SOD values in wheat plantlets after 7 days of treatment*

Treatment	**USOD/mg protein**
Control (distilled water)	5.43
$HgCl_2$	8.96
$NiCl_2$	14.36
$Cd(NO_3)_2$	10.21
$Pb(NO_3)_2$	7.87
$BaCl_2$	4.98
$CuCl_2$	9.51
$AgNO_3$	9.24

Quantitative determination of soluble vegetal proteins through the Bradford method

After the developing period of 7 days, plantlets were cut in 1 cm pieces, separating the root from the plantlet (stem), in view of separately quantitatively analyzing the soluble vegetal proteins from the two parts of the plant. They were suspended in 10 ml phosphate buffer and sonicated for 30 seconds 3 times, with 5 minute breaks, the extract being then centrifuged and held at a 4 °C temperature for 4-5 days.

To quantitatively determine soluble vegetal proteins, same steps as in the case of extract from the dinitroderivates treatment were followed, pipetting the same reactive amounts, and reading after 3 minutes of incubation and 5 minutes of irradiation. Determining the total concentration of protein from enzymatic extracts was achieved with the Bradford method, treating extracts with Bradford reactive.

From Table 3 one can notice that in the case of the treated samples extracted from roots, the total soluble protein concentration has different values from the blank which does not contain metallic extracts. Therefore, specific activities vary based on the type of used metallic extract, the largest protein quantity being identified when treating with $HgCl_2$ and $NiCl_2$, while treating with $CuCl_2$, $Pb(NO_3)_2$ or $Cd(NO_3)_2$ determines enzymatic inhibition.

Table 3. *Specific activity values based on absorbance and protein concentration of the protein extract obtained from wheat plantlets roots*

	Weight of roots (g)	**Absorbance (595 nm)**	**Protein concentration, µg/mL**	**Specific activity**
Control	0.040	0.0798	0.159	0.0756
$CuCl_2$	0.050	0.0724	0.159	0.0756
$AgNO_3$	0.050	0.0747	0.159	0.0717
$HgCl_2$	0.050	0.0688	0.159	0.0663
$Pb(NO_3)_2$	0.050	0.0878	0.159	0.0756
$NiCl_2$	0.050	0.0680	0.159	0.0705
$Cd(NO_3)_2$	0.050	0.0695	0.159	0.0745

In the case of wheat plantlets extract, specific activity values show significant differences, compared to their evolution in the root extract (Fig. 2). This increasing variation of activities corresponding to the treatments with 7 types of toxic indicates that there is a much larger protein specific activity in wheat plantlets than in roots, varying according to the applied treatment. Consequently, a lower activity was identified in case of treating with $AgNO_3$ and $CuCl_2$ and a larger one was identified when treating with $Cd(NO_3)_2$, $HgCl_2$, $NiCl_2$ and $Pb(NO_3)_2$.

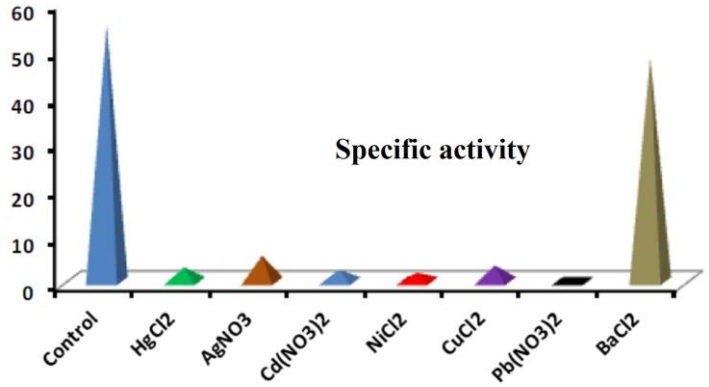

Fig. 2. *Specific activities of the protein extract obtained from wheat plantlets after treating with heavy metals*

Determining the peroxidase activity

The much more intense activity of peroxidase in the experimental batch can be clearly attributed to $NiCl_2$. In other words, Ni^{2+} interferes in the germination and growth processes of wheat plantlets. It is well known that the seed deterioration process starts immediately after harvesting, various intrinsic and extrinsic factors contributing to this. For this reason, to prevent rapid loss of vigor, viability and productivity, a controlled approach of their depositing is necessary, especially in environments where the deterioration rate is imposed by a hostile condition (high heat and increased humidity). Applying various treatments substantially slows down the deterioration rate and rapidly increases the seeds viability rate.

Tabel 4. *Peroxidase activity values in wheat plantlets after 7 days of treatment*

Treatment	UP/mg protein
Control	4.52
$HgCl_2$	7.52
$AgNO_3$	8.63
$Cd(NO_3)_2$	8.99
$NiCl_2$	15.98
$CuCl_2$	7.32
$Pb(NO_3)_2$	6.12
$BaCl_2$	5.73

Determining catalase activity

The intensification of the two enzymes (peroxidase and catalase) activity denotes the fact that the heavy metals treatment is capable of inducing a significant decoupling of the transport chain of electrons and of the oxidative phosphorylation, resulting in dissipating the membrane gradient and, consequently, increasing the production of oxygen reactive species. This explains the catalase activity intensification in plantlets treated with $NiCl_2$ (40.72 UC/mg protein), compared to plantlets from the control batch (15.18 UC/mg protein) (Fig. 3).

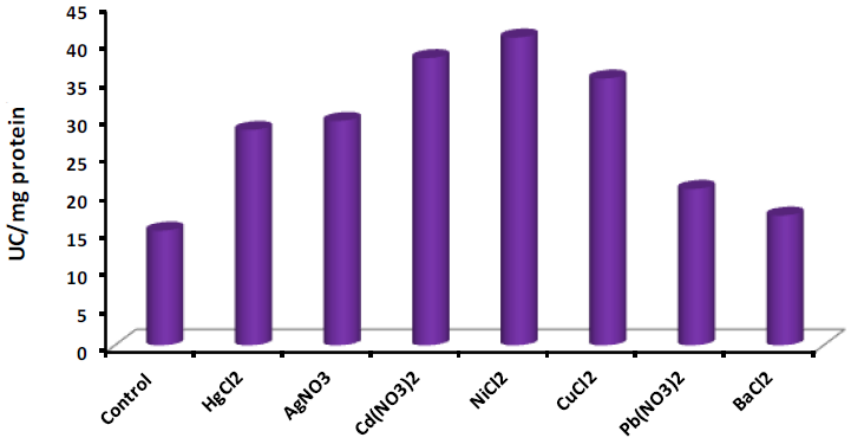

Fig. 3. *Determining catalytic activity from wheat plantlets exposed to 7 days of treatment*

4. Conclusions

The present paper proved the toxic effects of heavy metals on the viability of plants. This experiment revealed the sensitivity of wheat seeds to heavy metals, which inhibit the plants growth. Individual heights and the unitary average mass reflect the effects of various treatments more precisely. This could be explained by the fact that the effect owed to the number of unsprouted seeds is removed, only taking into account individual plants that had effectively suffered from the treatment. Also, these differences are also caused by the fact that each compound specifically influences each plant. Every living organism reacts specifically to exterior factors. Thus, dead seeds were not taken into account in case of individual height and unitary average mass.

Enzymatic activity of vegetal species was determined. Wheat extracts were concentrated and exposed to subsequent stages of concentration (ammonium precipitate) and dialyze. Enzymatic extracts stability was relatively high for short periods (1 week), but was substantially modified in case of storing for longer periods (remained enzymatic activity was 30-40% after 3 weeks).

Enzymes involved in respiratory processes are very attractive for understanding the evolution of life, from the prokaryote to the eukaryote stage, as well as for classifying pathological modifications that take place in malign processes, where the reversed

phenomenon of transition takes place (from normal respiration of cells to lactic fermentation, with all biochemical implications: pH modification of body fluids, degradation of ramified essential aminoacids etc.).

The method of enzymatic determinations can be successfully applied particularly in the case of plantlet roots, due to the more accentuated inhibition. The extraction degree is influenced by the dimensions of the plant parts. Enzymatic activity from various plant compartments significantly differs based on treatment or source. To conclude, the value of enzymatic activity in roots is superior to that in leaves, and the type of phenolic extract used influences the enzymatic activity.

Acknowledgments

Funding from the Romanian Government (PN-II-PT-PCCA-2013-4-1149, Contract 107/2014) is gratefully acknowledged. Marius Z. acknowledges the Grants for young researchers of UAIC (Contract 21754/03.12.2015) project from Alexandru Ioan Cuza University of Iasi.

References

[1]. Pintilie O., Andries C., Cosma A., Zaharia M., Drochioiu G., Vasilache V., Sandu I., *The influence of dinitrophenolic pesticides on the viability of plants*, *Rev. Chim. (Bucharest)*, 66 (9), p. 1321-1326, 2015.

[2]. Pintilie O., Cosma A., Zaharia M., Murariu M., Drochioiu G., Sandu I., *Conservarea genetică a varietăților vegetale autohtone și modificările biochimice*, Revista Tehnocopia, 2 (11), p. 18-23, 2014.

[3]. Pintilie O., Zaharia M., Tudorachi L., Cosma A., Ciobanu C., Drochioiu G., Sandu I., *Sisteme de apărare ale organismului împotriva otrăvirii cu metale grele*, Scientific, Technological and Innovative Research in Current European Context (International Workshop EUROINVENT), Alexandru Ioan Cuza University Publishing House, p. 109-118, 2014.

[4]. Drochioiu G., Sunel V., Oniscu C., Basu C., Murariu M., *The breakdown of plant biostructure followed by amino acids determination*, Roum. Biotechnol. Lett., 6 (2), p. 155-165, 2001.

[5]. Cosma A., Bontas D., Pintilie O., Zaharia M., Drochioiu G., Sandu I., *De la teoria biostructurala la determinarea aminoacizilor liberi din plante*, Revista Tehnocopia, 2 (11), p. 5-11, 2014.

[6]. Yuan H., Lu T., Wang Y., Chen Y., Lei T., *Sewage sludge biochar: Nutrient composition and its effect on the leaching of soil nutrients*, Geoderma, 267, p. 17-23, 2016.

[7]. Fodor F., *Physiological response of vascular plants to heavy metals*, Physiology and Biochemistry of Metal Toxicity and Tolerance in Plants, Ed. M. N. Prasad, Kazimierz Strzalka, Springer, 6, p. 149-177, 2002.

[8]. Georgiev P., Groudev S., Spasova I., Nicolova M., *Ecotoxicological characteristic of a soil polluted by radioactive elements and heavy metals before and after its bioremediation*, J. Geochem. Explor., 142, p. 122-129, 2014.

[9]. Philippe Vernay P., Gauthier-Moussard C., Hitmi A., *Interaction of bioaccumulation of heavy metal chromium with water relation, mineral nutrition and photosynthesis in developed leaves of* Lolium perenne *L.*, Chemosphere, 68, p. 1563-1575, 2007.

[10]. Lyubenova L., Schröder P., *Uptake and effect of heavy metals on the plant detoxification cascade in the presence and absence of organic pollutants*, Soil Biol, 19, p. 65-85, 2010.

[11]. Peyton D. P., Healy M. G., Fleming G. T. A., Grant J., Wall D., Morrison L., Cormican M., Fenton O., *Nutrient, metal and microbial loss in surface runoff following treated sludge and dairy cattle slurry application to an Irish grassland soil*, Sci. Total Environ., 541, p. 218-229, 2016.

[12]. Gergen I., Harmanescu M., *Application of principal component analysis in the pollution assessment with heavy metals of vegetable food chain in the old mining areas*, Chem. Cent. J., 6, p. 156-169, 2012.

[13]. Alloway B. J., *Heavy metals in soils*, Environ Pollution, 22, p. 3-9, 2013.

[14]. Pallardy S. G., *Physiology of woody plants*, Elsevier Inc., 2008.

[15]. Rees F., Sterckerman T., Morel J. L., *Root development of non-accumulating and hyperaccumulating plants in metal-contaminated soils amended with biochar*, Chemosphere., 142, p. 48-55, 2016.

[16]. Lal N., *Molecular mechanisms and genetic basis of heavy metal toxicity and tolerance in plants*, *Plant*, Adapt. Phytoremed., p. 35-58, 2010.

[17]. Garcia-Sánchez M., Garcia-Romera I., Cajthaml T., Tlustoš P., Száková J., *Changes in soil microbial community functionality and structure in a metal-polluted site: The effect of digestate and fly ash applications*, J. Environ. Manage, 162, p. 63-73, 2015.

[18]. Nosko P., Brassard P., Kramer J. R., Kershaw K. A., *The effect of aluminium on seed germination and early seedling establishment growth and respiration of white spruce (Picea glauca)*, Can. J. Bot., 66, p. 2305-2310, 1988.

[19]. Peralta J. R., Gardea-Torresdey J. L., Tiemann K. J., Gomez E., Arteaga S., Rascon E., Parsons J. G., *Uptake and effects of five heavy metals on seed germination and plant growth in alfalfa* (Medicago sativa L.), B. Environ. Contam. Tox., 66 (6), p. 727-734, 2001.

[20]. Munzuroglu O., Geckil H., *Effects of metals on seed germination, root elongation, and coleoptile and hypocotyl growth in* Triticum aestivum and Cucumis sativus, Arch. Environ. Contam. Toxicol, 43 (2), p. 203-213, 2002.

[21]. Pintilie O., Ion L., Surleva A., Zaharia M., Ciornea Todirascu E., Ciubotariu E., Balan A., Drochioiu G., Sandu I., *Monitoring methods of plants viability in genetic conservation*, Rev. Chim. (Bucharest), 67 (4), p. 687-691, 2016.

[22]. Artenie V. I., Ungureanu E., Negură A. M., *Metode de investigare a metabolismului glucidic şi lipidic*, Ed. Pim, Iaşi, 2008.

[23]. Cojocaru D. C., *Enzimologie practică*, Editura Tehnopress, Iaşi, p. 245-247, 2009.

[24]. Pintilie O., Zaharia M., Tudorachi L., Bancila S., Drochioiu G., Sandu I., *Emphasizing the Toxicity of Heavy Metal Ions on Plants: Monitoring with an Amino Acids Assay*, The annals of "Dunarea de Jos" University of Galati. Fascicle IX. Metallurgy and Materials Science, N°. 1, p. 51-57, 2014.

THE ANNALS OF "DUNAREA DE JOS" UNIVERSITY OF GALATI
FASCICLE IX. METALLURGY AND MATERIALS SCIENCE
N°. 1 - 2016, ISSN 1453 – 083X

THE ECO-EFFICIENCY OF RECYCLING ORGANIC WASTE FOR AGRICULTURE PURPOSES

Cristian BANACU[1], Bianca Georgiana OLARU[2]
[1]Bucharest University of Economic Studies, 6 Piata Romana,1st District, Bucharest, 010374, Romania
[2]University of Agronomic Sciences and Veterinary Medicine, no 59, Mărăști street, 1st District, Bucharest, 011464, Romania
[a]cristian.banacu@gmail.com, [b]biancageorgiana.olaru@gmail.com*

ABSTRACT

One of the problems of the cities is the raising of household waste, with polluting effects on the environment. On the other hand, in agriculture, through specific activities necessary to ensure food, fertilizers are needed, which could be used for the commands of sustainable development. Depending on environmental conditions, the negative impact can be indicated that they have on the human population by affecting plants, animals and, not least, people. Developed countries, such as the Netherlands, UK, Germany, France, Switzerland, have invested in technologies for the transformation of household organic waste into biofertilizers with low impact to the environment. The present article tries to analyze and underline the eco-efficiency of transforming organic waste into biofertilizers.

KEYWORDS: sustainable development, eco-development, organic waste, green development, eco-management, eco-efficiency

1. Introduction

The theme of this paper is important in terms of increasing the quality of life, so superficially treated for methodological and procedural aspects. Essentially, the mismanagement of waste is an important cause regarding environment pollution and threats to human health, at the same time reflecting the inefficient use of natural resources. Therefore, one of the highest risks for people is represented by ineffective and irresponsible collection and recycling of waste which pollutes the environment. For example, waste management technologies, such as land filling and incineration, do not represent a complete solution to existing problems. Some organizations have one of the most important tasks, i.e., the continuous improvement of waste disposal usage. Additionally, in order to protect the environment, it is necessary to eliminate waste or to transform it into useful products. In the same time, it may be required to review the identification of waste. The main focus of the present article is waste elimination, to ensure that the manufacturing sector progresses towards ecoefficient production processes and a hazard-free workplace environment. For example, in agriculture recycling organic wastes can preserve finite phosphate resources and the embodied energy from industrial nitrogen fixation, thus helping to increase sustainable food production. Some waste, such as wood waste and paper sludge, offer organic alternatives to animal use. The agricultural uses of wastes ensure the protection of human health and of the environment.

2. Literature Review

"Most countries have traditionally utilized various kinds of organic materials to maintain or improve the tilth, fertility and productivity of their agricultural soils" [2].

Recycling organic wastes in agriculture can reduce the need for fertilizers and even restore organic carbon deficiency in the soil.

Recycling of organic wastes (such as biogas residues and sewage sludge) to agriculture has been a widely-discussed subject for decades [5].

"Organic agriculture augments ecological processes that foster plant nutrition yet conserves soil and water resources. Organic systems eliminate agrochemicals and reduce other external inputs to improve the environment and farm economics. Among the benefits of organic technologies there are higher soil organic matter and nitrogen, lower fossil energy inputs, yields similar to those of conventional

systems, and conservation of soil moisture and water resources" [6].

Despite the economic crisis, people focus on buying organic products that do not harm health, the organic farming sector is increasingly popular because it is benefic to human health.

Additionally, it should be noted that a significant share of the whole quantity of waste is represented by non-biodegradable materials (plastic, glass, metal, etc.) that were considered by European legislation as agents of soil pollution and contaminants that are to be eliminated.

"Everyday waste consists of 45% food waste, 24% plastic, 7% paper and 6% iron. Approximately 95-97% of waste collected is taken to landfill for disposals. Wastes which remain are sent to small incineration plants, or diverted to recyclers/re-processors or is dumped illegally. Actually, *only 5% of waste is recycled, however the government aims to reach a ceiling of 22% in terms of waste recycled by 2020"* [9].

The good practice we teach is that the best strategy for guaranteeing high standards of waste is to separate at collection in new developments and restoration areas e.g. "*at door-to-door waste collection".*

"As global environment and climate change are challenges the world faces today, there is an increasing need to evaluate the impact of waste management on environmental quality and greenhouse gas emissions" [3.]

Currently, there are various treatment methods that can be applied to a good management of natural resources and ecological recycling options are a priority for the recovery of organic waste.

It additionally shows that *"current waste management practices in relation to composites are dominated by landfilling*" [12] *"which still is a relatively inexpensive option for industry in comparison to alternatives. However, it is the least preferred option according to legislation*" [7].

In addition, the approaches to eco-efficiency and resource development can be combined. This article may have implications on how eco-efficiency can be quantified in waste management.

"Sustainable consumption behavior occurs when consumers have two positive attitudes: firstly, as regards sustainability and environment and, secondly, when there is a greater personal responsibility and involvement displayed" [4].

Recycling included feeding vegetable waste to livestock and using eco-waste as fertilizer.

3. Research methodology

3.1. European Directives on Waste Management

a. Waste Framework Directive 2008/98/EC sets the basic concepts and definitions related to waste management, such as definitions of waste, recycling, recovery. It explains when waste ceases to be waste and becomes a secondary raw material (so called end-of-waste criteria), and how to distinguish between waste and by-products. The Directive lays down some basic waste management principles: it requires that waste be managed without endangering human health and harming the environment, and in particular without risk to water, air, soil, plants or animals, without causing a nuisance through noise or odors, and without adversely affecting the countryside or places of special interest. Figure 1 presents briefly the main features of waste management that must be taken into account,: (i) *waste prevention*, by application of "clean technologies" in waste generating activities; (ii) *reduction of waste quantities*, by implementing best practices in everyday waste generating activity; (iii) *valorification*, by reuse, material recycling and energy recovery; (iv) *disposal*, by incineration and landfill.

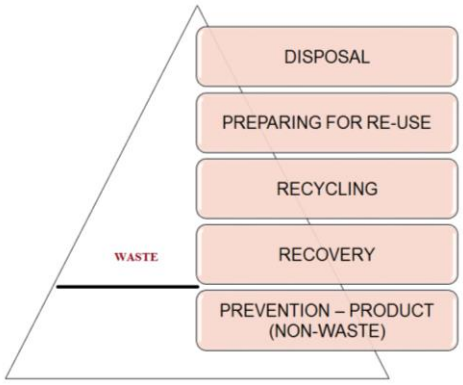

Fig. 1. *Waste recycling*

This Directive introduces the ***polluter pays principle*** and the "extended producer responsibility". It incorporates provisions on hazardous waste and waste oils (old Directives on hazardous waste and waste oils being repealed, in force since 12 December 2010), and includes two new recycling and recovery targets to be achieved by 2020: 50%.

Preparing for re-use and recycling of certain waste materials from households and other origins similar to households, and 70% preparing for re-use, recycling and other recovery of construction and demolition waste.

***b. Directive 2000/76/EC of the European Parliament* and of the Council of 4 December 2000 on incineration of waste.** The European Union imposes strict operating conditions and technical requirements on waste incineration plants and waste co-incineration plants to prevent or reduce air, water and soil pollution caused by the incineration or co-incineration of waste. Emission limits are introduced for certain pollutants released to air or to water.

c. The Landfill Directive

Council Directive 1999/31/EC on the landfill of waste (the Landfill Directive) was agreed in Europe at Council on 26 April 1999 and came into force in the EU on 16 July 1999. The Directive aims to harmonize controls on the landfill of waste throughout the European Union, and its main focus is to achieve common standards for the design, operation, and aftercare of landfill sites. It also aims to reduce the amount of methane, a powerful greenhouse gas, emitted from landfill sites.

3.2. Specific responsibilities for waste

The issue of responsibility for waste management implies an inherent hierarchy from individual and family responsibilities at the institutional, legal and community levels. Generally speaking, everybody is responsible regarding waste recycling. Additionally, it is important to understand that as the quantity of waste increases, there is also an accumulation of effects, some of which are evil because they lead to pollution and decrease in comfort, others are beneficial as they create a natural source of raw materials and recyclable materials. It is also essential to have clarity regarding the action of factors acting as producers of waste. Therefore, the legislation on waste management clearly imposes certain responsibilities incumbent upon the waste producer but not on processing such material. If reference is made to the guidance about `Waste Management: The Duty of Care - A Code of Practice` these responsibilities for the producer can be defined as: (i) "*the person who made the substance become waste e.g. by breaking or contaminating it"*; (ii) "*the person who decided that a substance was unwanted and therefore waste"* [10].

3.3. Indicators of eco-efficiency

Eco-efficiency indicators are used to illustrate whether there is a decoupling of environmental impact and the sectors' economic activity or not.

Quality of economic growth represents the making the green concept of growth operational for public policies, which requires a measurement that would capture the pattern.

The main indicators of eco-efficiency are the following: (i) measure the eco-efficiency of different sectors within the country; (ii) compare the eco-efficiency of economic growth of different countries; (iii) identify policy areas for improvement in achieving economic benefit.

The eco-efficiency indicators of the World Business Council for Sustainable Development are: *"(i). minimize the material intensity of goods and services; (ii) minimize the energy intensity of goods and services; (iii). minimize toxic dispersion; (iv) enhance material recyclability; (v) maximize the use of renewable resources; (vi). extend product durability; (vii) increase the service intensity of goods and services"* [11].

If reference is made to the economic instruments, for example user charges for managing municipal waste (e.g. 'pay-as-you-throw' schemes), landfill taxes and product charges can play a significant role in diverting waste from landfill if they are designed in such a way that they regulate the behavior of households, waste companies and producers effectively.

3.4. Comparative analyses

In Romania, currently there is still no system collecting organic waste separately from other waste categories even though there have been important steps towards selective waste selection.

Furthermore, there are no technology firms that would take over, process and transform organic household waste into compost and then into organic fertilizer. However, there is no legislative framework to stimulate and encourage initiative in this area. Therefore, studies should be carried out to evaluate the environmental impact of both domestic organic waste disposals in landfills and combustion (CO_2 emissions in conjunction with other sources, transport, industry, etc. that amplify the greenhouse effect and global climate change) and salting excess land and underground water sources compromised.

Generally, diverting waste from landfill has relied on combinations of policies aimed at households, waste companies and producers. And countries have progressed or plan to progress further towards the Landfill Directive targets by strengthening several alternative waste treatment paths, rather than focusing on just one. The strategies usually include a combination of recycling, incineration, and/or mechanical-biological treatment. On the other hand, the quality of the compost derived from separately collected biodegradable waste is not always sufficient.

"Countries with high dependence on landfill can take positive action against climate change by landfilling less biodegradable waste. Likewise, in

countries that have very low landfill rates, waste recycling and energy recovery can help avoid greenhouse gas emissions from the production of virgin material or energy" [1].

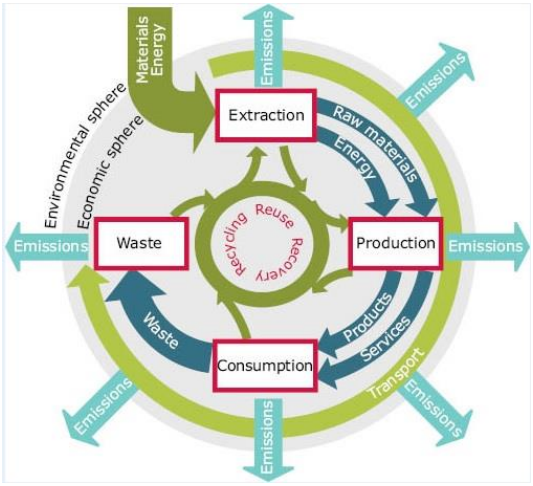

Fig. 2. *Life-cycle chain: extraction - production - consumption - waste (EEA, 2012)*

Figure 3 below exemplifies methods of waste treatment in several states; as for Romania, it can be noticed that recycling and disposal in landfills are most frequent [8].

According to Eurostat (2012), Figure 2 below shows that between 2004 and 2012 progress has been made in terms of waste recycling by using methods of incineration, but also reuse, especially in 2008, in European countries [8].

Figure 3 lists the quantities of waste from various sources of business, and in our country the highest amounts of waste resulting from mining and quarrying / mining and other economic activities similar and / or complementary.

In developed countries, such as Germany, UK, Sweden, the Netherlands, etc., materials and resources must be used to their full potential, and this has propagated a culture of reuse, repair and recycling.

Also, there are three main methods in which organic waste can be used: (i) soil improvement, (ii) animal raising and (iii) provision of source of energy.

	Total	Recycling	Energy recovery	Backfilling	Incineration	Disposal
EU-28	2 302 560	838 960	101 140	213 790	36 650	1 112 020
Belgium	41 328	30 237	4 612	0	3 331	3 148
Bulgaria	158 752	1 789	172	0	14	156 777
Czech Republic	18 263	8 420	959	5 137	76	3 670
Denmark	14 070	8 147	3 255	0	0	2 668
Germany	352 996	152 807	33 953	91 469	11 017	63 750
Estonia	20 610	7 903	349	4 196	0	8 162
Ireland	8 033	827	403	1 985	13	4 805
Greece	71 334	2 928	118	5 440	21	62 827
Spain	108 475	48 745	3 269	8 194	7	48 259
France	315 147	151 724	11 637	39 591	7 153	105 042
Croatia	2 999	994	39	42	0	1 923
Italy	130 460	98 809	2 593	160	5 814	23 084
Cyprus	2 077	409	2	232	7	1 429
Latvia	1 573	808	153	0	1	612
Lithuania	4 221	999	106	0	1	3 115
Luxembourg	10 302	4 691	36	1 934	134	3 507
Hungary	12 964	4 637	960	436	90	6 842
Malta	1 351	116	0	46	6	1 183
Netherlands	119 962	61 796	8 997	0	1 612	47 556
Austria	32 122	14 272	3 305	2 795	75	11 675
Poland	160 697	80 941	3 567	35 103	328	40 757
Portugal	10 188	4 598	1 735	0	70	3 785
Romania	264 647	18 849	1 708	1 037	182	242 871
Slovenia	5 068	2 965	326	1 102	36	639
Slovakia	7 052	2 651	270	0	71	4 059
Finland	90 478	31 700	10 317	0	445	48 015
Sweden	151 225	18 732	6 712	774	43	124 964
United Kingdom	186 163	77 467	1 585	14 114	6 102	86 895
Iceland	521	344	14	3	0	160
Norway	10 103	4 303	4 271	143	86	1 300
FYR of Macedonia	9 023	68	19	0	41	8 896
Serbia	55 023	793	49	0	0	54 180
Turkey	983 046	307 467	440	0	44	675 095

Source: Eurostat (online data code: env_wastrt)

Fig. 3. *Waste Treatment (Eurostat, 2012)*

In Figure 6 (diagram) the differing levels of processing required can be observed and in this section, we will take a brief look at just some of the common approaches to using organic waste.

The agricultural potential that Romania has may lead to the use of organic waste that allows the development of organic farming. Environmental policies are necessary to educate citizens / employees of companies on corporate responsibility actions involving recycling promotion. Ecological agriculture offers a modern alternative that helps reduce organic waste, thereby leading to the reduction / elimination

of pollution, better soil fertility and food production and providing a source of income for farmers.

Bio-fertilizers are an essential component of ecological agriculture and involve the preparations containing live or latent cells of efficient strains of nitrogen fixing, phosphate solubilizing or cellulolytic micro-organisms used for application to seed, soil or composting areas with the objective of increasing number of such micro-organisms and accelerate those microbial processes which augment the availability of nutrients that can be easily assimilated by plants.

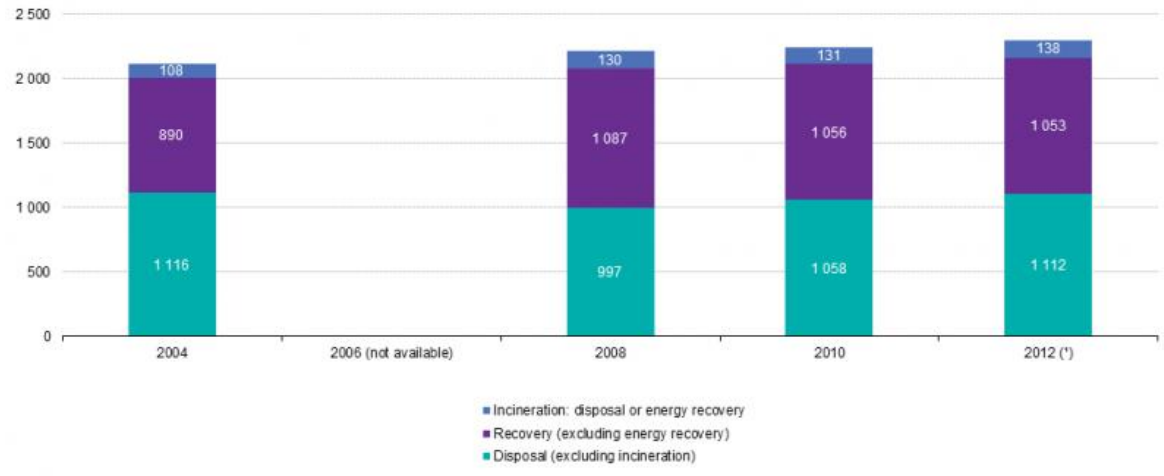

(*) Estimates.
Source: Eurostat (online data code: env_wastrt)

Fig. 4. *Recycling methods used in Europe (Eurostat, 2012)*

	Total	Mining and quarrying	Manufacturing	Energy	Construction and demolition	Other economic activities	Households
EU-28	2 515 110	733 980	269 690	96 480	821 160	380 390	213 410
Belgium	67 630	115	17 736	1 314	24 570	18 891	5 004
Bulgaria	161 252	141 083	3 009	9 533	1 033	3 841	2 755
Czech Republic	23 171	167	4 376	1 063	8 593	5 739	3 233
Denmark	16 332	18	1 610	893	3 867	6 216	3 727
Germany	368 022	8 625	56 596	8 050	197 528	60 752	36 472
Estonia	21 992	9 355	4 121	6 258	657	1 165	436
Ireland	13 421	2 025	4 599	396	366	4 379	1 657
Greece	72 328	47 832	4 183	12 259	813	2 383	4 859
Spain	118 562	22 509	14 594	5 772	26 129	28 333	21 224
France	344 732	2 477	21 431	2 100	246 702	42 024	29 996
Croatia	3 379	5	425	108	682	968	1 191
Italy	162 765	720	34 142	3 616	52 966	41 708	29 613
Cyprus	2 086	218	98	2	965	353	451
Latvia	2 310	2	396	133	8	558	1 213
Lithuania	5 679	26	2 551	29	419	1 477	1 177
Luxembourg	8 397	131	509	2	7 079	426	249
Hungary	16 310	91	2 991	2 872	4 038	3 638	2 681
Malta	1 452	45	9	2	1 041	201	155
Netherlands	123 613	179	14 115	1 342	81 354	17 758	8 864
Austria	34 047	51	3 636	622	19 471	6 247	4 020
Poland	163 378	68 035	31 135	20 706	15 368	18 809	9 324
Portugal	14 184	243	3 188	422	928	4 672	4 731
Romania	266 976	223 293	6 029	9 043	1 325	22 638	4 647
Slovenia	4 547	14	1 345	1 069	535	941	641
Slovakia	8 425	311	2 516	1 046	806	2 090	1 657
Finland	91 824	52 880	14 531	1 011	16 034	5 635	1 734
Sweden	156 367	129 481	6 218	1 852	7 656	6 967	4 193
United Kingdom	241 922	24 044	13 596	4 965	100 230	71 580	27 506
Iceland	529	0	93	2	11	191	233
Liechtenstein	467	29	12	0	107	2	316
Norway	10 721	470	2 639	89	1 881	3 205	2 438
Montenegro	386	1	33	351	0	0	0
FYR of Macedonia	8 472	802	1 304	6	0	6 360	0
Serbia	55 003	47 896	760	5 744	364	238	0
Turkey	1 013 226	950 587	13 141	18 424	0	289	30 785
Bosnia and Herzegovina	4 457	72	1 213	3 171	0	0	0
Kosovo	1 167	177	80	151	0	268	490

Source: Eurostat (online data code: env_wasgen)

Fig. 5. *Sources of provenance of the waste (Eurostat, 2012)*

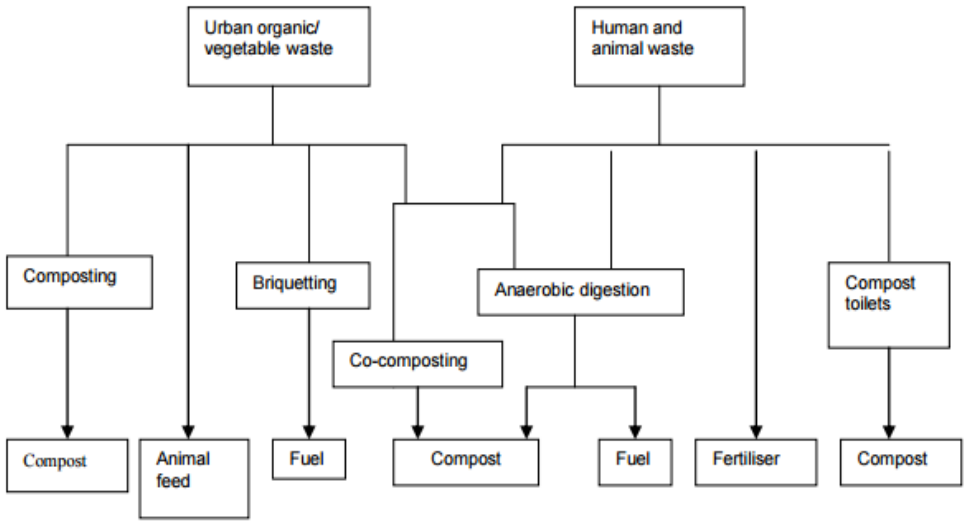

Fig. 6. *Structure of organic waste*

The importance of bio-fertilizers results from the following: (i) increase the yield of plants by 15-35%, (ii) bio-fertilizers are effective even under semi-arid conditions, (iii) farmers can prepare the inoculum themselves, (iv) improve soil texture, (v) bio-fertilizers do not allow pathogens to flourish, (vi) produce vitamins and growth promoting bio-chemical's, (vii) are non-polluting.

4. Conclusion

In conclusion, the difference between recycling methods in European countries is obvious. Finally, it may indicate that the responsibility of the government or municipality is waste collection and disposal. Also, in many cases the municipality is unable to fulfil this role either due to financial constraints, lack of will or lack of organizational skills. It has been noted that it is of great help if the organic and non-organic waste is separated at source. Many successful methods are only successful because of community participation in the activities on a day-to-day basis. Where waste is separated at source, this lessens the risk of contamination from items such as batteries, meaning that the organic waste is cleaner (and will therefore fetch a higher price), it is easier to sort and the incidence of injury and disease related to sorting is decreased. There is a number of good examples of community recycling or resource recovery schemes in developing countries.

The commonly used methods of recycling in Europe are landfills and incinerators, that is precisely why we need an ecological recycling.

Also, recycling organic waste plays an important role in agriculture through bio-fertilizers on soil that have beneficial properties.

References

[1]. EEA, *Better management of municipal waste will reduce greenhouse gas emissions*, EEA Briefing 1/2008, European Environment Agency, Copenhagen, 2008.
[2]. Parr J. F., Papendick R. I., Colacicco D., *Biological Agriculture and Horticulture*, Academic Publishers, Printed in Great Britain, vol. 3, p.115-13, 1986.
[3]. Lou X. F., Nair J., *The impact of landfilling and composting on greenhouse gas emissions - A review*, Bioresource Technology, 100, p. 3792-3798, 2009.
[4]. Luchs M. G., Phipps M., Hill T., *Exploring consumer responsibility for sustainable consumption*, J. Market. Manag., 31, p. 1449-1471, (CrossRef), 2015.
[5]. Odlare M., Arthurson V., Pell M., Svensson K., Nehrenheim E., Abubaker J., *Land application of organic waste - Effects on the soil ecosystem*, Applied Energy, 88, p. 2210-2218, 2011.
[6]. Pimentel D. *et al.*, *Environmental, Energetic, and Economic Comparisons of Organic and Conventional Farming Systems*, BioScence, vol. 55 n., 7, p. 573-582, 2005.
[7]. ***, *Council Directive 2008/98/EC*.
[8]. ***, *Eurostat*, 2012.
[9]. ***, *Malaysia Environment-Current*, issues-Geography, 2010.
[10]. ***, *Waste Management: The Duty of Care - A Code of Practice*, 2014.
[11]. World Business Council for Sustainable Development, http://www.wbcsd.org.
[12]. ***, *WRAP*, http://www.wrap.org.uk, 2013.

THE ANNALS OF "DUNAREA DE JOS" UNIVERSITY OF GALATI
FASCICLE IX. METALLURGY AND MATERIALS SCIENCE
N°. 1 - 2016, ISSN 1453 – 083X

THE INFLUENCE OF SPEED COOLING ON SOME PROPERTIES OF LAMINATED STEEL

Carmen Penelopi PAPADATU, Marian BORDEI
"Dunarea de Jos" University of Galati, Romania
e-mail: papadatu.carmen@ugal.ro

ABSTRACT

This study presents a possibility to predict the connection between the cooling regime and the properties of steel. An important factor to enhance the properties of steel is the speed of the cooling regime. To be in accordance with the experimental results, this study considered a correlation between the speed of cooling for laminated steel with a low carbon content and other properties of steel. It is important to choose the optimal cooling regime because the steel was laminated at high temperature.

KEYWORDS: steel properties; cooling speed, correlation; statistical model

1. Introduction

Carbon is the most important element of steel because this chemical element determines the chemical structure and its properties. In the case of steel with a low content of carbon, its structure has two important components: Ferrite (F) and pearlite (P). Ferrite has a low mechanical strength but has plastic properties. Cementite in steel has high hardness but is fragile. Therefore, an increased content of carbon increases the hardness and the strength of steel and decreases its plasticity.

For example, the literature shows that for steels with 0.11% C, 0.48% Mn, and 0.24% Si the microstructural parameters which determine their mechanical properties are the size and shape of pearlitic and ferritic grains. The microstructure of this type of steels is formed by pearlite (P) and ferrite (F) as constituents. These types of steels are used currently without chemical treatments, for metal construction and machine building, for elements of metal structures subjected to small requests. Because the steel with low carbon content has high plastic properties below 550 °C, the thermal stresses will not lead to the formation of cracks.

Damage of materials means the progressive or sudden deterioration of their mechanical strength due to loading, thermal or chemical effects (*see [4] Vuong Nguyen Van Do 2016*). It is important to know how the properties of steels can be improved. For this case, it is necessary to find a causal relation between a technological parameter (the speed of cooling regime) and the mechanical properties of steel (for example, the resilience – KV - of steel).

After an experimental program, the values obtained were used to determine a correlation between these variables through an empirical study.

2. Experimental results

Three groups of 8 steel samples were considered. The chemical composition of the material is presented in Table 1. Three cooling regimes were applied: (1) cooling regime in normal conditions; (2) cooling in airflow (in jet of air); (3) cooling in the metallic recipient.

Table 1. *Chemical composition of steel*

Steel grade	C (%)	Mn (%)	Si (%)	P (%)	S (%)	Al (%)
Fe510 (Euronorm); S355	0.14	1.51	0.31	0.010	0.010	0.041

The initial temperatures were: 850 °C (for the first batch of samples), 900 °C (for the second batch of samples), 950 °C (for the third batch of samples) and 1000 °C (for the last batch of samples). If the cooling mediums are different, the speeds of the cooling are different, too.

In Figure 1 was represented the evolution of the thinning of the samples (Z or Ψ) during the tensile

tests [6]. In Figure 2 was represented the evolution of the resilience (KV+20 °C) which depends on the initial temperatures, in the first case [6].

In Figures 3 and 4 are presented the variations of the resilience (KV +20 °C), in the other two different cooling regimes: in metallic box and in jet of air. The best values have been obtained in the cases of higher values of the cooling speed, in jet of air regime.

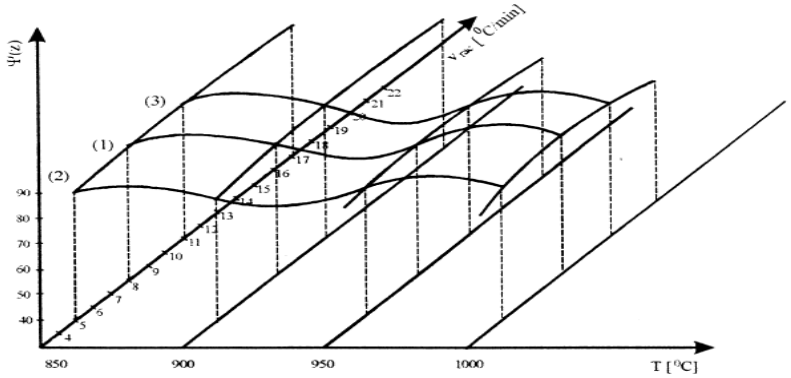

Fig. 1. *Thinning of the samples during the tensile tests depending on cooling regimes (1, 2 or 3) and on initial temperature*

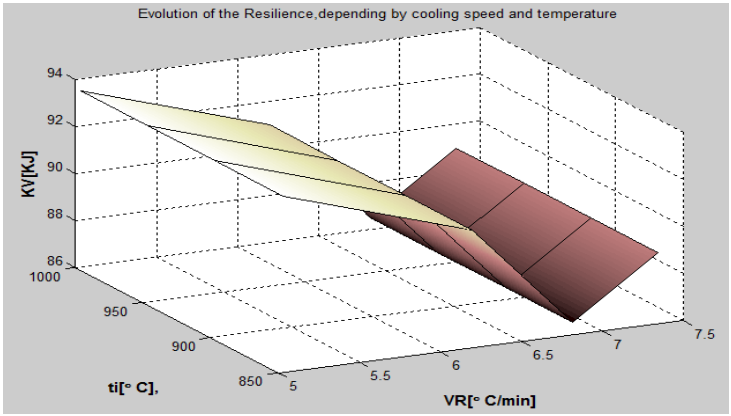

Fig. 2. *Evolution of resilience (KV), depending on cooling speed (VR) and initial temperature, for the cooling regime (1)*

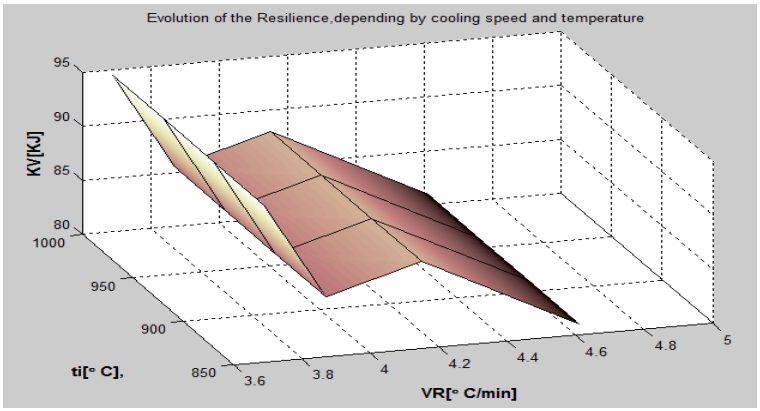

Fig. 3. *Evolution of resilience (KV), depending on cooling speed (VR) and initial temperature, for the cooling regime (3)*

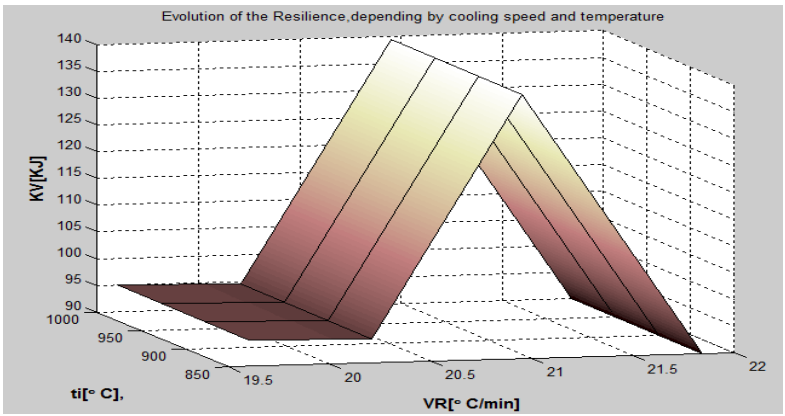

Fig. 4. *Evolution of resilience (KV), depending on cooling speed (VR) and initial temperature, for the cooling regime (2)*

The thinning of the samples (Z or Ψ) during the tensile tests is higher in the case of the initial temperature T = 1000 °C and the speed of cooling VR = 21.84 °C/s (cooling in jet of air). In the case of cooling in jet of air, the speed of the cooling will be the highest and the mechanical properties have the best results.

In Table 2 are presented some of the experimental results obtained [6].

Table 2. *Obtained experimental results*

Speed of cooling Vrac [°C/S]	HB	A5[%]	KV [KJ]	Cooling regime	Code samples
4.61 (cooling in metallic recipient)	162.5	31.05	89	(2)	2.8
7.35 (cooling in normal conditions)	181.5	32.5	81	(1)	2.4
21.84 (cooling in jet of air)	184	33.2	90	(3)	2.13

3. Statistical model

To determine the model parameters, this operation can be performed using the method of least squares. It starts from the regression equation of a simple linear model. For example, to prove the causation between the cooling speed (VR.) and the resilience (KV-20 °C) in the case of the initial temperature Ti = 850 °C, statistical methods were used to check the next assumption: we assume that there is a causal relationship between the independent variable "VR" and a dependent variable "KV". Between these variables there is a direct connection. In Figure 3 was represented the evolution of the resilience of steel at 850 °C, which depends on the type of the cooling regime.

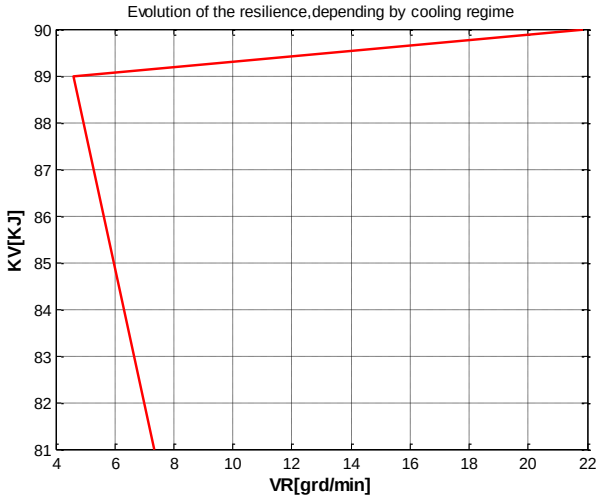

Fig. 5. *Resilience (KV) depending on cooling speed corresponding to different regimes*

To study the correlation between the variables we used unifactorial regression. Unifactorial regression can describe with success the relationship between two analyzed indicators. In the case of unifactorial regression, only the variable factor (x) has an action on the result feature (y) [3]. Other possibly factors have a constant action negligible (y-f(x)). The estimation function is given by the following expression:

$$\hat{y} = a + b \cdot x \quad (1)$$

We have the following expressions *(see [1-3] or Scradeanu 2015)*:

$$n\hat{a} + \hat{b}\sum_{i=1}^{n} x_i = \sum_{i=1}^{n} y_i \quad (2)$$

$$\hat{a}\sum_{i=1}^{n} x_i + \hat{b}\sum_{i=1}^{n} x_i^2 = \sum_{i=1}^{n} x_i y_i \quad (3)$$

It is estimated that the bond between these two variables (VR and KV) is represented by the equation of straight line. The mathematical model must continue with the characterization of the connection intensity between the two variables using the correlation coefficient "$r_{x,\ y}$" and the correlation report (*see Scradeanu, 2015 and Simofi, 2013*).

In this case, n = 3 and the system of the equations (4) will be:

$$3\ a + 33.79\ b = 260$$
$$33.79\ a + 552.259\ b = 2971.24$$

Solving the system and applying the substitution method, results:

$$b = 0.249 > 0$$
$$a = 83.860$$

The estimation function will be:

$$y = 83.860 + 0.249\ x \quad (5)$$

Comparing the real values of **y** with the adjusted values for the *resulting feature* ŷ, there are some differences, presented in Table 3.

Table 2

x	ŷ
4.61	85
7.35	85.69
21.84	89.29

Table 3

ŷ	ŷ - y
85	85-81= 4
85.69	85.69-89= -3. 31
89.29	89.29-90 = -0.71

Using Matlab Program, the correlation graphic corresponding to the equation (5) was obtained for the values corresponding to the adjusted values for resulting feature **ŷ** (see Tables 2 and 3 and Figure 6).

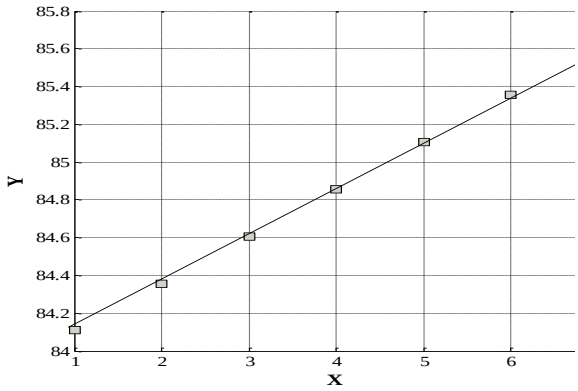

Fig. 6. *Graphic representation for adjusted values of resulting feature ŷ, calculated with relation: ŷ = 0.249 x + 83.860*

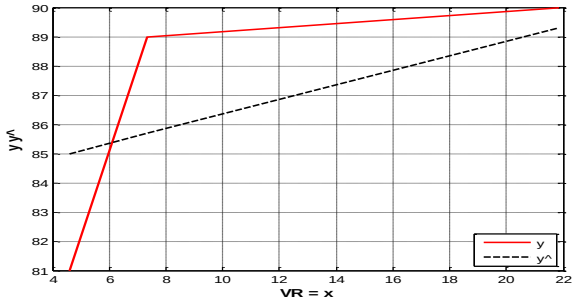

Fig. 7. *Graphic of correlation*

It is estimated that the bond between these two variables (VR and KV) is represented by the equation of straight line. The mathematical model must continue with the characterization of the connection intensity between these two variables using the correlation coefficient ($r_{x,y}$) and the correlation report (*see [1] Scradeanu, 2015*).

$$n\hat{y} = \sum_{i=1}^{n} x_i\ y_i \quad (6)$$

The above relation, for *covariance coefficient*, can be written (*see [1-3] or Breaz N., Craciun M. Gaspar P.2011, Curs)*:

$$M(x \cdot y) = n^{-1} \sum_{i=1}^{n} x_i y_i \quad (7)$$

For n =3, $\bar{y}$ = M(x y) = 2971.24/3 = 990.41

The simple correlation coefficient "r" will be:

$$r = \frac{n\sum x_t y_t - \left(\sum x_t\right)\left(\sum y_t\right)}{\sqrt{n\sum x_t^{\,2} - \left(\sum x_t\right)^2} * \sqrt{n\sum y_t^{\,2} - \left(\sum y_t\right)^2}} \quad (8)$$

In this case, r = 0.5.

The simple correlation coefficient is positive: $r_{x,y} > 0$ shown that a direct connection between the variables (VR and KV) exists. This result indicates the correlation, a direct connection between these two variables.

4. Conclusions

This work wants to demonstrate that the model of linear unifactorial regression- commonly used in economics - has applications in steel engineering. This study determined a correlation between the variables. Because r = 0.5 < 0.95, we cannot talk about a relative deterministic connection but it was statistically proved that a direct and strong connection between the variables exists.

References

[1]. Scradeanu D., *Modele cantitative statistice*, *Note de curs*, Bucuresti, 2015.
[2]. Breaz N., Craciun M., Gaspar P., s.a., *Modelarea matematica prin Matlab*, Note de Curs, Bucuresti, 2011.
[3]. Baron T., Korka M., Pecican E., Stanescu M., *Statistica*, Editura Didactica si Pedagogica, Bucuresti, p. 128-138, 1981.
[4]. Vuong Nguyen Van Do, *The Behavior of Ductile Damage Model on Steel Structure Failure*, Procedia Engineering, 142, p. 26-33, 2016.
[5]. Papadatu C. P., *Cercetari privind ameliorarea proprietatilor si cresterea fiabilitatii unor oteluri folosite in constructia utilajelor metalurgice*, *PhD.Thesis*, "Dunarea de Jos" University of Galati, 2005.
[6]. Papadatu C. P., *Studii si cercetari privind influenta vitesei de racire asupra proprietatilor si structurii otelurilor*, Graduated Project, "Dunarea de Jos" University of Galati, Romania, 1994.
[7]. Baker L. J., Daniel S. R., Parker J. D., *Metallurgy and processing of ultra-low carbon bake hardening steels*, Mater. Sci. Tech., 18 (4), p. 355-368, 2002.
[8]. Geru N., s.a, *Analiza structurii materialelor metalice*, Editura Tehnica, Bucuresti, 1991.

THE ANNALS OF "DUNAREA DE JOS" UNIVERSITY OF GALATI
FASCICLE IX. METALLURGY AND MATERIALS SCIENCE
N°. 1 - 2016, ISSN 1453 – 083X

DESIGN AND FLOW MODELLING OF BALLAST TANK IN-LINE EJECTOR

[1]Constantin DUMITRACHE, [2]Corneliu COMANDAR, [3]Bogdan HNATIUC
[1,3]Maritime University of Constanta, Romania, [2]"Ghe. Asachi" Technical University of Iasi, Romania
e-mail: ldumitr@yahoo.com

ABSTRACT

The purpose of this paper is to present the stages of designing a water in-line ejector used for ballast tanks stripping operation. The design operation was performed using NX Siemens CAD and ANSYS 15 for computer fluid dynamic analysis CFD. This ejector' design was based on descriptive drawings of component parts, all dimensions being chosen from a worldwide supplier of high quality marine products. Computer Fluid Dynamic analysis is based on the finite element method (FEM), meshing, boundary condition and loads. Finally, we reached important conclusions regarding velocities, pressure and temperature of the fluid.

KEYWORDS: in-line ejector, CAD NX Siemens, revolve, extrude, velocities, total pressure, temperature, CFD

1. Introduction

On board of commercial ships there are a lot of auxiliary devices, such as ejectors, emergency fire pumps, transfer pumps and electrical control, which are most used in maritime industries [1].

An ejector is a static piece of equipment with no moving parts (Figure 1). There are three major components of an ejector: the house with suction chamber (1), the motive nozzle (2) and the diffuser (3).

The operating principle of an ejector is to convert pressure energy of high pressure motive liquid into velocity. High velocity liquid emitted from a motive nozzle is then used to work on the suction fluid. This work occurs in the suction chamber and inlet diffuser.

The remaining velocity energy is then turned back into pressure across the diffuser. In simple terms, high pressure motive liquid is used to increase the pressure of a fluid that is at a pressure well below motive liquid pressure [2].

The ejectors are used in a large range of applications in maritime industry:

- stripping of bilges from the bottom of the vessel;
- filling and stripping of ballast tanks;
- stripping of all sorts of mediums from cargo holds includes oil, gas, water and sewage;
- stripping of bilge from chain lockers.

In the engine room ejectors, can both be used for stripping of bilge and for ventilation of exhaust or other gasses, and removal of ashes from incinerators.

Multiple use portable ejectors are designed for multiple suction purposes. These ejectors can be installed with hoses, in order to utilize the ejector various places on the ship. Portable ejectors are favorable to use where various suction quantities are low or where coarse vacuum cleaning are needed. Peak tanks are situated either in the front or the rear of the vessel. Ejectors can both be used for stripping and filling these tanks.

In the priming of centrifugal pumps the ejector creates vacuum which will initiate the function of pumps.

2. Construction of in-line ejector

All dimensions for the in-line ejector were presented in the supplier's technical documentation [1]:

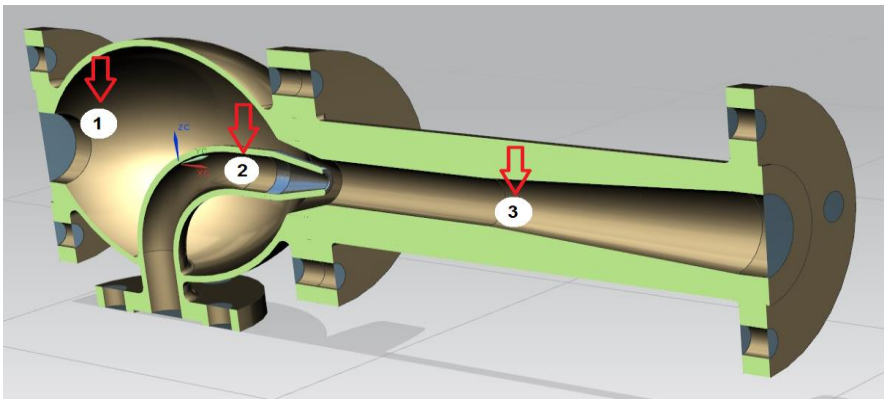

Fig. 1. *Assembly NX cross section viewing parts of in-line ejector; 1- the house, central part of ejector, containing suction and motive inlet; 2 - the motive nozzle is mounted in the house with the purpose of regulating motive liquid; 3 - the diffuser, contains the process of mixing and ejecting the motive and sucked fluid*

2.1. 3D Design of house ejector

The essential feature of the ejector is the house (1) presented in Figure 2.

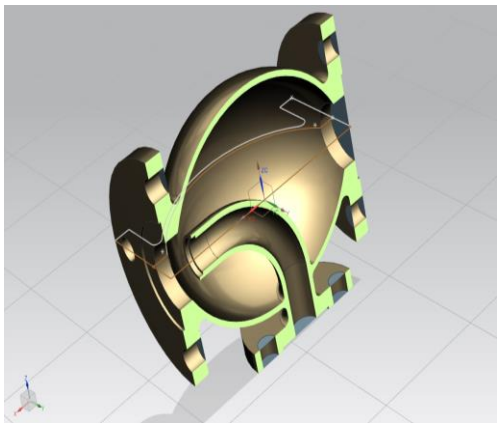

Fig. 2. *Section view of house ejector*

Achieving a 3D house representation starts with the sketch drawn with the yellow line in Figure 2 and goes on with the use of the *Revolve* option that gives the final shape with two flanges at the extremities.

The third flange, also known as motive inlet, is done initially in the form of sketch which is then extruded with the *Extrude* operation. The diameter pipe flange is crossing the ejector body and makes a rounded angle of 90 degrees that was done with the option *Sweep along Guide.*

2.2. 3D Design of motive nozzle

The easiest 3D part is motive nozzle constructed with 2D yellow sketch revolved with *Revolve* operation (Figure 3). The nozzle is considered the heart of the ejector because it converts the energy of pressure to velocity and directs the flow of motive liquid into the diffuser.

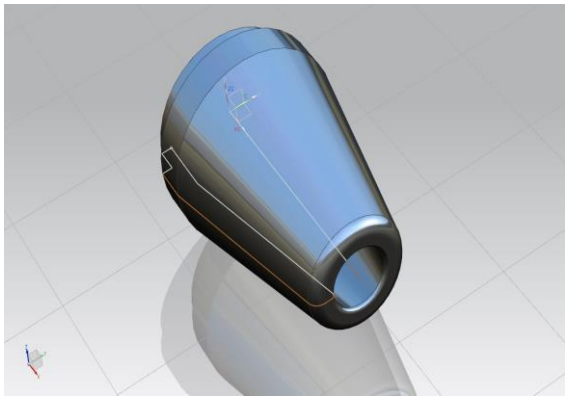

Fig. 3. *Main view of motive nozzle*

2.3. 3D Design of diffuser

The diffuser (Figure 4) is constituted of three parts:

- inlet diffuser;
- throat section;
- outlet diffuser.

Inlet diffuser provides a correctly shaped introductory section and converging diffuser section to handle the high velocity flow of fluids. It is in this section that entrainment and mixing of the motive and load fluids is completed and the energy of liquid velocity is converted to pressure.

The throat section is the transition piece between the converging inlet diffuser and the diverging outlet diffuser.

The outlet diffuser provides a correctly shaped diverging diffuser section for completing the conversion of velocity to pressure. The outlet diffuser

section further reduces the fluid velocity to a reasonable level so as to convert practically all the velocity energy to pressure energy [3].

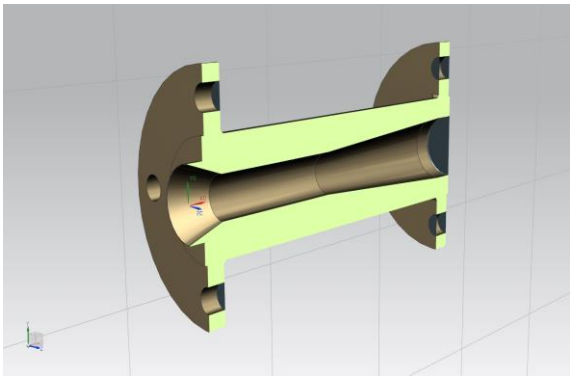

Fig. 4. *Section view of diffuser*

2.4. Assembly of component parts

Our in-line ejector is 25-50-50F type (25 mm - inner diameter of motive inlet, 50 mm - inner diameter of suction inlet, 50 mm - inner diameter of discharge outlet) and has the best efficiency for ballast tanks and cargo tanks [1].

All three parts of the assembly were added using touching (on flanges), infer center axis (on holes), concentric constraints. The final assembly is created when the component objects are added to the assembly part file, each component object being mated with the corresponding objects. The 3D Design of the ejector is presented in Figure 1.

Copper alloy was used for the house ejector and the diffuser, and stainless steel with mechanical properties presented in Table 1 was used for the motive nozzle.

Table 1. *Mechanical properties*

Material	**Yield Strength [N/mm^2]**	**Ultimate Tensile Strength [N/mm^2]**
Copper alloy	280	430
Stainless Steel	207	586

Both materials show excellent resistance to corrosion in sea-water because of main constituents, copper and nickel. This alloy has excellent service under high-velocity conditions, where cavitations erosion is important. But stainless steel is a little more resistant to mechanical-wear than copper alloy due to the superior hardness.

3. Computer fluid dynamics - CFD

CFD has become a powerful tool that can be employed either for pure/applied research or for industrial applications. Computational simulations and analyses are increasingly performed in many fluid-engineering applications, which include aerospace engineering (airplanes, rocket engines), automotive engineering, biomedical engineering (blood flow in artificial hearts), chemical engineering (fluid flow through pumps and pipes), civil and environmental engineering [4].

The first step in our CFD analysis is the creation of the geometry of the flow region using NX Siemens software (Figure 1). This assembly was imported in ANSYS 15 to extract the ejector flow region presented in section viewing in Figure 5.

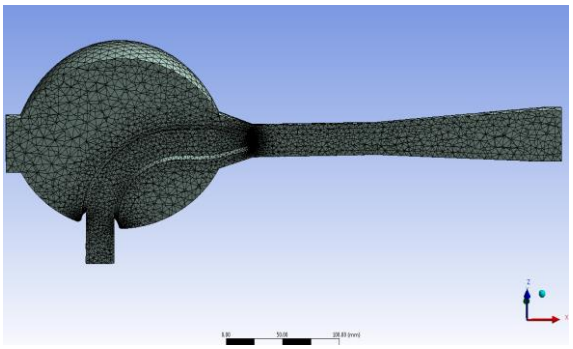

Fig. 5. *Section view of flow meshed region*

The second step is meshing operation (Figure 5) which generates 292884 nodes and 1496290 elements.

3.1. Boundary conditions

We considered that the ballast tank in-line ejector is assigned water as the fluid, with a 7 bar pressure at the motive inlet and a temperature of 25 °C. It is called "in-line" ejector because the suction inlet and outlet discharge are placed on the same line; both suction inlet and outlet have the atmospheric pressure and opening temperature 15 °C.

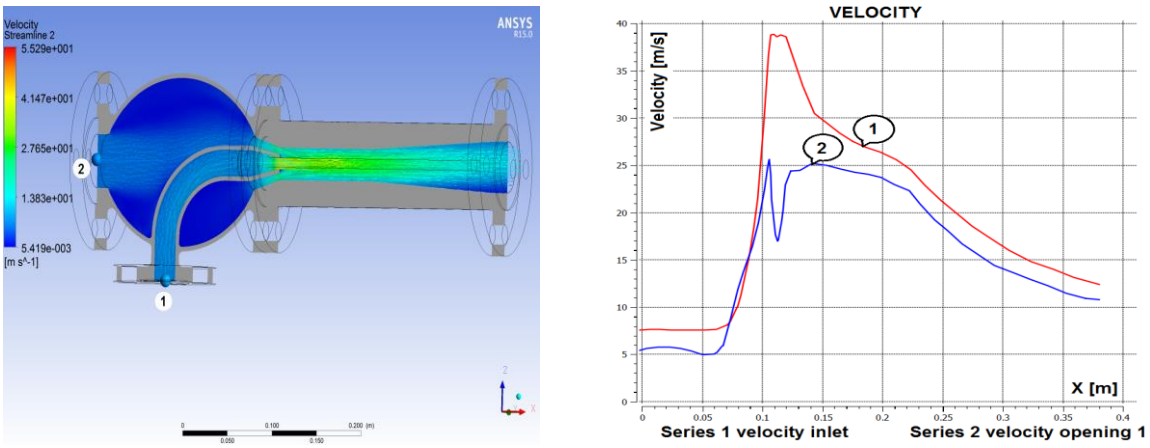

a b

Fig. 6. *Velocity distribution: a) ejector section plane; b) centered streamlines variation 1 (inlet) and 2 (opening 1)*

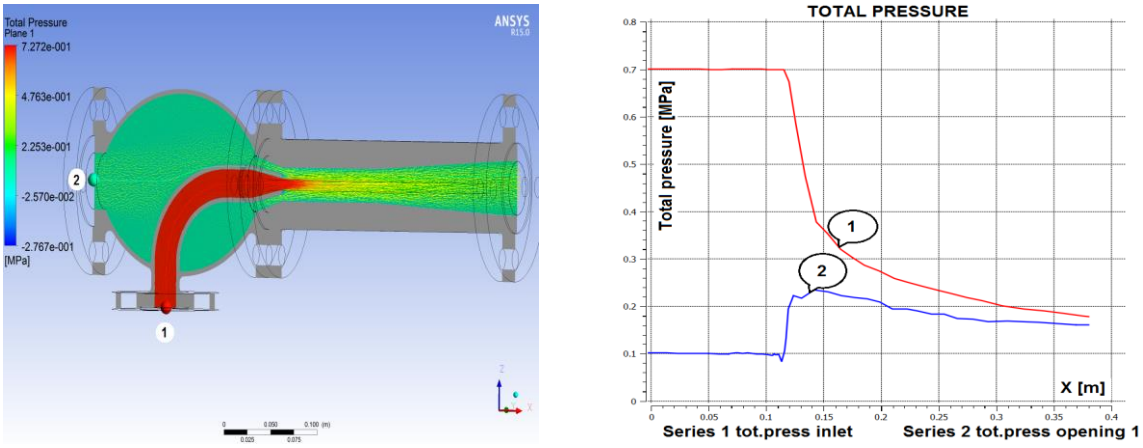

a b

Fig. 7. *Total pressure distribution: a) ejector section plane; b) centered streamlines variation 1 (inlet) and 2 (opening 1)*

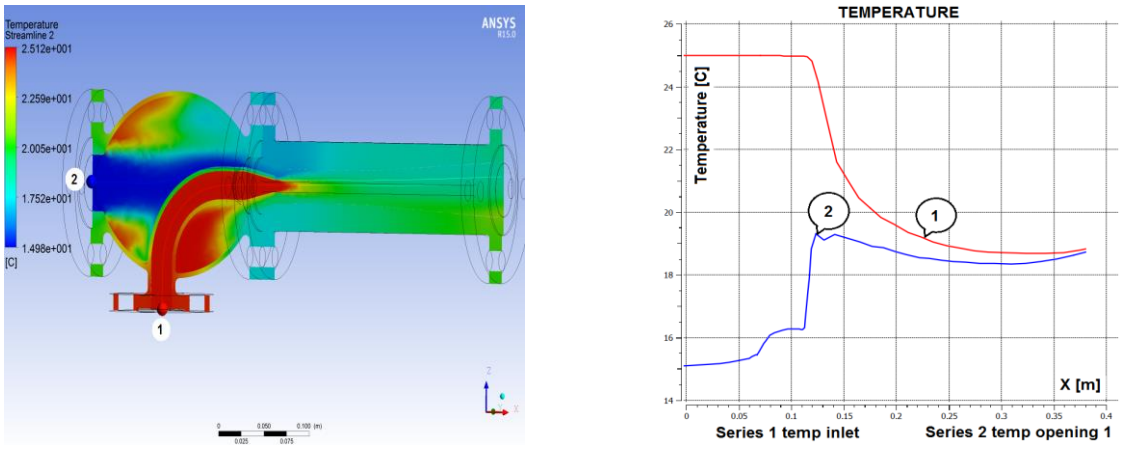

a b

Fig. 8. *Temperature distribution: a) ejector section plane; b) centered streamlines variation 1 (inlet) and 2 (opening 1)*

4. Conclusions

As can be seen in Figure 7, motive liquid pressure is very important because it ensures the minimum pressure on the suction inlet. Generally, it is recognized that the manufacturer has designed the system to maintain stable operation with liquid pressures at or above a minimum liquid pressure. In our example, the motive inlet pressure is 7 bar and for this value the pressure at the suction inlet is around 1 bar. When the velocity of the fluid starts to increase at the motive nozzle, in the same time the suction velocity at opening 1 is increasing (Figure 6b). If the motive liquid supply pressure falls below design, then a motive nozzle will pass less liquid. When this happens, the ejector is not provided with sufficient energy to compress the suction fluid to the design discharge pressure. The same problem occurs when the supply motive liquid temperature rises above its design value, resulting in increased specific volume, and consequently, less liquid passes through the motive nozzle [2].

An ejector may operate unstably if it is not supplied with sufficient energy to allow compression to its design discharge pressure [5]. Unstable ejector operation is characterized by dramatic fluctuations in operating pressure. If the actual motive liquid pressure is below design or its temperature above design, then, within limits, an ejector nozzle can be rebored to a larger diameter. The larger nozzle diameter allows more liquid to flow through and expand across the nozzle. This increases the energy available for compression. If the motive liquid supply pressure is more than 20-30% above design, then too much liquid expands across the nozzle. This tends to choke the diffuser. When this occurs, less suction load is handled by the ejector and suction pressure tends to rise. If an increase in suction pressure is not desired, then ejector nozzles must be replaced with ones having smaller throat diameters or the motive liquid pressure corrected.

In conclusion, an ejector is designed to operate at exact motive pressure and motive capacity, any changes in motive flow can result in [1]:

- Varying motive flow will decrease ejector performance.
- Decreasing motive flow from the specifications might result in an insufficient or even non-performing ejector.
- Increasing motive flow might cause the ejector to malfunction.

Ejectors are designed for maximum suction capacity; therefore, increasing motive flow might not increase suction capacity.

References

[1]. Maritime Diesel Electric, *Marine Consulting, Engineering & Technical Purchasing*, www.mardiesel.com.
[2]. J. R. Lines, R. T. Smith, *Ejector system troubleshooting*, The International Journal of Hydrocarbon Engineering, UK, 1997.
[3]. F. Duncan Berkeley, *Ejectors*, Graham Manufacturing Company, Iinc., BATAVIA, N. Y., Reprinted from Petroleum Refiner, December 1958.
[4]. Jiyuan Tu, Guan-Heng Yeoh, Chaoqun Liu, *Computational Fluid Dynamics, A Practical Approach*, Second Edition, Butterworth-Heinemann is an imprint of Elsevier.
[5]. Yveline Marnier Antonio, Christelle Périlhon, et al., *Thermodynamic Modelling of an Ejector with Compressible Flow by a One-Dimensional Approach*, open access Entropy 2012, 14, p. 599-613, ISSN 1099-4300.

MANUSCRISELE, CĂRŢILE ŞI REVISTELE PENTRU SCHIMB, PRECUM ŞI ORICE CORESPONDENŢE SE VOR TRIMITE PE ADRESA:

MANUSCRIPTS, REVIEWS AND BOOKS FOR EXCHANGE COOPERATION, AS WELL AS ANY CORRESPONDANCE WILL BE MAILED TO:

LES MANUSCRIPTS, LES REVUES ET LES LIVRES POUR L'ECHANGE, TOUT AUSSI QUE LA CORRESPONDANCE SERONT ENVOYES A L'ADRESSE:

MANUSCKRIPTEN, ZIETSCHRITFTEN UND BUCHER FUR AUSTAUCH SOWIE DIE KORRESPONDENZ SID AN FOLGENDE ANSCHRIFT ZU SEDEN:

After the latest evaluation of the journals by the National Center for Science Policy and Scientometrics (**CENAPOSS**), in recognition of its quality and impact at national level, the journal will be included in the B^+ category, 215 code (http://cncsis.gov.ro/userfiles/file/CENAPOSS/Bplus_2011.pdf).

The journal is already indexed in:

EBSCO: http://www.ebscohost.com/titleLists/a9h-journals.pdf

Copernicus: http://journals.indexcopernicus.com/karta.php

The papers published in this journal can be viewed on the website of "Dunarea de Jos" University of Galati, the Faculty of Engineering, pages: http://www.sim.ugal.ro/Annals.htm, http://www.imsi.ugal.ro/Annals.html.

Name and Address of Publisher:
Contact person: Elena MEREUȚĂ
Galati University Press - GUP
47 Domneasca St., 800008 - Galati, Romania
Phone: +40 336 130139, Fax: +40 236 461353
Email: gup@ugal.ro

Name and Address of Editor:
Prof. Dr. Eng. Marian BORDEI
Dunarea de Jos University of Galati, Faculty of Engineering
111 Domneasca St., 800201 - Galati, Romania
Phone: +40 336 130208
Phone/Fax: +40 336 130283
Email: mbordei@ugal.ro

AFFILIATED WITH:

- THE ROMANIAN SOCIETY FOR METALLURGY
- THE ROMANIAN SOCIETY FOR CHEMISTRY
- THE ROMANIAN SOCIETY FOR BIOMATERIALS
- THE ROMANIAN TECHNICAL FOUNDRY SOCIETY
- THE MATERIALS INFORMATION SOCIETY (ASM INTERNATIONAL)

Edited under the care of the FACULTY OF ENGINEERING

Annual subscription (4 issues per year)

Editing date: 15.03.2016
Number of issues: 200
Printed by Galati University Press (accredited by CNCSIS)
47 Domneasca Street, 800008, Galati, Romania